ISTANBUL TECHNICAL UNIVERSITY ★ GRADUATE SCHOOL OF SCIENCE ENGINEERING AND TECHNOLOGY

SYNTHESIS AND CHARACTERIZATION OF POROUS MACROMOLECULAR MATERIALS, AND THEIR APPLICATIONS

Ph.D. THESIS

Ömer Suat TAŞKIN

Department of Chemistry

Chemistry Programme

OCTOBER 2014

ISTANBUL TECHNICAL UNIVERSITY ★ GRADUATE SCHOOL OF SCIENCE ENGINEERING AND TECHNOLOGY

SYNTHESIS AND CHARACTERIZATION OF POROUS MACROMOLECULAR MATERIALS, AND THEIR APPLICATIONS

Ph.D. THESIS

Ömer Suat TAŞKIN
(509102071)

Department of Chemistry

Chemistry Programme

Thesis Advisor: Prof. Dr. Yusuf YAĞCI

OCTOBER 2014

İSTANBUL TEKNİK ÜNİVERSİTESİ ★ FEN BİLİMLERİ ENSTİTÜSÜ

GÖZENEKLİ MAKROMOLEKÜLER MALZEMELERİN SENTEZİ, KARAKTERİZASYONU VE UYGULAMALARI

DOKTORA TEZİ

Ömer Suat TAŞKIN
(509102071)

Kimya Anabilim Dalı

Kimya Programı

Tez Danışmanı: Prof. Dr. Yusuf YAĞCI

EKİM 2014

Ömer Suat Taşkın, **a Ph.D.** student of ITU **Graduate School of Science Engineering and Technology** student ID 509102071, successfully defended the **thesis** entitled "**SYNTHESIS AND CHARACTERIZATION OF POROUS MACROMOLECULAR MATERIALS, AND THEIR APPLICATIONS**", which he prepared after fulfilling the requirements specified in the associated legislations, before the jury whose signatures are below.

Thesis Advisor :	**Prof. Dr. Yusuf YAĞCI** Istanbul Technical University	.....
Jury Members :	**Prof. Dr. B. Filiz ŞENKAL** Istanbul Technical University	.....
	Prof. Dr. Nuray BALKIS Istanbul University	.....
	Doç. Dr. Özkan SEZER Istanbul Technical University	.....
	Prof. Dr. Mehmet EROĞLU Marmara University	.....

Date of Submission : 19 Eylül 2014
Date of Defense : 17 Ekim 2014

To my family and friends,

FOREWORD

I cannot express enough thanks to my advisor, Professor Yusuf Yağcı for his continued support and encouragement. My completion of this thesis could not have been accomplished without the supervision of Professor Yağcı. He educated me how to develop the focus on scientific research. He always advices the scientific imagination more important than the accumulation of knowledge. He also gives inspiration from polymer chemistry to every aspect of life. Even we were playing soccer, he was teaching me. I will never forget Professor Yağcı's famous catchphrase; 'I am sorry to say so, but this is the fact.'

I would also like to express my gratitude to Professors, Nuray Balkıs and B. Filiz Şenkal for serving on my committee and making valuable suggestions.

I also want to express my special thanks to Assoc. Prof. Dr. Barış Kışkan, Assoc. Prof. Dr. M. Atilla Taşdelen and Assist. Prof. Dr. Abdullah Aksu for helping me with my laboratory work and thesis all the time, without any impatience and annoyance. Each time they advised me how to handle problems and helped me with them.

I wish to thank to my past and current laboratory colleagues for all their help and guidance. In particular, Assist. Prof. Dr. Binnur Aydoğan, Dr. Demet Çolak, Dr. Füsun Şeyma Kışkan, Assist. Prof. Dr. Muhammet U. Kahveci, Ali Görkem Yılmaz, Mustafa Çiftçi, Gökhan Açık, Çağatay Altınkok, Muhammed Aydın, Cansu Aydoğan, Faruk Oytun, Manolya Kukut, Cemil Dizman, Kübra Demir, Mustafa Arslan, Hüseyin Akbulut, Elyesa Murtezi, Abdurrahman Musa, Sajjad Dadashi, Sean Doran, Senem Körk, Betül Hanbeyoğlu, Hatice Şahin, Semiha Bektaş Bozdemir, Emre Tunç, Umut Uğur Özköse and Sinem Yener, with all of you, it has really been a great pleasure.

I also thank to my best friends, Erhan Karabayır, Res. Asst. M. Abdussamed Maldar, Res. Asst. A. Talha Üzümcü, Res. Asst. Ümit Gülyüz, Res. Asst. Alperen Bal, Eliften Semerci, and the MoSpect group members, Res. Asst. Sevcan Tabanlı, Res. Asst. Nesrin Çelebioğlu, Res. Asst. Alptekin Yıldız, for always beeing next to me.

Finally, I would like to dedicate my thesis to my dearest father and mother Kadir and Makbule Taşkın, brothers (Ertuğrul and Muhammed), sister (Şeyma), sister-in-law (Zeynep) and my little nephew (Emir Talha), their love and support over the years makes my life more meaningful and valuable.

This work is supported by Öğretim Üyesi Yetiştirme Programı (ÖYP) and ITU Institute of Science and Technology.

October 2014 Ömer Suat TAŞKIN

TABLE OF CONTENTS

Page

FOREWORD ..... **ix**
TABLE OF CONTENTS ..... **xi**
ABBREVIATIONS ..... **xiii**
LIST OF TABLES ..... **xv**
LIST OF FIGURES ..... **xvii**
LIST OF SYMBOLS ..... **xix**
SUMMARY ..... **xxi**
ÖZET ..... **xxv**
1. INTRODUCTION **1**
2. THEORETICAL PART **5**
2.1 Porosity 5
2.2 Microporous Polymers 9
2.2.1 Disordered microporous polymers 11
2.2.1.1 Microporous network polymers 11
2.1.1.2. Microporous non-network polymers 13
2.1.2 Ordered microporous polymers 14
2.3 Meso- and/or Macroporous Polymers 15
2.3.1 Radical polymerization 15
2.3.2 Polycondensation 16
2.4 Materials Characterization 18
2.5 Microporous Materials and Their Applications 19
2.5.1 Polybenzoxazines 19
2.5.2 General introduction to Schiff base chemistry 23
2.5.2.1 Chromatography 26
2.5.2.2 Surface chemistry 28
2.5.2.3 Selectivity 28
2.5.3 Click Chemistry 29
2.5.3.1 Copper(I)-catalyzed azide -alkyne cycloaddition (CuAAC) 30
2.5.3.2 Mechanistic considerations on the Cu(I) catalysis 31
3. EXPERIMENTAL PART **35**
3.1 Materials and Chemicals 35
3.1.1 Solvents 35
3.1.2 Other chemicals 36
3.2 Characterization 39
3.2.1 Nuclear magnetic resonance spectroscopy (NMR) 39
3.2.2 Infrared spectrophotometer (FT-IR) 39
3.2.3 UV-visible spectrophotometer 39
3.2.4 Fluoresans spectrophotometer 39
3.2.5 Gel-permeation chromatography (GPC) 40
3.2.6 Differential scanning calorimeter (DSC) 40

3.2.7 Thermal gravimetric analysis (TGA) 40
3.2.8 Nitrogen sorption analysis 41
3.2.9 Scanning electron microscopy (SEM) 41
3.3 Preparation of Polybenzoxazines 41
3.3.1 Synthesis of 6,6-(propane-2,2-diyl)bis(3-allyl-3,4- dihydro-2H-benzo[e][1,3] oxazine) (B-ala) 42
3.3.2 Preparing of polybenzoxazine sorbent resin 43
3.3.3 Analytical method for mercury analysis 43
3.3.4 Preparation of microporous organic polymer 44
3.3.5 Analytical method for analysis 45
3.3.6 Operating conditions 45
3.3.7 Synthesis of 1,5-bis(prop-2-yn-1-yloxy)anthracene-9,10-dione 46
3.3.8 Synthesis of 2-azidomethyl pyrene (Py-N_3) 46
3.3.9 Synthesis of propargyl functionalized MOP (c-MOP) 47
3.3.10 Post-functionalization of propargyl-MOP by click reaction 48
4. RESULTS AND DISCUSSIONS 49
4.1 Polybenzoxazine Based Microporous Material 49
4.2 Schiff Base Chemistry Based Microporous Materials 57
5. CONCLUSIONS 69
REFERENCES 73
CURRICULUM VITAE 95

ABBREVIATIONS

^{1}H NMR	**:** Hydrogen Nuclear Magnetic Resonance Spectroscopy
C NMR	**:** Carbon Nuclear Magnetic Resonance Spectroscopy
BET	**:** Brunauer-Emmett-Teller
FT-IR	**:** Fourier Transform Infrared Spectrophotometer
UV	**:** Ultra Violet
GPC	**:** Gel Permeation Chromatography
DSC	**:** Differential Scanning Calorimetry
HPLC	**:** High Performance Liquid Chromatography
GC	**:** Gas Chromatography
PAH	**:** Polycyclic Aromatic Hydrocarbons
PMDTA	**:** *N, N, N',N'', N''*- Pentamethyldiethylenetriamine
CH_2Cl_2	**:** Dichloromethane
$CDCl_3$	**:** Deuterated Chloroform
THF	**:** Tetrahydrofuran
St	**:** Styrene
PS	**:** Poly(styrene)
CuAAC	**:** Copper Catalyzed Azide-Alkyne Cycloaddition
TEA	**:** Triethylamine
EtOAc	**:** Ethyl Acetate
DMF	**:** *N*,*N*-dimehthylformamide
DMSO	**:** Dimethyl Sulphoxide

LIST OF TABLES

Page

Table 3.1 : Composition of the prepared artificial sea water and its comparison with natural seawater..... 44
Table 3.2 : Conditions on packing material in different chromatographic modes. ... 46
Table 4.1 : Column properties of various materials for naphthalene and anthracene samples. 62

LIST OF FIGURES

Page

Figure 2.1 : Illustration of porosity existing in nature and synthesized materials with a decreasing pore size: (a) bamboo; (b) honeycomb; (c) SEM image of alveolar tissue in mouse lung 5
Figure 2.2 : Schematic illustration of size of the pores..... 7
Figure 2.3 : Illustration of pore geometry, pore surface, pore size, and framework structure of porous polymers 8
Figure 2.4 : SEM photos of microporous polymer. 10
Figure 2.5 : Synthesis of benzoxazine monomers..... 22
Figure 2.6 : Schematic illustration of condensation of an aldehyde or ketone with a primary amine. 23
Figure 2.7 : The formation of a Schiff base from an aldehydes or ketones is a reversible reaction..... 23
Figure 2.8 : General mechanism a Schiff base formation. 24
Figure 2.9 : Applications of Schiff bases in organic synthesis. 26
Figure 2.10 : General represantation of copper catalyzed cycloaddition. 30
Figure 2.11 : Proposed catalytic cycle for CuAAC. 32
Figure 3.1 : Thermally activated ring opening polymerization of a bisbenzoxazine monomer. 41
Figure 3.2 : Synthesis of B-ala monomer. 42
Figure 3.3 : Synthesis of B-ala derived polybenzoxazine resin. 43
Figure 3.5 : Schematic representation of synthesis of 1,5-dihydroxy-9,10-dione dipropargyl ether..... 46
Figure 3.6 : Azidation of 1-pyrenemethanol. 47
Figure 4.4 : DSC profiles of B-ala (a) and polybenzoxazine resin (b). 51
Figure 4.5 : N_2 adsorption/desorption isotherms of polybenzoxazine resin obtained at 77.3K..... 52
Figure 4.6 : Sorption behaviour of polybenzoxazine resin against several metal ions, based on retained metal salt. 53
Figure 4.7 : Load capacity trends of polybenzoxazine resin for various metal salts. 54
Figure 4.8 : Chemisorption-adsorption and desorption cycle of mercury (II) salt on polybenzoxazine resin. 55
Figure 4.9 : IR spectra of Hg(II) loaded polybenzoxazine resin (a) and pristine polybenzoxazine resin (b). 56
Figure 4.10 : Sorption values of polybenzoxazines after reuse experiments. 57
Figure 4.11 : 3D Structure of porous packing material..... 58
Figure 4.12 : SEM photos of porous packing material. 58
Figure 4.13 : Fourier transform infrared (FTIR) spectra of porous packing material. 59
Figure 4.14 : Gas adsorption/desorption isotherms under nitrogen and CO_2. 59

Figure 4.15a : The analysis of [1]PAH standards mixture chromatogram by using acetonitrile as mobile phase. 60
Figure 4.15b : The analysis of [2]PAH standards by using methanol and water as mobile phase. 60
Figure 4.16 : The analysis of pesticide standards. 61
Figure 4.17 : The analysis of flavonoid group standards. 61
Figure 4.18 : The analysis of phenolic acid group standards. 62
Figure 4.19 : Representative scheme of principal solute/sorbent interaction mechanism. 63
Figure 4.20 : N_2 adsorption/desorption isotherms obtained at 77.3 K; CO_2 adsorption/desorption isotherms obtained at 273 K. 64
Figure 4.21 : SEM photos of to **a)** porous alkyne, **b)** porous click product..... 65
Figure 4.22 : FT-IR spectra of the c-MOP (a), 2-azidomethyl pyrene (b) and pyrene functionalized porous network Py-MOP (c). 66
Figure 4.23 : Solid state C-NMR spectra of the c-MOP. 66
Figure 4.24 : Flourescence spectra of functional porous material a) before and b) after “click” reaction. 67

LIST OF SYMBOLS

λ	**:** Wavelength
h*ν*	**:** Radiation
E	**:** Energy
nm	**:** Nanometer
µm	**:** Micrometer
c	**:** Concentration
A	**:** Absorbance
ε	**:** Molar extinction coefficient
ppm	**:** Parts per million
K	**:** Kelvin
^{o}C	**:** Celsius
M_n	**:** The number average molecular weight
M_w	**:** The weight average molecular weight
M_w/M_n	**:** The molecular weight distribution

SYNTHESIS AND CHARACTERIZATION OF POROUS MACROMOLECULAR MATERIALS, AND THEIR APPLICATIONS

SUMMARY

The contamination of water by metal ions has been a central environmental concern throughout the world. Among various other hazardous metals, mercury has received a particular attention since mercury and most of its compounds are extremely toxic to living organisms. The need for analytical techniques capable of removing mercury from environment is crucial. In order to remove aqueous mercury salts, the conventional approaches that can be used are adsorption, chemisorption, coagulation, precipitation, reduction, ion exchange and membrane separation methods.

In the first part of the thesis, a reusable macroporous polybenzoxazine resin with high specific surface area was prepared as sorbent material for the removal of mercury salts. For this purpose, ally functional bisbenzoxazine was cured in dimethyl sulfoxide by thermally activated ring opening polymerization at 180 °C for 3 days followed by freeze-drying processes. The porous structure of the resin was confirmed by SEM analysis and N_2 adsorption/desorption studies at 77.3 K. Among various metal salts, namely Pb(II), Fe(II), Mn(II), Cu(II), Zn(II), and Cd(II), the porous polybenzoxazine resin exhibited a specific sorption behaviour against Hg(II) salt. Mainly chemisorption and to some extend adsorption mechanisms were proposed for the observed high loading capacity of the resin. As evidenced by FT-IR spectral analysis, the chemisorption is attributed to the coordination system formed between free OH and tertiary amine groups present in the polybenzoxazine structure with Hg(II) ions. It was also demonstrated that the porous polybenzoxazine can be regenerated simply by treatment with acids. The recycling ability of the resin is up to 7^{th} cycle without any significant loss of activity and proved by the sorption and desorption experiments.

Figure 1 : Schematic illustartion of mercury sorption mechanism.

An ‘‘ideal’’ HPLC polymeric packing should be mechanically robust, inert, pH stable, compatible with both polar and non-polar organic solvents and even water. These conditions are best met by the new generation of polymeric adsorbent materials. Principally differing from conventional porous packing materials, the material was obtained by only using melamine and anthraquinone in the presence of dimethyl sulfoxide.

In the second part of the thesis, the column packing material obtained with the inventive method was manually filled in the high performance liquid chromatography (HPLC) column under high pressure. The analysis of compounds such as polycyclic aromatic hydrocarbons (PAH), pesticides, flavonoids and phenolic acids was performed after porous packing material was synthesized by heating at 180°C for 3 days followed by freeze-drying processes. The resulting rigid and black porous polymer network displayed high surface area (215 m^2/g) and similar solvent uptake in both polar and non-polar media, which explains good compatibility of the material with all mobile phases, from acetonitrile to methanol and water.

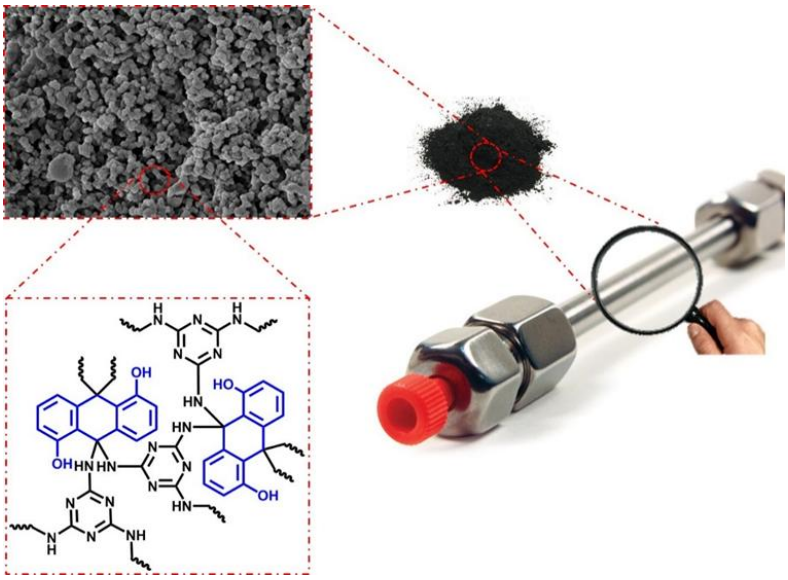

Figure 2 : Graphical illustration of porous packing material.

The modification of polymers after the successful achievement of a polymerization process represents an important task in macromolecular science. The “click” - type reactions provide possibilities for such modifications under various conditions. Among them, the metal catalyzed azide/alkyne reaction, which is a variation of the Huisgen type click reaction between terminal acetylenes and azides, appears to be the most suitable process

In the third part of the thesis, in order for post-functionalization via click chemistry of microporous organic polymer (MOP), the corresponding propargyl containing antraquinone was synthesized and reacted with melamine to form clickable MOP. The obtained MOP was successfully modified with azido pyrene resulting in fluoresans property with high surface area.

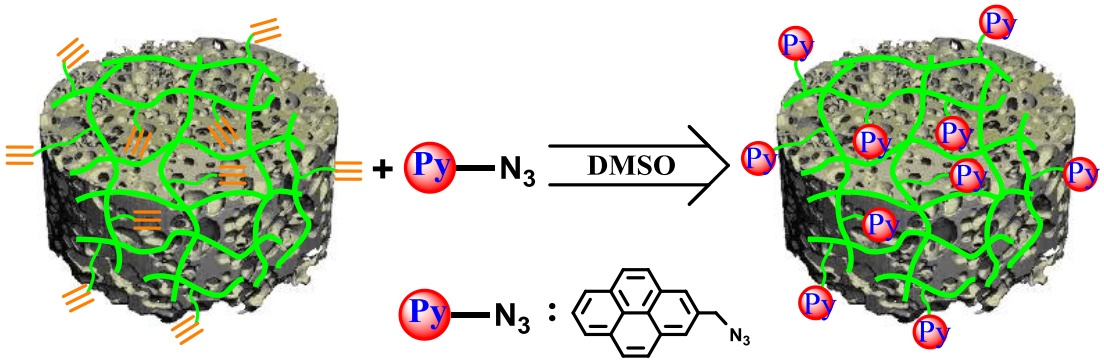

Figure 3 : Graphical illustration of functional porous clickable material.

GÖZENEKLİ MAKROMOLEKÜLER MALZEMELERİN SENTEZİ VE KARAKTERİZASYONU VE UYGULAMALARI

ÖZET

Günümüzde civa kirliliğinin insan sağlığı üzerindeki olumsuz etkisi bilinmekte ve bu kirliliğinin giderilmesi büyük önem taşımaktadır. Sentezlediğimiz malzemenin civanın uzaklaştırılması için spesifik olması bu malzemeyi diğer reçinelerden ayrı tutar. Organik maddelerle ligand yapan d-bloğu elementlerinden iyonlaşma enerjisi en düşük ve kovalent bağ yapma karakteri en fazla olan 12. grup elementleridir. Doğadaki davranış durumları incelendiğinde civanın bu elementlere göre daha yüksek oranlarda kararlı organik formları halinde bulunduğu bilinmektedir. Bu özellik arıtma ve/veya tutulma süreçlerinde civa seçiciliğini açıklayabildiği gibi polimerin karışım süresi, fonksiyonel grupların civaya bağlanma açısı da etken faktörler arasındadır.

Çalışmanın ilk bölümünde, cıva tuzlarının çapraz bağlı polibenzoksazin bazlı malzeme kullanılarak uzaklaştırılması amaçlanmıştır. Kemisorpsiyon (kimyasal tutunma) ilkesine dayanan bu çalışmada, elde edilen gözenekli malzeme civa tuzlarını bağlayabilme özelliğine sahiptir. Malzeme, maliyeti düşük olan formaldehit, birincil amin ve fenol kullanılarak hazırlanan benzoksazin monomeriyle sentezlendiği için önemli bir avantaja sahiptir. Gözenekli ve belirli bir metali kendine bağlayan yapıların sentezi için değişik yöntemler geliştirilmiştir. Çeşitli ligand moleküllerini barındıran gözenekli yapılar sentezlenebilir. Fakat bu ligandların kilolarca hatta tonlarca üretilmesi ekonomik açıdan maliyetlidir. Bu nedenle gerçekten endüstriyel olarak çok miktarda üretilen ticari maddeler ile istenen kimyasal tutunmayı sağlamak, uygulanabilirlik ve maliyet açısından önemlidir. Çalışmamızdaki temel yaklaşım, oldukça düşük maliyeti olan reçinelerin kullanımını sağlamaktır. Kullandığımız reçine klasik epoksi veya fenol formaldehit reçinelerinden farklı olarak polibenzoksazinlerdir. Civa adsorplama oranı kısa süreli adsorpsiyon deneyleri için %98 olarak belirlenmiştir. Suda bulunan civanın sadece %2'si tutuklanamamıştır. Zira, günümüzde endüstriyel olarak ton mertebesinde üretilen polibenoksazinler istenen maliyet-fayda ilişkisini yüksek oranda karşılayabilmektedir. Sentezlenen yeni polibenoksazinlerin başlangıç maddeleri de ucuz maliyetli maddelerden oluşmaktadır. Polibenoksazinlerin civa bağlamasından sonra seyreltik asit ve ardından baz ile yıkanarak tekrar kullanılabilirliği gösterilmiştir.

Şekil 1 : Cıvanın uzaklaştırılma mekanizmasının şematik gösterimi.

Kromatografi, bir karışımın gözenekli bir ortamda, hareketli bir çözücü etkisiyle, karışım bileşenlerinin farklı harkeketleri sonucu birbirinden ayrılması olgusuna dayanır. Hareket eden faza hareketli faz, bahsedilen gözenekli ortama ise adsorban veya sabit faz denir. Kromatografi olayında adsorpsiyon, dağılma ve değiştirme kuvvetleri rol oynar. Bu kuvvetlere göre de farklı kromatografik yöntemler farklı gruplarda toplanırlar.

Çalışmanın ikinci bölümünde, sentezinde düşük maliyetli melamin ve antrakinon kullanılarak gözenekli malzemenin elde edilmesi ve bu malzemenin HPLC uygulaması incelenmiştir. Ekonomik açıdan yüksek maliyet gerektiren eşdeğerlerine göre elde edilen malzeme önemli bir avantaja sahiptir. Bu yeni malzeme, ısısal koşullarda gözenekli hale getirilmesi sayesinde yüksek adsorpsiyon kapasitesine sahiptir. Sentezlenen bu malzemeyle yapılan kromatografik çalışmalarla, poliaromatik hidrokarbonlar, pestisitler, alkoloidler ve flavonoidler için, bu malzemenin uygun bir adsorban olduğu ortaya konmuştur. Ayrıca, malzemenin sentezinin de sadece iki aşamada gerçekleşmesi, bu yöntemi farklı kılmaktadır.

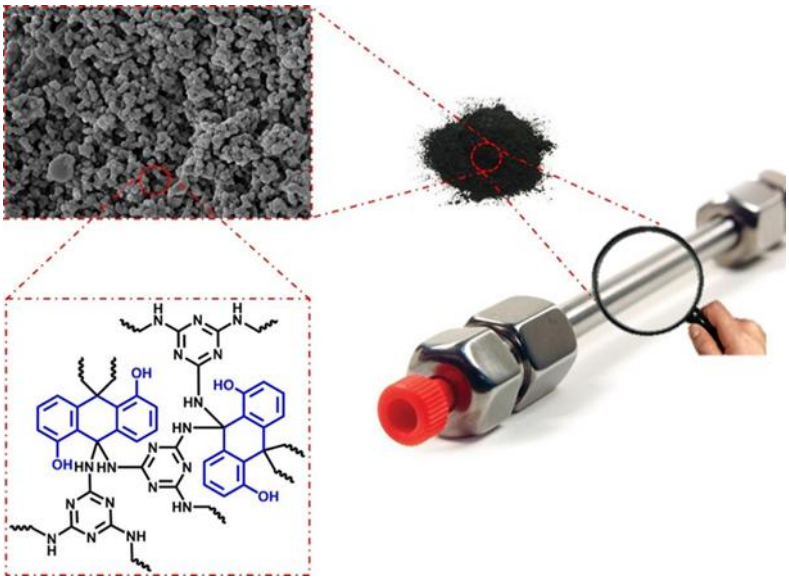

Şekil 2 : Gözenekli kolon malzemesinin şematik gösterimi.

“Çıt çıt (Click) Kimyası” kavramı makromoleküllerin modifikasyonunda kullanılan etkin bir yöntemdir. Bu bağlamda geliştirilen birçok “Çıt-çıt” kimyası arasında Cu(I)’in, azit ve alkinlerin 1,2,3-triazolleri verdiği tepkimenin en etkin ve seçici bir yöntem olduğu ortaya konmuştur. NHC-Cu(I) komplekslerinin bu dönüşümlerde yüksek katalitik aktivite gösterdikleri bildirilmiştir.

Çalışmanın üçüncü bölümünde “Çıt-çıt” kimyası kullanarak piren fonksiyonel gruplu floresans özellikli gözenekli malzemenin sentezi gerçekleştirilmiştir. Başlangıçta 215 m^2/g olan gözenekli malzemenin yüzey alanı “Çıt-çıt” reaksiyonundan sonra 202 m^2/g olarak ölçülmüştür.

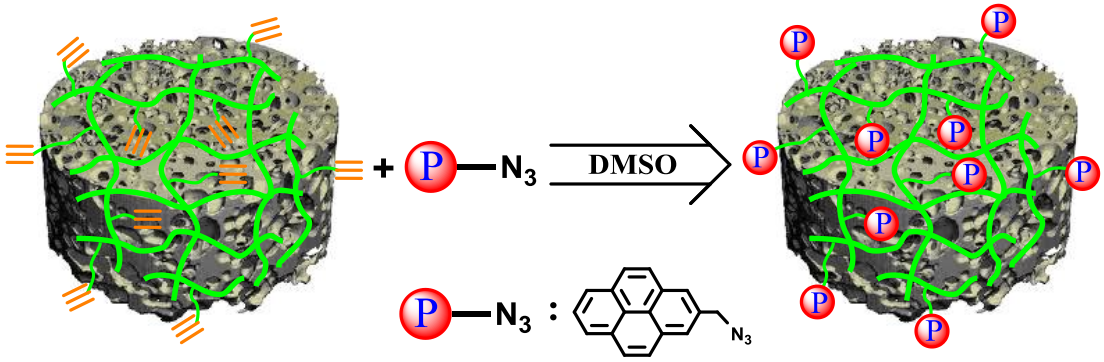

Şekil 3 : Fonksiyonel gözenekli malzemenin şematik gösterimi.

1. INTRODUCTION

Porosity can be considered as a profound concept that helps us to understand nature and create advanced structures. There are some interesting examples in nature, such as hollow bamboo, honeycomb with hexagonal cells, and alveoli in the lungs. Design and construction of porous architectures that mimic structures found in nature in synthesized materials, down to the micro- and nanoscale range, have long been an important science subject. Porous polymers especially have received an increased level of research interest because of their potential to merge the properties of both porous materials and polymers [1, 2]. First, porous polymers can be designed to show the advantages of high surface area and well-defined porosity. Second, the porous polymers have easy processability. For example, they can be produced in a molded monolithic form or in thin films, which generates significant advantages in many practical applications. Moreover, some of them can even be dissolved in a solvent and then processed directly using solvent based techniques without destroying the porosity, which is almost impossible to imagine for other types of porous materials like activated carbons, zeolites, or porous silicas. Third, the diversity of synthetic routes for polymers facilitates the design and construction of numerous porous polymers capable of incorporating multiple chemical functionalities into the porous framework or at the pore surface. The functional porous polymers can be designed to demonstrate stimuli-responsive characteristics capable of reversibly changing the pore structure or even switching between the open and closed porous state after exposure to environmental stimulation. Such unique characteristics are generally unavailable in other porous materials. Last but not least, due to their organic nature, the polymeric frameworks are composed of light elements providing a weight advantage in many applications [3, 4].

Porous polymers can be used as gas storage and separation materials, encapsulation agents for controlled release of drugs, catalysts, supports for catalysts and sensors, precursors of nanostructured carbon materials, supports for biomolecular immobilization and cell scaffolds, low-dielectric constant materials, photonic band

gap materials, filtration/ separation membranes, proton exchange membranes, templates for structure replication, masks for nanopatterning or lithography, packing materials in chromatography, electrode materials for energy storage, antireflection coating, and for many other applications. Therefore, these high value applications drive the recent emphasis on development of reliable methods for preparation of porous polymers, with designed pore architectures as well as customized framework and pore surface functionalities [5-9].

The interest in 1,3-benzoxazine chemistry is growing rapidly due to many unique properties of benzoxazines and their resins. They have various advantages in comparison to other types of thermosets such as phenolic, epoxy, bismaleimide, or cyanate ester resins [10-16]. These extraordinary properties of benzoxazines can be listed as near zero volumetric change upon curing, no strong acid catalysts or additives requirement for curing, high thermal stability, good mechanical performance, low water absorption and high char yield of the cured products. Additionally, another attractive feature of benzoxazine chemistry is the preparation of monomers from inexpensive, commercially available phenols, primary amines, and formaldehyde, easily. By varying the starting phenols and amines a wide range of molecular design flexibility can also be achieved [17-19].

The most common method for preparing imines is the original reaction discovered by Schiff. It consists in the reaction of an aldehyde (respectively a ketone) with a primary amine and elimination of one water molecule. This reaction can be accelerated by acid catalysis and is generally carried out by refluxing a mixture of a carbonyl compound and an amine, in a Dean Stark apparatus in order to remove the water [8].

Cu(I)-catalyzed azide-alkyne cycloaddition, commonly known as “Click Chemistry,” has proven to be the most influential method for the preparation of complex macromolecular structures, polymeric networks, and biomaterials. In our laboratory, CuAAC click reactions in particular were successfully used for the preparation of functional polymers and networks. Such reactions have also been employed in the synthesis of hyperbranched-type complex structures. It can be focused on the use of these types of click reactions for the synthesis of various macromolecular architectures. It seemed that click chemistry could be an important tool for extending possible combinations of conventional polymers with polyconjugated systems [20].

In this thesis, three different strategies were described for the fabrication of porous macromolecules to benefit from their adsorption properties in different applications. Polybenzoxsazines were used for sorbent porous material in order to remove mercury salts. Another strategy was to the synthesis of porous column packing material for chromatographic systems. Finally, this strategy was also extended to synthesize clickable porous polymer to introduce desired functionality to porous systems.

2. THEORETICAL PART

2.1 Porosity

Many solid and powder materials both natural (stones, soils, minerals, etc.) and manufactured (catalysts, cement, pharmaceuticals, metal oxides, ceramics, carbons, zeolites, etc.) contain a certain void volume of empty space. This is distributed within the solid mass in the form of pores, cavities, and cracks of various shapes and sizes. The total sum of the void volume is called the porosity (Figure 1) [1, 21].

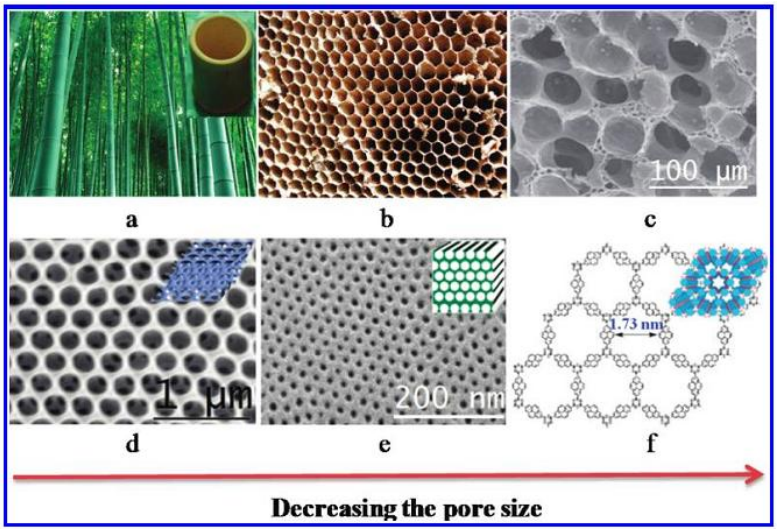

Figure 2.1 : Illustration of porosity existing in nature and synthesized materials with a decreasing pore size: (a) bamboo; (b) honeycomb; (c) SEM image of alveolar tissue in mouse lung [1].

Porous polymers are widely applied as adsorbents, ion exchangers, catalysts, and permeable materials. The first resins with some of these properties were obtained by D'Aleleio in 1944 based on the copolymerization of styrene and divinylbenzene. Unfunctionalized polystyrene resins crosslinked with divinylbenzene (Amberlites) and other types of polymeric resins are porous materials that are widely applied as adsorbents. In addition, functionalized polystyrene–divinylbenzene resins and other porous materials are extensively used as cation and anion exchangers in industry and science. Cation and anion-exchange resins are also significantly used as catalysts. In addition, polymers are the materials that are most extensively applied for membrane

preparation. Often, porous polymers are obtained during the crosslinking used to form thermoset networks that do not flow during heating. These are materials with a permanent porous structure produced during their synthesis and preserved in the solid state. These polymers are often synthesized by suspension polymerization, where the polymerization mixture includes a crosslinking monomer, a comonomer, an initiator, and a porogenic agent. Another method applied to produce porous polymers is based on the addition of an inorganic matrix of a known porosity, for example, silica gel or aluminum oxide, to the reacting mixture. Subsequent to polymerization the inorganic template is eliminated by dissolution without destruction of the polymer. Physical, mobile, and immobile adsorption that is in the application of adsorption for the characterization of porous materials, interested in physical adsorption. For this type of adsorption process there is no need for a reaction involving the exchange of electrons between the solid surface and the gas molecules and the formation of chemical bonds. Physical adsorption is mobile when adsorbed molecules act as a gas in the adsorption space and is immobile when the adsorbed molecule is constrained to vibrate around an adsorption site [22-32].

Porous polymers generally have many pores, but polymers with a single pore, commonly called hollow polymers such as hollow polymeric spheres and tubes, can also be included. Furthermore, according to the IUPAC recommendation, it can be defined microporous polymers as polymeric materials with pore size smaller than 2 nm in diameter, mesoporous polymers with pore size in the range of 2-50 nm, and macroporous polymers with pore size larger than 50 nm. Such a definition is necessary because sometimes polymers with pores in the micrometer scale are also called microporous polymers. There are several important structural characteristics of porous polymers that should be described, including pore geometry, pore size, pore surface functionality, and polymeric framework structure including composition, topology, and functionality [33-41].

Porous polymer particles, especially those spherical in shape, have been utilized in numerous applications for decades. They have been classified as macro-, meso- and microporous depending on the size of the pores.

- Materials with different pore sizes (from nanometer to millimeter)
- Ordered or irregular arrangement of pores

- Various chemical compositions (metal, oxides)
- Different preparative approaches

The International Union of Pure and Applied Chemistry (IUPAC) classifies the different pore widths of porous adsorbents. IUPAC classifies;

Microporous, smaller than 2 nm,

Mesoporous, between 2 and 50 nm,

Macroporous, larger than 50 nm,

Macropores have larger than standard mean free path length of typical fluid. Mesopores exhibit same order or smaller than the mean free path length. Micropores, pore size is comparable to the molecules [42-45].

Adsorption in porous materials that is the concept of gas adsorption in solids, in a very general sense, describes the increase in concentration of gas molecules in an adjacent solid surface. The adsorptive, sorptive, or adsorbate is the gas adsorbed by the solid adsorbent. Adsorption is an important unit operation in industry and a very useful method for the characterization of porous materials. In a general sense, the adsorbents applied for practical purposes are normally porous. The pore width Dp is defined as the diameter in the case of cylindrical and spherical pores and as the distance between opposite walls in the case of slit-shaped pores.

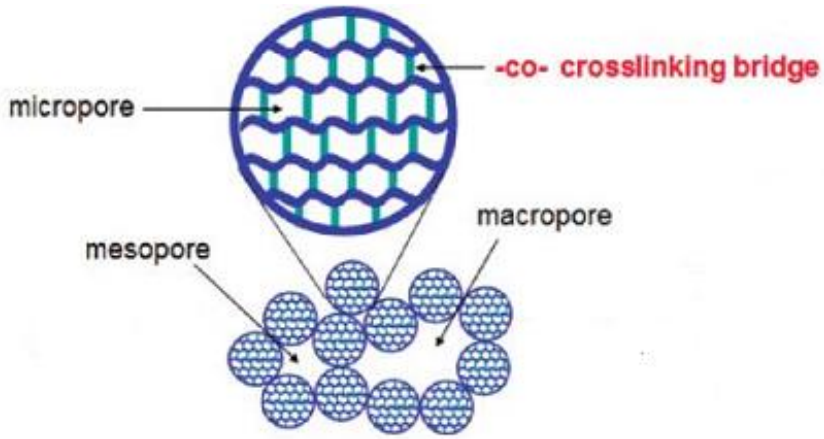

Figure 2.2 : Schematic illustration of size of the pores [1].

Pore geometry includes spherical, tubular, and network-type morphologies that can be either disordered or assembled into ordered arrays. Surface area is a very important parameter that is employed to evaluate the pore structure; generally, pores with a smaller size (e.g., micropores) contribute predominantly to the generation of

materials with high surface area. In addition to the physical structure of the pores, the functionalities of the polymer framework and pore surface are also important. The framework and pore surface functionalities can be engineered through the use of functional monomers or by postmodification processes. The ability to control the structure of pores and incorporate desired functionalities into the material has benefited from the great strides being made in the preparation of porous polymers by various synthetic methods, from directed at preparing porous polymers, including direct templating, block copolymer self-assembly to direct synthesis methodologies.

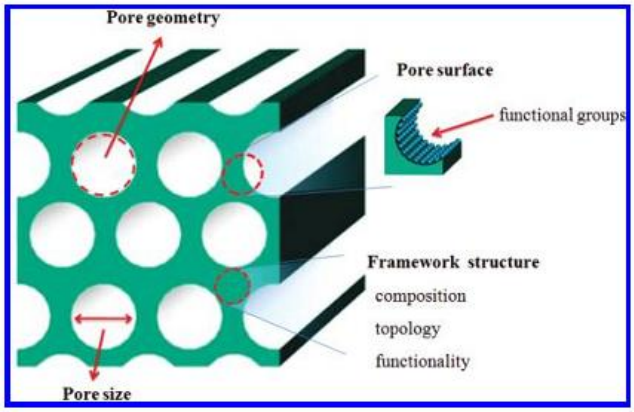

Figure 2.3 : Illustration of pore geometry, pore surface, pore size, and framework structure of porous polymers [1].

Two main features, their porous nature and higher crosslinking degree, differentiate them from gel-type polymer particles. These differences give rise to different characteristics such as high surface area, ability to uptake various solvents with different polarity and increased brittleness. Size, size dispersity, chemical nature and functionality can be mentioned as the other features that porous particles share with their nonporous counterparts, the gel-type particles. The variety of applications requires different combinations of the mentioned features. For instance, while chromatography requires highly monodisperse (uniform in size, low coefficient of variation (CV)) sub 5 μm beads, solid phase peptide synthesis (SPPS) is usually conducted with 100–200 μm beads and monodispersity is not that crucial. On the other hand, functionality is necessary for SPPS but can be undesired for chromatography. In general, polymer particles are produced by heterogeneous polymerizations using the immiscibility of two or more liquids. Suspension, dispersion, precipitation, multistage, membrane/microchannel emulsification and microfluidic polymerizations are the main techniques to form porous particles. In all

cases, the application should be kept in mind prior to choosing the method of production [46, 47].

2.2 Microporous Polymers

Microporous materials are defined as solids that contain interconnected pores of less than 2 nm in size and consequently, they possess large and accessible surface areas typically 300-1500 $m^2.g^{-1}$ as measured by gas adsorption. In the past decades, there has been an intense international effort to optimise conventional microporous materials, such as zeolites (aluminosilicates) and activated carbons, for specific applications in adsorption, separations and heterogeneous catalysis. However, it is recognised that there is a pressing requirement to find entirely novel approaches to the synthesis of microporous materials to benefit fundamental research and to provide new technological opportunities. In recent years, there has been a growing emphasis on using organic components for the construction of microporous materials. It is anticipated that by careful selection of organic precursors it will be possible to exert precise control over the chemical nature of the accessible surface and to introduce specific molecular recognition or catalytic sites, thus facilitating chemoselective adsorption and the design of highly efficient heterogeneous catalysts. Ordered crystalline structures have considerable visual impact, and none are more pleasing than those of the zeolites and related microporous solids. Therefore, it is understandable that the synthesis of "organic zeolites", in which rigid organic units are assembled into a microporous, crystalline structure by metal–ligand or hydrogen bonds, has developed into a major research area in the past decade. Initially, such materials were classified as "microporous" simply on the basis of X-ray crystal structures, even when the removal of solvent from the void space destroyed the crystalline order. Early examples also suffered from interpenetration of one lattice within the pores of another, resulting in restricted access to the internal void space. However, impressive advances based on coordination chemistry, especially by Yaghi and co-workers, have provided highly porous crystalline zeolite-like materials termed metal-organic frameworks (MOFs), which demonstrate vast accessible surface areas by the reversible adsorption of gas. Recently, this methodology has been applied to the assembly of microporous structures by using porphyrin derivatives with catalytic potential. It is also apparent that some coordination solids

derived from more flexible organic ligands demonstrate dynamic behaviour with microvoids that can expand in the presence of an adsorbate [3, 5, 7, 42, 43].

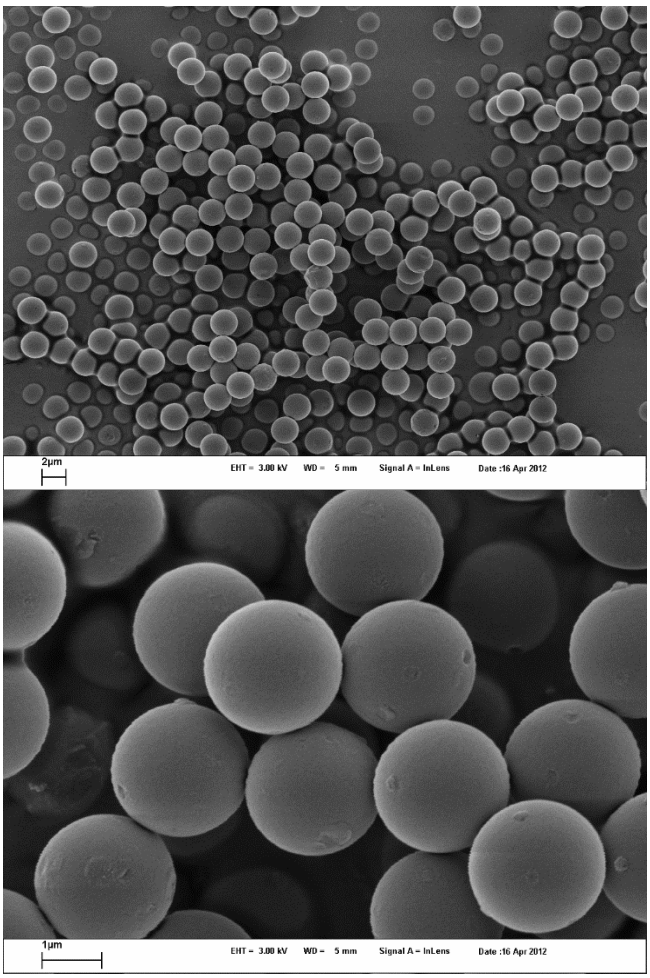

Figure 2.4 : SEM photos of microporous polymer.

The preparation of microporous polymers is a great challenge, due to much higher surface energies and larger capillary pressures exerted on the micropores, compared with meso-/ macroporous counterparts. This places a series of limitations of selection of the monomers and their linking chemistries. The predominant synthetic strategies have focused on polycondensation of multifunctional monomers. The monomers are almost always selected to provide a very robust framework structure, whether it is planar or contorted, in order to impart the resultant polymeric frameworks with sufficient mechanical stability. When compared with the other porous polymers, microporous polymers are unique in that they exhibit permanent porosity with extremely high BET surface area up to 6000-6500 $m^2.g^{-1}$. On the other hand, compared with other microporous materials such as zeolites, silicas, and carbons prepared for molecular sieving applications, microporous polymers have an

advantage in that they could be prepared via diversified chemical synthetic routes. This provides a wealth of opportunities to control the porous structures as well as framework and surface functionalities to cater to the needs of targeted applications. As summarized before, there has been a significant expansion in synthesis methods have been developed in the past few years. Control over the micropore structure and functionality of a targeted porous material is a major goal in materials science and will continue to provide multiple opportunities for a fundamental breakthrough in numerous applications because of superior properties that can be incorporated into design articles. Many parameters inherent in the selected synthetic route influence the final porous structure and targeted site specific functionalities, for example, the chemical synthesis routes, monomer structure and reactivity, phase behavior, molecular weight, and reaction conditions, including solvent, temperature, catalyst, concentration of reactants, and their ratios. Evaluation of all these interacting factors is a challenge but is necessary to optimize porous properties and maximize cost-performance ratio for a given microporous polymer. Particular emphasis is paid to those elements that tailor the microporous structure and incorporate organic functional groups directly into the framework by designing monomer with targeted structures [48].

2.2.1 Disordered microporous polymers

A promising class of disordered microporous polymers consisting of non-network polymer chains has been successfully developed; they are soluble and can be processed directly using solvent-based techniques.

2.2.1.1 Microporous network polymers

A typical example of microporous network polymers is hyper-cross-linked styrenic polymers formed via Friedel-Crafts (F-C) alkylation reactions. These materials are generally prepared by hyper-cross-linking linear PS, poly(vinylbenzyl chloride), or their pre-cross-linked copolymers. The polymer precursors are dissolved in or swollen by a solvent and are then quickly cross-linked to lock in place a stable network structure that closely resembles their solvated state. The structure of the prepolymer, composition, catalyst, solvent, and reaction temperature and time all influence the structure of the final microporous polymers. It is found that the F-C

reaction is rapid, judging from the fact that stable pores providing a majority of surface area are formed in less than 1 h and there is no further increase in surface area with longer reaction times. This means that such reactions are relatively hard to control and the resultant molecular chemical structure is complex and difficult to differentiate. Recently, direct polycondensation via the F-C chemistry has been demonstrated with dichloromethyl-containing aromatic monomers or with aromatic monomers and an additional cross-linker. The porosity in these polymers is controlled not only by the level of cross-linking but also by subtle changes in the design of the rigid monomer unit [49-57]. Likewise, atomistic simulation of the structure becomes possible in such systems providing further information required for deeper understanding the porous structure. Although significant progress has been made in the preparation of microporous hyper-cross-linked polymers, they also continue to possess some limitations: (1) most of porous polymeric frameworks are restricted to styrenic polymers, and (2) control over the pore size is rather difficult, and attaining a surface area exceeding 3000 $m^2.g^{-1}$ is a challenge [3, 7].

Microporous polymers with conjugated frameworks show promise in addressing some monomer types. Although the monomers are planar, they can form 3D networks due to the easy rotation about the alkyne bonds. The porous structure can be manipulated by judicious design of the monomer. This represents an important step toward fine control of the structure of the micropores in disordered amorphous microporous polymers. These conjugated frameworks can be further functionalized by designing monomers bearing pendant functional substituents such as methyl, hydroxyl, carboxyl and amine groups. This combination allows control over the properties of the network polymers such as micropore structure, hydrophobicity, and incorporation of surface functional groups for applications such as CO_2 capture, molecular separations, and catalysis [58].

Most of the above synthetic approaches require costly reaction conditions and use metal catalysts, which inevitably results in the entrainment of trace amounts of metals in the porous polymers. This results in increased research efforts directed at metal-free synthesis strategies with facile polymerization conditions and low-cost monomers. Some catalyst-free reactions with inexpensive monomers, such as Bakelite type chemistry, Schiff-base chemistry and imidization reaction have been developed to prepare microporous network polymers. A typical example is the

catalyst-free one-pot preparation of melamine based microporous networks, which was developed via Schiffbase chemistry with a large industrial-scale monomer, melamine, and monomers containing multiple aldehyde functional groups. Polymers with high surface area, up to 1500 $m^2.g^{-1}$, can be obtained with tailorable microporosity by designing the structure of the multialdehyde monomers. The porous framework can possess up to 40 wt % nitrogen, which is very significant for many applications [59, 60].

2.1.1.2. Microporous non-network polymers

Generally, this approach is plausible for a large range of monomers, but does sometimes fail because of monomer incompatibility with the used MOP synthesis reaction. Another drawback, in large quantities, the use of functional monomers could be uneconomical. Alternative to functional monomers, the incorporation of functional groups by post modification into MOPs has been scarcely been investigated, there are only few examples in the literature. For example, chemical hydrolysis of the pendant nitrile functionalities in MOP to produce carboxylic acids, reaction of MOP with NaN_3 to form tetrazole rings for the separation of CO_2. Reduction of imine bonds in covalent organic framework (COF) followed by treatment with acetic anhydride to form amide. Post functionalization of MOPs by thiol-yne and thiol-ene chemistry and post metallation of bypridyl-containing MOPs to obtain catalytic activity.

The pores in microporous non-network polymers are derived from the space-inefficient packing of highly rigid and contorted nonnetwork polymer chains, which is also named as their “intrinsic porosity”. Thus these polymers are also called polymers with intrinsic microporosity (PIMs). There are two key issues that are generally required in order to prepare such porous structures: (1) polymer chains are generally aromatic heterocyclic ladder polymers with a non-network structure, and (2) polymer chains should be rigid and contorted enough to prevent rotational freedom along the polymer backbone otherwise the conformation of the polymer chains can rearrange to collapse the porous structure. The primary advantage of this type of materials is its solution processability. The polymers can dissolve in a solvent and be processed by solvent-casting to form a film without destroying the porosity [2, 45, 46, 48].

Microporous polymers with non-network frameworks are particularly attractive because of their solution processability. In addition, it is possible to carry out the quantitative evaluation of molecular weight and molecular weight distribution. Up to now, their surface area has been relatively low compared with microporous network polymers, which did not exceed 1000 $m^2.g^{-1}$, and only three classes of chemical synthetic routes have been developed. Ongoing researches focus on exploring other efficient routes for synthesis of soluble porous polymers and designing new monomers to further enhance the surface area, control the porous structure, and expand the framework complexity. Particular care should be taken when using gas (e.g., nitrogen) adsorption to evaluate the porous structure, because of the activated adsorption effect, swelling effects, or limited access of nitrogen molecules to the pores. Such phenomena can also be seen in some porous network polymers, e.g., hyper-cross-linked styrenic polymers. Consequently, complementary measurements are sometimes needed for a more trustworthy examination, such as small-angle X-ray scattering, positron annihilation spectroscopy, or computer simulation. Nevertheless, very definitive control over pore size appears difficult in most disordered microporous polymers, whether based on network or non-network structures, owing to the predominantly statistical nature of these amorphous frameworks, complicated phase behaviors, and side reactions. These limitations resulted in the development of ordered microporous polymers with crystalline frameworks by linking molecular building blocks into an extended structure, which paves the way for rational pore size engineering at a molecular level and specific control over the topology and functionality of a network structure [61, 62].

2.1.2 Ordered microporous polymers

Crystalline microporous polymers with ordered porous structure, also named covalent organic frameworks (COFs), were prepared for the first time by Yaghi et al., [63-68] based on judicious choice of reaction conditions that proceed under thermodynamic control, that is, reversibility of condensation. The crucial point in developing ordered crystalline COFs is to ensure that the polycondensation reactions are sufficiently reversible to link monomer building blocks under thermodynamic control to form an extended, ordered porous structure. The monomers and the corresponding ordered polymers with different pore sizes and surface areas. Pore size is usually controlled in the micropore range (<2 nm) but in some cases can be

extended to small mesopores (2-4.7 nm). BET surface area ranges from about 700 to 4000 $m^2.g^{-1}$ [33, 34, 42].

2.3 Meso- and/or Macroporous Polymers

Polymers containing meso-/macropores can be prepared using the direct synthesis methodology by reaction-induced phase separation. Simply speaking, during the course of the polymerization reaction, the polymers progressively segregate from the solution to form nano- or microscale cross-linked agglomerate/particles that can be considered as network units, followed by covalent cross-linking in various directions into a 3D nano- or microscale network. Extracting a porogenic solvent from the resulting network leaves numerous meso-/macropores in the 3D network framework. It should be noted that, unlike the case of microporous network polymers, the cross-linked/network polymeric frameworks themselves for these meso-/macroporous polymers usually do not demonstrate microporosity. This is probably because they exhibit a much lower structural rigidity, judging from the fact that for most polymer aerogels, their nanopores cannot be retained without supercritical drying. The pore size for the meso-/macropores depends on the size of particulate network units themselves and their compact/loose cross-linked aggregation. Attention should be paid to two crucial points with regards to the design and fabrication of meso-/macroporous polymers: (1) exploring an appropriate reaction system, including reagent, solvent, catalyst, and initiator, to guarantee the occurrence of phase separation; and (2) ensuring the appropriate rigidity of the monomer unit and resultant network structure to avoid the collapse of internetwork pores during drying, especially in the case of mesoporous networks [69-71].

2.3.1 Radical polymerization

Many meso-/macroporous polymers with pore size up to the micrometer scale have been successfully prepared by free radical polymerization. In a typical process, a homogeneous single-phase solution including monomer, cross-linker, porogen, and initiator is in situ polymerized to induce the phase separation between the cross-linked polymer chains and the porogenic solvent. Styrene- and (meth)acrylate-based divinyl monomers are frequently used. The resultant pore framework has a cross-linked structure, but the rigidity is less pronounced than that of microporous network

polymers. UV irradiation initiated polymerization, γ-radiation initiated polymerization, and electron-beam initiated polymerization have been used, as well as thermally initiated polymerization. The porogenic solvent employed in the reaction should be a relatively good one for the monomers, but a thermodynamically poor one for the resulting polymer networks. Conventional free radical polymerization often results in the formation of heterogeneous polymer networks consisting of tiny micrometer-scaled particulate network units. This is because the slow initiation and fast chain propagation and termination results in an abrupt increase in the local degree of polymerization and high degree of cross-linking density, leading to a fast phase separation for the formed microgel in the local regions. Recently, some efforts have been made to overcome such a structural inhomogeneity; for example, a more homogeneous 3D bicontinuous macroporous structure has been successfully constructed by addition of a socalled phase separator, poly(butyl methacrylate-*b*-glycidyl methacrylate), to delay the phase separation process. Controlled/living radical polymerization (CRP) methods have better ability to prepare the homogeneous 3D bicontinuous macroporous polymeric monoliths compared with conventional free radical polymerization. In the CRP procedures, the DP progressively increases with time in a stepwise manner, and then the rapid formation and phase separation of highly cross-linked microgel particles can be effectively suppressed. A series of wellcontrolled 3D bicontinuous macroporous polymers have been prepared by various CRP methods in the presence of proper phase separators [72-74].

2.3.2 Polycondensation

Two major steps can usually be distinguished in the preparation of porous polymers via polycondensation sol-gel chemistry. The first stage is the sol-gel polymerization of the reagents, followed by curing the resulting gel. During the phase separation process, the homogeneous single-phase reaction solution is transformed into the solid−liquid two-phase monolithic gel. The second stage is the removal of solvent from the gel to form the meso-/ macroporous structure. Resorcinol and formaldehyde are the most often used monomers for preparation of the framework of phenolic resin networks, whose network units are resorcinol-formaldehyde resin-based nanoparticles without any micropores because of their low structure rigidity. The

covalent aggregation of these particulate network units leads to numerous nanopores ranging from mesopores to macropores [75-77].

The 3D network structures are largely dependent on variation in the conditions used for sol-gel synthesis, which provides considerable opportunities to control the pore structure. Conditions selected for the solvent drying step are often crucial to avoid pore collapse from the capillary pressure, and generally, supercritical or freeze-drying techniques are utilized for solvent removal. However, these additional procedures undoubtedly raise production costs. Thus, there is continuing effort to simplify this preparation process and explore the suitability of cheap phenolic monomers or prepolymers to replace relatively expensive resorcinol.

Recently, a new ambient pressure drying technique was developed for the synthesis of polymeric aerogels, which can be carbonized into carbon aerogels, using a microemulsion templated sol-gel polymerization method. It should be noted that carbonization is an important approach to provide novel structures and properties to polymer-based materials, such as achieving conductive and electrochemical performances and generating micropores, which greatly extends their applications. The particulate network units and interparticle pores of polymeric aerogels and related carbon aerogels can be easily controlled from micrometer to nanometer scale by increasing the surfactant/ resorcinol molar ratio. Moreover, the respective role of gel strength, pore size, and surfactant in decreasing the drying shrinkage at ambient pressure has been investigated in detail. Currently, this simple and effective technique has been scaled up for the production of polymeric and carbon aerogels, and they have found utility in some applications, such as advanced supercapacitor electrode materials, catalyst supports for fuel cells, and adsorption of small organic molecules from aqueous solution. Additionally, some relatively cheap raw materials for polymeric and carbon aerogels, such as phenol-formaldehyde, phenol-furfural, and tannin-formaldehyde, have been developed. The polymeric and carbon aerogels prepared by various aforementioned procedures have been proved to have extensive application prospects in many fields, such as adsorption, energy, catalysis, and environment [1, 48].

The direct synthesis methodology utilizing the phase separation process can be used effectively to produce meso-/macroporous polymers. During the dying step, micropores inside the network framework collapse, because the less rigid polymeric

chains collapse to pack the space effectively, while the interstitial meso-/macropores among the nano- or micronetwork are retained after drying. Therefore, procedures to lock in the intraframework micropores while maintaining the interframework meso-/macropores are an interesting and important research subject.

2.4 Materials Characterization

For chromatographic separation materials, parameters like specific surface area and pore size distributions, elemental surface and bulk composition, as well as morphology are essential. Theese parameters are all determined or assessed on materials in their state, in contrast to the chromatographic application were the material are wetted by the eluent and then most certainly have quite different properties. There is, however, a chromatographic technique, and like in modeling and simulaton are still done on silica monoliths. Among other things detection might be a problem and this makes the technique difficult to use especially for polymer capillary monoliths. Therefore, new sample preparation techniques used for transmission electron microscopy (TEM) to asses the macroporous structure of porous polymeric monoliths might be necessary. The most commonly used dry state pore characterization technique is nitrogen sorptiometry according to the BET. In terms of surface elemental composition X-ray photoelectron spectroscopy (XPS) is superior, fourier transform infra red spectroscopy (FT-IR) and bulk elemental analysis aera important when the bulk material is considered [54].

Nitrogen Sorptiometry – BET

In 1938, Brunauer, Emmett and Teller published a theory of adsorption of gases in multimolecular layers, which has later become known as the BET scheme. This was an improvement of the Langmuir monolayer theory and considered a multilayer formation. However, an over-simplified model of physiosorption like the Langmuir theory, assumes that there is no interaction between adsorbed molecules on the surface. Thereby a perfect close packing independent on surface morphology of the adsorbent is formed. Since no interactions are allowed, the assumption of liquid-like properties on the second, third and so on layers is contradictory [63].

2.5 Microporous Materials and Their Applications

Microporous organic polymers (MOPs) attracted a great deal of attention, because of their potential uses in various applications such as catalysis, sensors, batteries, light harvesting and photoluminescence, carbon dioxide capture, gas storage and separation. MOPs have superior properties over many other microporous materials regarding synthesis of various architectures, ultrahigh surface areas and their stability against polar solvents especially water, which distorts the structure of many metal organic frameworks (MOFs). Syntheses of MOPs are generally non-complicated and many functional groups can be incorporated to the structure by predesigned monomers. MOPs can contain polar pendant functionalities such as amines, phenols, alcohols and carboxylic acids that can prove more difficult in MOFs, since these groups can coordinate metals or be incompatible with MOF forming reactions. Typically, stable permanent microporosity in MOPs requires the use of highly rigid linkages. Thus, most of the MOPs are based on fully aromatic conjugated structures or kinked aromatic high-performance polymer systems (e.g. polyimides, polyaromatic ethers). Hence, the selection of the monomers and the synthesis methods are crucial in MOP synthesis. In general, polycondensation reactions, especially metal catalyzed e.g. Sonogashira-Hagihara of aryl halides with aryl ethynylenes, or by Suzuki coupling coupling of aryl halides with bisboronic acids are used with the selected rigid monomers. Moreover, various chemistries also can be used for such purposes, such as imine formation, aromatization, etherification etc. Due to the synthetic convenience and vast number of possible monomers, there is an increased interest in preparing functional MOPs, in order to utilize benefits of high surface area. The classical way to achieve desired functionality on the MOP network is to use functional monomers.

2.5.1 Polybenzoxazines

Polybenzoxazines are advantageous materials since they provide the benefits of phenolic resins and have a wide variety of attractive features such as (I) their curing occurs without any need of strong acid catalysts, (II) during curing, they do not or limitedly release any by products, (III) low shrinkage upon curing, (IV) uptaking water hardly any despite having many hydrophilic groups, (V) for some benzoxazines, glass transition temperature is higher than curing temperature and (VI)

high char yield. Moreover, they can be easily prepared by commercially available and inexpensive phenols, amines and formaldehyde. They can be used for a number of applications due to their adjustable molecular architecture. The polymerization reaction of benzoxazines is a thermally induced self- polymerization without any curative or initiator [1, 48, 78, 79].

Even though polybenzoxazines have a lot of fascinating features superior to other resin materials, they are not adequately processable because of powdery form of their monomers and fragility of their networks. Therefore, a number of studies involving polymeric precursor developments has been performed. Recently, main-chain, side-chain and telechelic type precursors are in the centre of polybenzoxazine studies. The main aim of these investigations is to improve the processability, solubility and to cast thin films from polybenzoxazines without distorting the favorable properties of polybenzoxazines such as superior mechanical property [17-19, 80-87].

Benzoxazine-based phenolic thermosets have gained an increasing interest in the field of polymer research owing to the superior properties that overcome several shortcomings of conventional novolac and resole-type phenolic resins. These materials offer low water absorption, high char yield, resistance against flame, high modulus, high strength, high glass transition temperatures, chemical resistance, long shelf life, they have very limited volumetric change upon curing and strong acid catalysts are not required for curing. Moreover, the molecular design flexibility of benzoxazines is enormous. Basically, the synthesis of a monomer is carried out by the reaction of any suitable phenols, formaldehyde, and primary amines (aliphatic or aromatic). Synthesis of polybenzoxazine network is a thermally induced ring-opening polymerization of precursor 1,3-benzoxazines which can be accomplished without any initiator or curing agent. Despite their various attractive properties, polybenzoxazines have drawbacks and limitations related to their processability, brittleness, high curing temperatures (200 ^{o}C or more), and low degree of polymerization for mono-functional monomers. To overcome these problems, various modification strategies have been proposed. To improve the performance of polybenzoxazines, additional sites such as allyl-, acetylenyl-, nitrile-, and propargyl groups have been introduced into benzoxazine monomers. These groups take part in further crosslinking reactions, yielding three-dimensional networks that exhibit high thermal and mechanical stability, and high solvent and moisture resistance. Similarly,

incorporating some functional groups such as carboxylic and phenolic groups allows lowering curing temperature. The side-, main-, and end-chain polymeric benzoxazine precursors or blending benzoxazines with a highperformance polymer, filler, and fiber have been successfully used to reduce brittleness and improve thoughness [88, 89].

For decades, the contamination of water by metal ions has been a central environmental concern throughout the world. Among various other hazardous metals, mercury has received a particular attention since mercury and most of its compounds are extremely toxic to living organisms [90-92]. Even relatively low doses can cause serious kidney, liver, brain and central nervous system disorders for human and animals. Therefore, the control of its circulation in society and the environment through air, water, sediments and living organisms is a global challenge. Despite its highly toxic nature, mercury has many unique properties that make it indispensable in various industrial applications, ranging from fungicides and bactericides in the agriculture industry to heat transfer agents and catalysts in the chemical industry. Thus, the need for analytical techniques capable of removing mercury from environment is crucial [93-112]. In order to remove aqueous mercury salts, the conventional approaches that can be used are adsorption, chemisorption, coagulation, precipitation, reduction, ion-exchange and membrane separation methods. Among these approaches, chemisorption reinforced adsorption processes have been widely studied due their simple operational conditions. Materials that are effective for mercury removal generally carry sulfur, nitrogen and oxygen containing functional groups as mercury ion binding sites. Accordingly, many S, O and N atoms containing adsorbents were used for mercury removal. For example adsorbents having ligands such as xanthate, thiourea, pyridine-based thiols and dithiozone iminodiacetamide, dipridylamide and polythiourea on charcoal were successfully used for binding Hg(II) ions [113-144].

Moreover, many other alternative adsorbents for mercury including activated carbons, polymers, silicates, bacteria, chitosan clays, iron oxides, natural minerals and pyrite have also been extensively studied. In particular, the binding capability of Hg(II) to N and O atoms can give rise to design of many alternative materials for removal of mercury salts. From this point of view, an important high performance

material, polybenzoxazines, which contains both nitrogen (amino) and O (phenolic) becomes a cost-effective alternative for mercury removal purposes [145-151].

Polybenzoxazines are 1,3-benzoxazine based phenolic thermosets that have gained an increasing interest in the field of polymer research as alternative to phenolic resins.These materials offer low water absorption, high char yield, resistance against flame, high modulus, high strength, high glass transition temperatures, chemical resistance, long shelf life and they have very limited volumetric change upon curing. The synthesis of these materials is performed by non-catalytic thermally activated ring opening of corresponding benzoxazine monomers. Depending on the monomer structure, their polymerization temperatures vary between ca. 160-250 °C [17, 19, 85, 89, 152, 153].

Even though benzoxazines were first synthesized by Cope and Holly in 1940s, the potency of polybenzoxazines has been recognized much later. There has been a massive work on new monomers to improve several properties of polybenzoxazines to further expand their application fields by taking advantage of design flexibility of benzoxazine monomers, coming from simple preparation by using inexpensive and commercially available phenols, primary amines, and formaldehyde (Figure 2.5). In related studies, a wide range of conventional polymers were combined with polybenzoxazines [154-164].

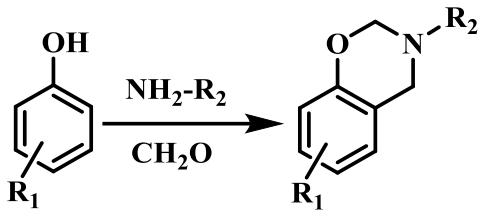

Figure 2.5 : Synthesis of benzoxazine monomers.

The features of polybenzoxazines are mainly caused by the Mannich base bridges –CH_2–N(R)–CH_2– and the hydrogen bonds between nitrogen and phenolic –OH groups. Moreover, this structure has a potential of binding mercury salts over phenolic oxygen and nitrogen on the structure. As part of our continues interest in developing new applications of polybenzoxazines we present a simple route to fabricate functional polybenzoxazines for the removal of mercury salts by taking advantage of the above mentioned structural features. As will be shown below, the surface area of polybenzoxazine material is significantly increased by conducting the

polymerization in a high boiling point solvent. Thus, porous polybenzoxazine material with a high chemical resistance to both alkaline and acidic conditions is obtained [80, 115, 165, 166].

2.5.2 General introduction to Schiff base chemistry

A Schiff base is a nitrogen analog of an aldehyde or ketone in which the C=O group is replaced by C=N-R group [167]. It is usually formed by condensation of an aldehyde or ketone with a primary amine according to the following figure:

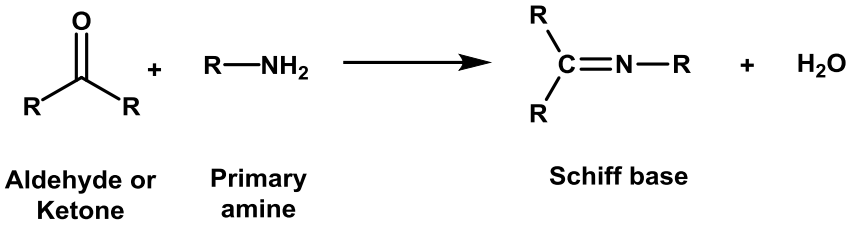

Figure 2.6 : Schematic illustration of condensation of an aldehyde or ketone with a primary amine.

where R, may be an alkyl or an aryl group. Schiff bases that contain aryl substituents are substantially more stable and more readily synthesized, while those, which contain alkyl substituents, are relatively unstable. Schiff bases of aliphatic aldehydes are relatively unstable and readily polymerizable while those of aromatic aldehydes having effective conjugation are more stable. The formation of a Schiff base from an aldehydes or ketones is a reversible reaction and generally takes place under acid or base catalysis, or upon heating [7, 8, 44, 59, 71].

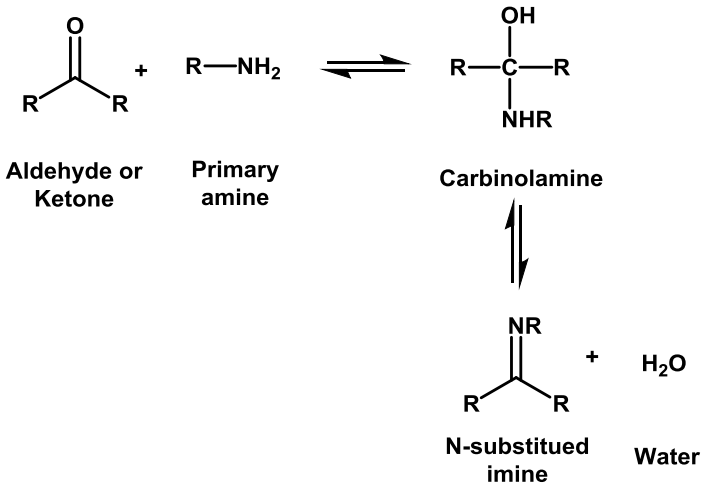

Figure 2.7 : The formation of a Schiff base from an aldehydes or ketones is a reversible reaction.

The formation is generally driven to the completion by separation of the product or removal of water, or both. Many Schiff bases can be hydrolyzed back to their aldehydes or ketones and amines by aqueous acid or base. The mechanism of Schiff base formation is another variation on the theme of neucleophilic addition to the carbonyl group. In this case, the neucleophile is the amine. In the first part of the mechanism, the amine reacts with the aldehyde or ketone to give an unstable addition compound called carbinolamine.The carbinolamine loses water by either acid or base catalyzed pathways. Since the carbinolamine is an alcohol, it undergoes acid catalyzed dehydration [4, 8].

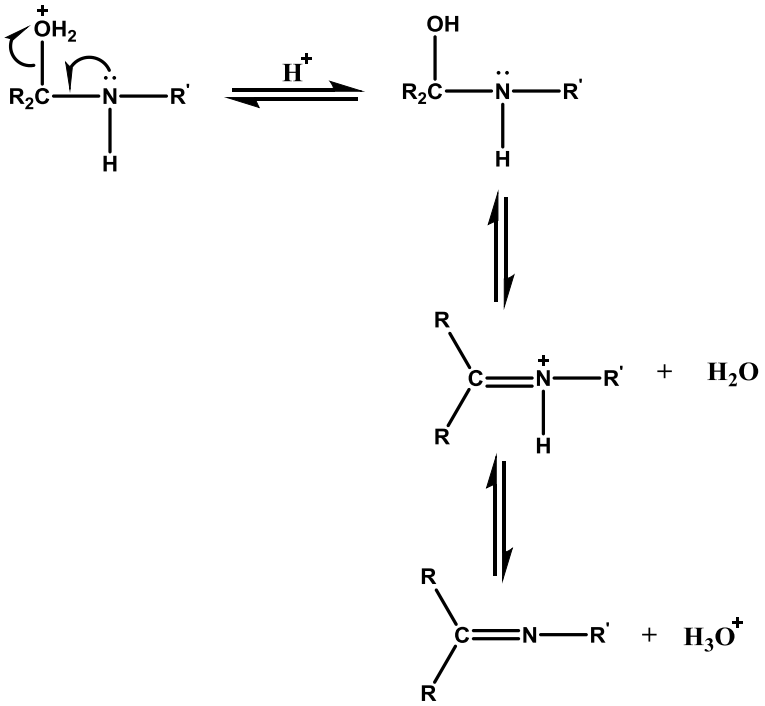

Figure 2.8 : General mechanism a Schiff base formation.

Typically the dehydration of the carbinolamine is the rate-determining step of Schiff base formation and that is why the reaction is catalyzed by acids. Yet, the acid concentration cannot be too high because amines are basic compounds. If the amine is protonated and becomes non-neucleophilic, equilibrium is pulled to the left and carbinolamine formation cannot occur. Therefore, many Schiff bases synthesis are best carried out at mildly acidic pH.

The dehydration of carbinolamines is also catalyzed by base. This reaction is somewhat analogous to the E2 elimination of alkyl halides except that it is not a concerted reaction. It proceeds in two steps through an anionic intermediate.

Schiff bases have a large number of synthetic uses in organic chemistry. Acylation of Schiff bases by acid anhydrides, acid chlorides and acyl cyanides is initiated by attack at the nitrogen atom and leads to net addition of the acylating agent to the carbon-nitrogen double bond. Reactions of this type have been put to good use in natural product synthesis.

Schiff bases appear to be an important intermediate in a number of enzymatic reactions involving interaction of an enzyme with an amino or a carbonyl group of the substrate. One of the most important types of catalytic mechanism is the biochemical process which involves the condensation of a primary amine in an enzyme usually that of a lysine residue, with a carbonyl group of the substrate to form an imine, or Schiff base. Stereochemical investigation carried out with the aid of molecular model showed that Schiff base formed between methylglyoxal and the amino group of the lysine side chains of proteins can bent back in such a way towards the N atom of peptide groups that a charge transfer can occur between these groups and oxygen atoms of the Schiff bases. In this respect pyridoxal Schiff bases derived from pyridoxal and amino acids have been prepared and studied from the biological point of view. Transition metal complexes of such ligands are important enzyme models. The rapid development of these ligands resulted in an enhance research activity in the field of coordination chemistry leading to very interesting conclusions.

The carbon-nitrogen double bond of Schiff bases like the carbon-oxygen double bond is readily reduced by complex metal hydrides. Reduction of this type is probably the most efficient and convenient method for the conversion of C=N into amino compounds. Thus lithium aluminium hydride in THF at room temperature (or in difficult cases at elevated temperature) smoothly reduces Schiff bases in high yield (> 90 %) to secondary amines. Sodium borohydride is an equally effective reducing agent and is preferred to lithium aluminium hydride because of its inertness to a wider range of solvent media and because of its greater specificity in that other substituents such as nitro or chloro reducible by lithium aluminium hydride are unaffected by sodium borohydride. An even more effective reagent of this type is sodium cyanoborohydride ($NaBH_3CN$).

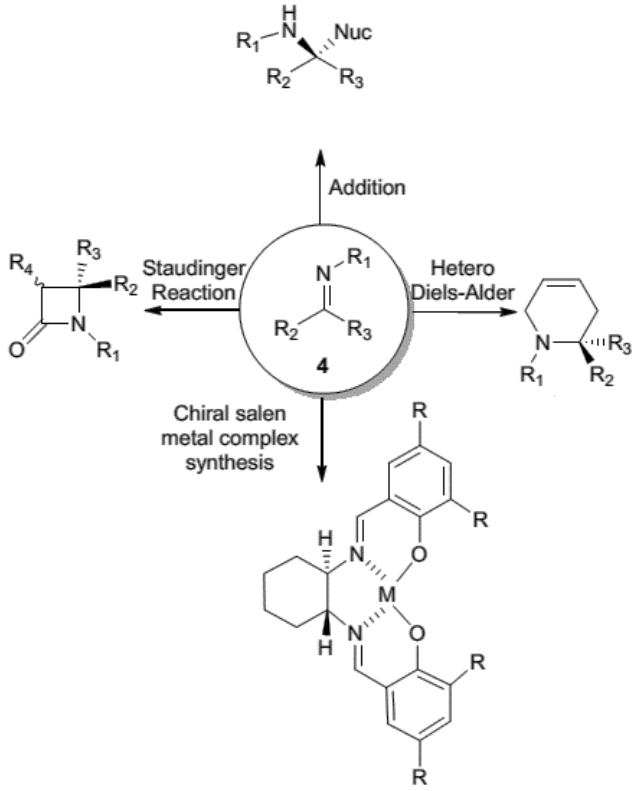

Figure 2.9 : Applications of Schiff bases in organic synthesis.

2.5.2.1 Chromatography

Chromatography is a strong composition and purification method used to separate material mixtures. It can be defined as separating a composition to its components on a porous stationary phase by means of a solvent as a result of different movements. The composition which is wanted to be separated is passed through the stationary phase with the help of the mobile phase. Since the compo-nents forming the composition keeps in different values by the stationary phase, each component leaves the system in different times. Therefore, it is possible to separate the compounds from each other, define and collect separately [168-170]. Even though the chromatography can be classified in different ways, it essentially operates through adsorption and partition mechanisms. The porosity of the material to be used as column filling material being high is preferred since it will increase the adsorption. Producing a material with high porosity is very costly. Today, the production of materials used as filling material in chromatography is realized in different methods and requires high costs [171-174].

When we consider the role of high-performance liquid chromatography (HPLC) column technology, porous packings have a large specific surface area, and this

creates a larger retention and a larger loadability, i.e. Fully porous packings are less prone to exhibit broad peaks with increased injection [175-179]. A typical specific surface area is in the range of 200-300 m^2/g. This quite sizeable surface area resides in the pores of the packing. The pore size must be sufficiently large to allow access of the analytes to the surface of the packing [180-182].

An important element of column performance is the particle size of the packing. However, there is much more to the story than just the particle size. The pore size must be sufficiently large to allow access of the analytes to the surface of the packing. For the analysis of small molecules (molecular weight 100-500), a pore size of 10 nm is about right. Some packings have a slightly smaller pore size (around 8 nm), some have a bit larger pores (about 13 nm). One needs to be careful with some of these designations though, since the methods used for the pore size measurements are not consistent from manufacturer to manufacturer, and often only nominal values are given. The 10 nm (or 100 A) packings can be used for peptide analysis as well, but for larger molecules (proteins) a larger pore size, nominally 30 nm (or 300 A), is needed. The larger pore size provides a smaller specific surface area, therefore these larger pore packings are less retentive, and they are not commonly used for small molecules [183-187]. The most important properties of a porous particle are the specific surface area and the specific pore volume. "Specific" means that these values are given per gram of packing. This approach is acceptable for a comparison of different silica-based packings, but such values can be misleading, if silica-based packings are compared to zirconia-based packings or polymer-based packings. Chromatographers are usually more interested in which packing would result in more retention or less retention. The retentivity of a particle can be estimated quickly by looking at the ratio of the specific surface area to the specific pore volume [188-190].

The advantage of fully porous packings is clear: they have a much larger surface area than non-porous particles [191]. Therefore, their retentivity and loadability is much larger. It is important to get a true understanding of the basic properties of different particles to obtain a proper assessment of their value in chromatography. It can be found that the true phase ratio gives you quite a different impression than the surface area alone. One is a silica packing with a specific surface area of 350 m^2/g and a specific pore volume of 1 mL/g; the other is also a silica packing, but now with a specific surface area of 200 m^2/g and a specific pore volume of 0.5 mL/g. The

strength of a particle depends on its specific pore volume. For normal HPLC applications, strength is of no issue, if the specific pore volume is 1 mL/g or less. For ultra-high-pressure applications, a slightly lower pore volume is needed [192, 193].

2.5.2.2 Surface chemistry

The most common ligand in chromatography is the C_{18} ligand, an 18-carbon hydrocarbon chain. This chain creates the hydrophobic retention of the reversed-phase packing. As an alternative, a C_8 ligand is sometimes used. Due to the shorter chain length, it provides a bit less retention than the C_{18} ligand, but it is occasionally preferred for several reasons. Sometimes, a shorter retention is desired. Some C_8 packings give a slightly improved peak shape compared to a C_{18} ligand, since the smaller ligand can result in a slightly better surface coverage. Or, a slightly different selectivity is desired. It should be pointed out that the selectivity differences between C_{18} and C_8 packings based on the same substrate and with the same surface coverage are rather small, but they still can be useful on occasion. If one is looking for an appreciable difference in selectivity, packings with an embedded polar group are recommended as the first choice. These packings have a polar group incorporated into the long-chain ligand, three carbons away from the silicon group that is used to attach the ligand to the surface. In order to be effective, the polar group is best selected from the group of amide, carbamate, or urea, which all provide excellent hydrogen bonding capability [6, 9, 58, 189, 194-197].

2.5.2.3 Selectivity

The general selectivity properties of commercial columns are of significant interest to the applied chromatographer. Several researchers have dedicated large resources to attempt to characterize the main features of commercially available columns. However, with the exception of the judgement about the hydrophobicity of different packings, the agreement between the different methods is rather poor. The reasons for these discrepancies are not understood. One possibility is that the mobile phase plays a more significant role, and that the dismissal of its influence is the underlying cause for the differences between the characterization methods. From the stand-point of the practitioner, this simply means that one needs to look at the described column features as paintings that have been created with a broad brush, and that one

can only extract a general character of a column from the measured values. However, this is still of significant value [62, 192].

2.5.3 Click Chemistry

"Click chemistry" is a chemical term introduced by Sharpless in 2001 and describes chemistry tailored to generate substances quickly and reliably by joining small units together. Click chemistry can be summarized only one sentence: Molecules that are easy to make. Sharpless also introduced some criteria in order to fullfill the requirements as reactions that: are modular, wide in scope, high yielding, create only inoffensive by - products, are stereospecific, simple to perform and that require benign or easily removed solvent. Nowadays there are several processes have been identified under this term in order to meet these criterias such as nucleophilic ring opening reactions; non - aldol carbonyl chemistry; thiol additions to carbon-carbon multiple bonds (thiol-ene and thio l-yne); and cycloaddition reactions. Among these selected reactions, copper(I)- catalyzed azide- alkyne (CuAAC) and Diels- Alder (DA) cycloaddition reactions and thiol-ene reactions have gained much interest among the chemists not only the synthetic ones but also the polymer chemists [203-207].

The modification of polymers after the successful achievement of a polymerization process represents an important task in macromolecular science. The "click" - type reactions, among them the metal catalyzed azide/alkyne "click" reaction (a variation of the Huisgen 1,3- dipolar cycloaddition reaction between terminal acetylenes and azides) or the Diels- Alder reaction (DA), [4 + 2] system, generally consists of a coupling of a diene and a dienophile by intra- or intermolecular reaction represent a n important contribution towards this endeavor. This approach brings an enormous potential in material science. The key features in "click" chemistry is represented by quantitative yields, high tolerans of functional groups, simple product isolations, lack of by-product, superior regioselectivity, and mild and simple reaction conditions. Since their fast growth, click chemistry strategies have been rapidly integrated into the field of macromolecular enginering and extensively been used in the synthesis of polymers ranging from linear to complex structures [198-202].

2.5.3.1 Copper(I)-catalyzed azide -alkyne cycloaddition (CuAAC)

1,3-Dipolar cycloaddition reactions have also been the subject of intensive research, most notably by Rolf Huisgen and co-workers in the 1950s to the 1970s., whose work led to the formulation of the general concepts of 1,3 - dipolar cycloadditions. The process is strongly thermodynamically favored (ΔH^o = -45 to -55 kcal/ mol) due to the high potential - energy content of the two reaction components, but has a relatively high kinetic- energy barrier (ca. 26 kcal/mol for methyl azide and propyne) that renders the reaction cycloaddition chemistry h as found widespread applications in organic synthesis and has been the subject of several reviews. Cu(I) catalysis of the Huisgen 1,3- dipolar cycloaddition reaction of organic azides and alkynes was introduced in 2001 by Tornøe and Meldal. The Cu(I) 4 catalysis has transformed this cycloaddition into an essentially quantitative and regioselective "click" reaction, as realized independently by the Meldal and the Sharpless laboratories. The Cu-catalyzed azide–alkyne 1,3- dipolar c ycloaddition (CuAAC) dramatically accelerates the reaction of azides with terminal alkynes (Figure 2.10) and exhibits several features. It is very robust, general, insensitive, and orthogonal to most other chemistries used in synthesis of polymers [203].

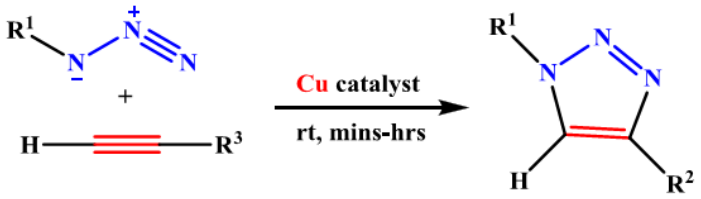

Figure 2.10 : General represantation of copper catalyzed cycloaddition.

The uncatalyzed thermal cycloaddition of azides to alkynes usually requires prolonged heating and results in mixtures of the 1,4-and 1,5-disubstituted regioisomers. In contrast, CuAAC produces only 1,4-disubstituted- 1,2,3-triazoles at room temperature in excellent yields [204-206].

1. The reaction is not significantly affected by the steric and electronic properties of the groups attached to the azide and alkyne reactive centers. For example, azides carrying a primary, secondary, or tertiary group; electron- deficient or electron-rich group; and aliphatic, aromatic, or heteroaromatic substituent usually react well with variously substituted terminal alkynes.

2. The reaction is unaffected by water and by most organic and inorganic functional groups; thus, all but eliminating the need for protecting - group chemistry.

3. The rate of the Cu-catalyzed process is approximately 10^7 times that of the uncatalyzed version, making the reaction conveniently fast in the temperature range of 0 to 25 °C. Furthermore, ligand-accelerated-catalysis effects are also significant, resulting in further increases in the reaction rate.

4. The 1,2,3-triazole unit that results from the reaction has several advantageous properties:

(i) a high chemical stability (in general, being inert to severe hydrolytic, oxidizing, and reducing conditions, even at high temperature),

(ii) a strong dipole moment (5.2-5.6 D),

(iii) an aromatic character, and

(iv) a good hydrogen - bond- accepting ability.

Thus, it can interact productively in several ways with biological molecules, and serve as a replacement for the amide linkage in some circumstances [207, 208].

2.5.3.2 Mechanistic considerations on the Cu(I) catalysis

A mechanistic picture of the copper catalyzed reaction was first proposed by Meldal and co-workers and Sharpless and co-workers, and has later been verified by computational methods.

The intermediacy of copper(I) acetylides in CuAAC was postulated early on based on the lack of reactivity of internal alkynes. Soon thereafter, a computational study of the elementary steps of the sequence was performed. The initial computations focused on the possible reaction pathways between copper(I) acetylides and organic azides (propyne and methyl azide were chosen for simplicity). The key bondmaking steps are shown in Figure 2.11. The formation of copper acetylide 2 (Step A) was calculated to be exothermic by 11.7 kcal/mol. This is consistent with the well - known facility of this step, which probably occurs through the intermediacy of a - alkyne–copper complex. The coordination of an alkyne to copper is calculated to move the pKa of the alkyne terminal proton down by ca. 10 units, bringing it into the proper range to be deprotonated in an aqueous medium. A concerted 1,3-dipolar

cycloaddition of the azide to the copper acetylide has a high calculated potential energy barrier (23.7 kcal/mol), thus the metal must play an additional role. In the proposed sequence, the azide is activated by coordination to copper (Step B), forming the intermediate 3. This ligand exchange step is nearly thermoneutral computationally (2.0 kcal/mol uphill when L is a water molecule). The key bond forming event takes place in the next step (Step C), when 3 is converted to the unusual 6 membered copper metallacycle 4. This step is endothermic by 12.6 kcal/mol with a calculated barrier of 18.7 kcal/mol, which is considerably lower than the barrier for the uncatalyzed reaction (approximately 26.0 kcal/mol), thus accounting for the enormous rate acceleration accomplished by Cu(I). The CuAAC reaction is therefore not a true concerted cycloaddition, and its regiospecif icity is explained by the binding of both azide and alkyne to copper prior to the formation of the C–C bond. The energy barrier for the ring contraction of 4, which leads to the triazolyl–copper derivative 5, is quite low (3.2 kcal/mol). Proteolysis of 5 releases the triazole product, thereby completing the catalytic cycle [209, 210].

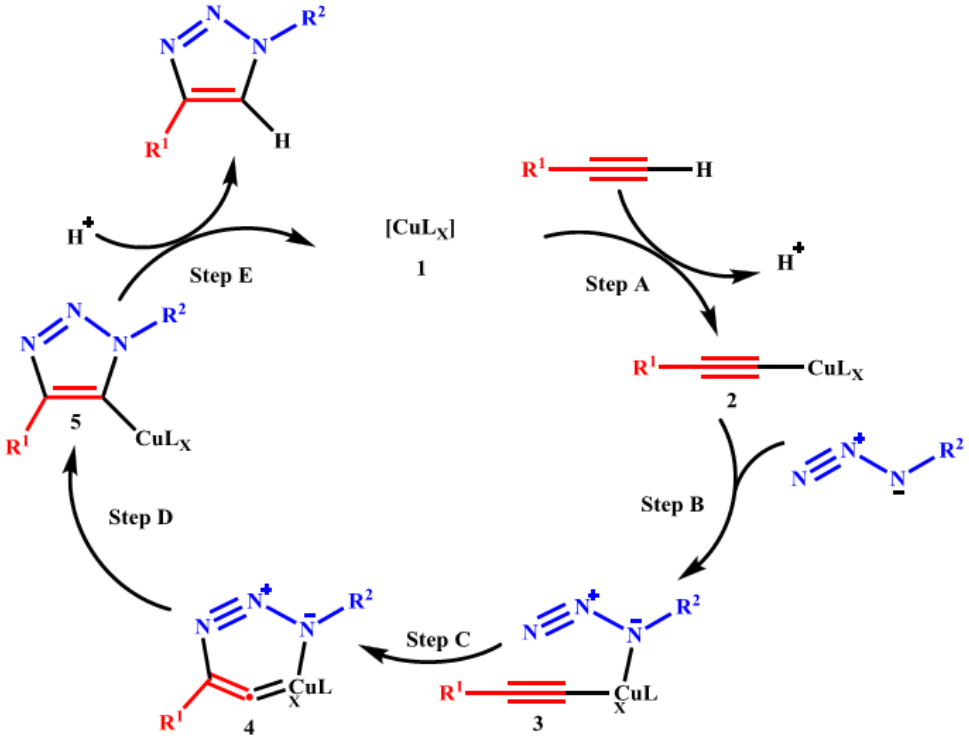

Figure 2.11 : Proposed catalytic cycle for CuAAC.

For post-functionalization of organic materials copper catalyzed Huisgen reaction was studied extensively during the last years and called “click” chemistry. Accordingly, the use of Huisgen-type click reactions has yielded many research

papers within post modification of a wide range of polymers. Moreover, apart from post-functionalization, various block, star-shaped, and graft copolymers, and telechelics have been successfully constructed using click chemistry. Hence, it is clear that the power of this chemistry can be used in synthesis and post modification of MOPs. The use of Huisgen-type click reaction in MOPs was first performed by Cooper's group. Multifunctional azide and etynyl containing monomers were reacted under mild conditions to yield a porous material having a Brunauer-Emmett-Teller (BET) surface area with 1128 m^2/g. Despite this study, there are no previous examples of the use of click chemistry for post-functionalization of MOPs. It can be synthesized the corresponding propargyl containing antraquinone and reacted with melamine to form clickable MOP. The obtained MOP was successfully modified with azido perylenes resulting in fluoresans property with high surface area [20, 211].

3. EXPERIMENTAL PART

3.1 Materials and Chemicals

3.1.1 Solvents

N,N-Dimethyl formamide (99.0 %, Aldrich)

It was used as received.

1,4-dioxane (≥99.0%, Sigma-Aldrich)

It was used as received.

Tetrahydrofuran (THF, 99.8%, J.T.Baker)

(a) It was used as eluent for chromatography as received (High Performance Liquid Chromatography Grade).

(b) For use in the chemical reactions, it was dried and distilled over benzophenonesodium.

Diethyl ether (≥99.0%, J.T. Baker)

It was used as received.

Toluene (99.9%, Acros)

It was used as received.

Methanol (Technical)

It was used for the precipitation of polymers without further purification.

n-Hexane (99.0%, Aldrich)

It was used as received.

Chloroform (≥99%, Aldrich)

It was used as received.

1-Pyrenemethanol (98%, Aldrich),

It was used as received.

Pyridine (98%, Merck),

It was used as received.

Toluene-4-sulfonyl chloride (98%, Aldrich),

It was used as received.

Acetone (99%, Aldrich),

It was used as received.

N,N,N',N'',N'''-Pentamethyldiethylenetriamine (PMDTA, Aldrich),

It was used as received.

Dichloromethane (≥99%, J.T. Baker)

It was used as received.

Acetic acid (99-100%, Merck)

It was used as received.

Dimethyl sulfoxide (DMSO) (≥99.5%, Sigma)

It was used as received.

Ethanol (≥99.5%, Aldrich)

It was used as received.

3.1.2 Other chemicals

Melamine (99%, Aldrich),

It was used as received.

1,5-dihydroxy anthraquinone (98%, Aldrich),

It was used as received.

Pb (II), Fe (II), Mn (II), Cu (II), Zn (II), Cd (II) and Hg (II) solutions (Aldrich, 99%)

It was used as received.

Sodium azide (NaN_3, 98%, Aldrich),

It was used as received.

Magnesium sulphate ($MgSO_4$, 99%, Aldrich),

It was used as received.

Potassium carbonate (K_2CO_3, 99%, Aldrich),

It was used as received.

Paraformaldehyde (powder, 95%, Sigma-Aldrich),

It was used as received.

Phenol (loose crystals, ≥99.0%, Sigma-Aldrich),

It was used as received.

Allylamine (≥99%, Sigma-Aldrich)

It was used as received.

Copper(I) bromide (CuBr) (≥98.0%, Sigma-Aldrich)

It was used as received.

Sodium hydroxide (Granulated, ≥98%, Merck)

It was used as received.

Sodium sulfate (≥99.0 %, Merck)

It was used as received.

Triethylamine (≥99%, Aldrich)

It was dried with NaOH pellets and distilled.

Propargyl bromide (~80 volume % in toluene, Fluka)

It was used as received.

HCl (37%, Sigma-Aldrich)

It was used as received.

Naphthalene: Dr. Ehrenstorfer GmbH (C 20905000),

Acenaphthylene: Dr. Ehrenstorfer GmbH (C 20510000),

Acenaphthene: Dr. Ehrenstorfer GmbH (C 20505000),

Flourene: Dr. Ehrenstorfer GmbH (C 20800000),

Phenanthrene: Dr. Ehrenstorfer GmbH (C 20920000),

Anthracene: Dr. Ehrenstorfer GmbH (C 20520100),

Pyrene: Dr. Ehrenstorfer GmbH (C 20930000),

Fluoranthene: Dr. Ehrenstorfer GmbH (C 20795000),

Benzo(a) anthracene: Dr. Eh-renstorfer GmbH (C 20545100),

Chyresene: Dr. Ehrenstorfer GmbH (C 20670000),

Beta-hexachlorocyclohexane (HCH): Dr. Ehrenstorfer GmbH (C 14072000),

Alpha-hexachlorocyclohexane (HCH): Dr. Ehrenstorfer GmbH (C 14071000),

4,4’-dichlorodiphenyldichloroethane (DDD): Dr. Ehrenstorfer GmbH (C 12031000),

4,4’-dichlorodiphenyldichloroethylene (DDE): Dr. Ehrenstorfer GmbH (C 12041000),

Dieldirin: Dr. Ehrenstorfer GmbH (C 12590000).

Cadechin hydrate, rutin hydrate, quercetin, 4-hydroxhy benzoic acid, p-coumaric acid, caffeic acid, gallic acid (≥98% (HPLC), powder)

It was used as received.

3.2 Characterization

3.2.1 Nuclear magnetic resonance spectroscopy (NMR)

All ^{1}H NMR spectra were recorded on an Agilent NMR System VNMRs 500 spectrometer at room temperature in $CDCl_3$ with $-Si(CH_3)_3$ as an internal standard. Samples were investigated further by 13C CPMAS NMR using an Inova 500 MHz NMR Varian system fitted with a Jacobsen brand CP-MAS probe. 13C CPMAS spectra were acquired at 125.654 MHz using Si_3N_4 rotors set to 6 Hz. Pulses were separated by a 1 s delay. Cross polarization contact time (1 ms), 10 ms data acquisition time, 32 kHz 1 H decoupling field and a spinning rate of 10 kHz were the parameters used during experiments. Two thousand scans were acquired for measurements.

3.2.2 Infrared spectrophotometer (FT-IR)

FT-IR spectra were recorded on a Perkin Elmer FTIR Spectrum One B spectrometer.

3.2.3 UV-visible spectrophotometer

UV-Visible spectra were recordedon a Shimadzu UV-1601 UV-visible spectrophotometer.

3.2.4 Fluoresans spectrophotometer

The fluorescence measurements were carried out by using a Varian Cary Eclipse model spectrometer. The source of spectrophotometer is Xenon flash lamp. The samples thus prepared were put in the sample holder of the spectrometer, then they were excited at 465 nm light. The fluorescence spectra were monitored starting from

excitation wavelength of light. All measurements were performed at a 90° position and slit widths were kept at 480 nm.

3.2.5 Gel-permeation chromatography (GPC)

a) Gel permeation chromatography analyses were performed with a set up consisting of a Waters 410 Differential Refractometer, a Waters 515 HPLC Pump and an apparatus equipped with three Waters ultrastyragel columns (HR series 4, 3, 2 narrow bore), with THF as the eluent at a flow rate of 0.3 mL/min. Molecular 515 weights were calculated on the basis of a calibration curve recorded with mono disperse polystyrene standards.

b) Gel permeation chromatography analyseswere measured on a Shimadzu system equipped with a SCL 10A system controller, a LC-10AD pump, a RID-10A refractive index detector, a SPD-10A UV detector and both a PSS Gram30 and a PSS Gram1000 column in series, whereby N, N-dimethyl acetamide with 5 mmol LiCl was used as eluent at 1mL/min flow rate and the column oven was set to 60°C. The molecular weight and the molecular weightdistribution of the prepared polymers were calculated by using poly(methylmethacrylate) standards.

c) Gel permeation chromatography instrument equipped with a Waters 1515 pump and Waters styragel column (HT4) utilizing DMF containing 5 mM NH4PF6at a flow rate of 0.5 ml/min and the column oven set to 50°C.

3.2.6 Differential scanning calorimeter (DSC)

Differential scanning calorimeter was performed on a Perkin Elmer Diamond DSC with a heating rate of 10 °C min -1 under nitrogen flow.

3.2.7 Thermal gravimetric analysis (TGA)

TGA was carried out on Perkin Elmer Diamond TA/TGA with a heating rate of 10°C min^{-1} under nitrogen flow.

3.2.8 Nitrogen sorption analysis

Nitrogen sorption experiments and micropore analysis were conducted at -195.8 °C using an Autosorb-1 from Quantachrome Instruments. Before sorption measurements, the samples were degassed in vacuum overnight at 150 °C.

3.2.9 Scanning electron microscopy (SEM)

SEM measurements were performed on a LEO 1530 field emission scanning electron microscope.

3.3 Preparation of Polybenzoxazines

Polybenzoxazines are 1,3-benzoxazine based phenolic thermosets that have gained an increasing interest in the field of polymer research as alternative to phenolic resins. These materials offer low water absorption, high char yield, resistance against flame, high modulus, high strength, high glass transition temperatures, chemical resistance, long shelf life and they have very limited volumetric change upon curing. The synthesis of these materials is performed by non-catalytic thermally activated ring opening of corresponding benzoxazine monomers (Figure 3.1). Depending on the monomer structure, their polymerization temperatures vary between ca. 160-250 °C

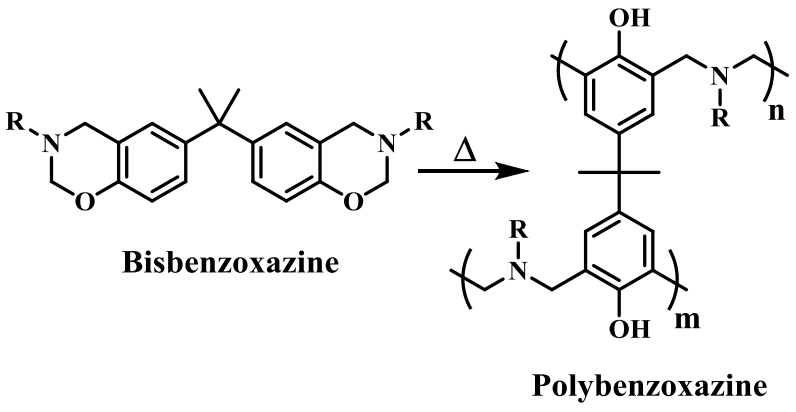

Figure 3.1 : Thermally activated ring opening polymerization of a bisbenzoxazine monomer.

3.3.1 Synthesis of 6,6-(propane-2,2-diyl)bis(3-allyl-3,4- dihydro-2H-benzo[e][1,3] oxazine) (B-ala)

In a 250 mL flask, allyamine (30.8 g, 0.54 mol) was dissolved in 200 mL of 1,4-dioxane at room temperature. The solution was cooled in an ice bath, followed by portion-wise addition of paraformaldehyde (32.5 g, 1.08 mol) during 10 min of stirring in an ice bath. Then, bisphenol-A (61.6 g, 0.27 mol) was added to the cooled solution. The content was refluxed for 24 h. After the removal of 1,4-dioxane under vacuum, the resulting crude product was purified by dissolving in 200 mL of diethyl ether and washing various times with 0.1 N sodium hydroxide, and finally two times with distilled water. Pale yellowish oily product was obtained after drying with Na_2SO_4, filtering and evaporating diethyl ether. The oily viscous product was dissolved in 20 mL of MeOH; water was added to this solution until it became turbid, and then the mixture was refrigerated. The precipitated sticky mass was obtained after decantation and subsequently washing with water. The mass was dried under vacuum at 60 °C for 24 h to afford solid (Yield, 62%) (Figure 3.2). The ^1H NMR spectrum of B-ala is as follows: δ ($CDCl_3$) 6.94 (dd, J = 8.3 and 2.1 Hz, 2H, ArH); 6.79 (dd, J = 2.0 Hz, 2H, ArH); 6.67 (dd, J = 8.3 Hz, 2H, ArH); 5.89 (multiplet, 2H, CH_2 = CH); 5.23 (dd, J = 12.2 and 1.5 Hz, 2H, CH=CH_2); 5.17 (dd, J = 5.3 and 1.3 Hz, 2H, CH=CH_2); 4.82 (s, 4H, N-CH_2-O); 3.93 (s, 4H, Ar-CH_2-); 3.37 (d, 4H, CH_2=CH-CH_2-); 1.58 (s, 6H, -CH_3).

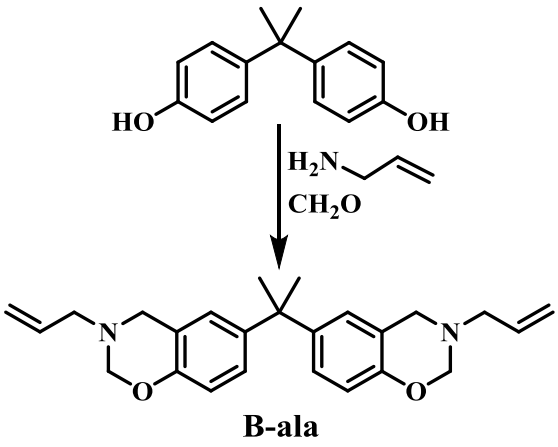

B-ala

Figure 3.2 : Synthesis of B-ala monomer.

3.3.2 Preparing of polybenzoxazine sorbent resin

Benzoxazine (2 g, 5.12 mol) was contained into a 100 mL flask and dissolved in 15 mL of dimethyl sulfoxide (DMSO) at room temperature. This mixture was heated at 180 °C for 72 h. At the end of the reaction, the precipitated material was thoroughly washed with acetone, tetrahydrofuran and 1,4-dioxane. Finally, the obtained black powder insoluble material was swelled in 1,4-dioxane and freeze-dried.

In the subsequent step, curing of B-ala was performed to obtain polybenzoxazine resin as sorbent material (Figure 3.3). Allyl functional bisbenzoxazine was deliberately selected as difunctional monomer so as to provide additional curable sites for the network formation. For the applications of polybenzoxazines in high performance needs, such as those requiring high mechanical strength, thermal stability etc., solventless curing of benzoxazines is usually preferred. Polybenzoxazine obtained by this way is a very stiff material, and meets the abovementioned requirements.

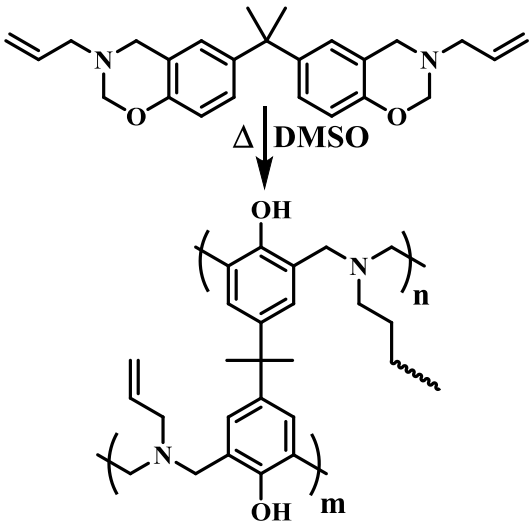

Figure 3.3 : Synthesis of B-ala derived polybenzoxazine resin.

3.3.3 Analytical method for mercury analysis

In order to determine the capacity of metal adsorptions, one ppm Pb (II), Fe (II), Mn (II), Cu (II), Zn (II), Cd (II) and Hg (II) salt solutions were prepared in synthetic sea water (pH=8.2, Table 3.1). Polybenzoxazine resin (100 mg) and metal solutions (1 ppm) were mixed in magnetic stirrer for 3 hours. In order to determine the optimum pH for removing mercury salts, experiments have been performed under different pH

values. The pH of solutions was arranged by using either 1 M HCl or NaOH solutions. The best sorption behavior was found to be at pH=6 and the results reported according to this pH. After filtration process, supernatant was separated to measure metal concentrations. All metal analyses except mercury were done by using ICP-MS (Perkin Elmer-Optima 7300 V). The mercury concentration was determined by using AAS-HVG (Shimadzu-6701).

Table 3.1 : Composition of the prepared artificial sea water and its comparison with natural seawater (Salinity 35‰) [128].

Ion	Artificial Seawater (g/kg)	Natural Seawater (g/kg)
Cl^-	19,353	19,353
Na^+	10,764	10,76
SO_4^{2-}	2,701	2,712
Mg^{2+}	1,297	1,294
Ca^{2+}	0,406	0,413
K^+	0,387	0,387
HCO_3^-	0,142	0,142
Br^-	0,066	0,067
Sr^{2+}	0,014	0,008
H_3BO_3	0,026	0,026
F^-	0,001	0,001

3.3.4 Preparation of microporous organic polymer

A flame dried Schlenk flask fitted with a condenser and a magnetic stirring bar was charged with melamine (0.6 g, 4.75 mmol), 1,5-dihydroxy anthraquinone (1.711 g, 7.12 mmol) and dimethyl sulfoxide (15.5 ml). After degassing by nitrogen bubbling the mixture was heated to 180 °C for 72 h under an inert atmosphere. After cooling to room temperature the precipitated porous network was isolated by filtration over a Buchner funnel and washed with excess acetone, tetrahydrofuran and chloroform. The solvent was removed under vacuum at room temperature to afford the materials as off-black powders in 53 % yield.

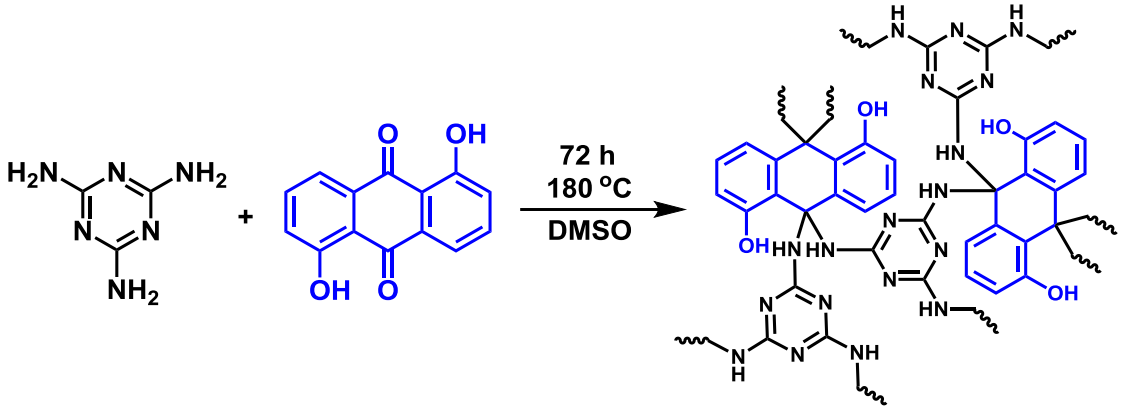

Figure 3.4 : Synthesis of microporous packing material.

3.3.5 Analytical method for analysis

Synthesized column packing material (1 g) is filled in a steel pipe (length: 150 cm x diameter: 4.6mm). Frits are put to the ends of the column so as not to let the packing material pass through. Ends of the column are closed by screws. Helium gas is passed through the column under pressure (10 bar) for 1 hour to compress the filling material. Spaces that occur are refilled by using packing material. This procedure is repeated until all of column is filled. Later solvent mixture (methanol: acetonitrile, 50:50 v/v) is passed through the column for 12 hours. This operation is also continued under both 200 bar pressure and 2 ml/min flow rate. If there is a space in the column, packing material is re-added and solvent mixture is repassed through the column. In this part, this procedure has been applied seven times.

3.3.6 Operating conditions

In HPLC measurements, firstly 100% acetonitrile, methanol or water has been used as the mobile phase for [1]PAH, pesticides and flavonoid determinations (Table 1). Secondly, acetonitrile:methanol solutions in different proportions as the mobile phase. After all the experiments, acetonitrile 100% and A: methanol 85% B: water %15 for [2]PAHs; A: methanol 90% B: acetonitrile 10% for flavonoids have been obtained as the mobile phase whilst 100% methanol has been seen as the only phase for pesticides. PAHs, organo-chlorine pesticide compounds, phenolic acids and flavonoids were prepared with hexane at 10 ppm concentration from the stock solutions which are given below:

Table 3.2 : Conditions on packing material in different chromatographic modes.

Compound	Mobile Phase		Flow rate (ml/min)	Wavelength (nm)
[1]PAHs	100% ACN	-	1	250-450
[2]PAHs	85% Methanol	15% Water	0.8	200-450
Pesticides	100% Methanol	-	2	190-360
Phenolic acids	85% ACN	15% Phosphoric acid*	0.8	200-450
Flavonoids	85% ACN	15% Phosphoric acid	0.8	200-450

ACN: Acetonitrile *0.01% Phosphoric acid solution

3.3.7 Synthesis of 1,5-bis(prop-2-yn-1-yloxy)anthracene-9,10-dione

A mixture of 1,5-dihydroxy anthraquinone (14 g, 49 mmol), propargyl bromide(80% w/w in toluene, 7.28 g, 49 mmol), and potassium carbonate (K_2CO_3, 20.3 g, 147 mmol) in acetone (200 mL) was refluxed for 12 h. Two portions of propargyl bromide were added after 12 h and 24 h respectively and the reaction mixture was continually refluxed for additional 12 h. After the reaction mixture was cooled to room temperature, water (200 mL) was added. It was then extracted with DCM in three times. The combined organic phase was washed with brine, dried over Na_2SO_4, filtered and concentrated (Figure 3.5). Purification by flash column chromatography gave as a yellow solid. ^{1}H NMR (500 MHz, $CDCl_3$) δ 2.49 (t, J = 2.4Hz, 2H), 4.71(d, J1 = 2.4Hz, J2 = 2Hz, 2H), 4.78 (d, J1 = 2.4Hz, J2 = 2Hz, 2H), 5.42 (s, 1H), 6.37 (s, 1H), 6.73(dd, J1 = 0.9Hz, J2 = 8.1Hz, 2H), 6.91-7.00 (m, 4H), 7.08 (d, J = 7.2Hz, 2H), 7.35-7.38 (m, 1H), 7.44-7.47 (m, 1H); Melting point: 214-216 ^{o}C.

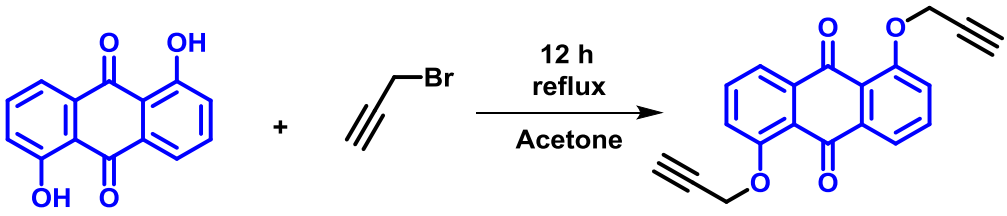

Figure 3.5 : Schematic representation of synthesis of 1,5-dihydroxy-9,10-dione dipropargyl ether.

3.3.8 Synthesis of 2-azidomethyl pyrene (Py-N_3)

1-pyrenemethanol (0.8 g, 3.65 mmol) was dissolved in 10 mL chloroform under nitrogen atmosphere and cooled down in an ice bath (0 °C) and pyridine (0.6 mL, 7.3 mmol) was added. Then, toluene-4-sulfonyl chloride (1.1 g, 5.48 mmol) dissolved in

10 mL of chloroform was slowly added to the reaction flask at cold. The reaction mixture was stirred overnight at room temperature. The solvent was removed under vacuum and the obtained viscous liquid tosylate was used in azidation reaction without any purification. Sodium azide (0.2 g, 3.1 mmol) was added to solution of the obtained tosylate (0.4 g, 1.04 mmol) in DMF and the reaction mixture was stirred for 2 days at 65 ºC. After extraction of the crude product with CH_2Cl_2/water, the organic layer was dried with anhydrous $MgSO_4$ and solvent was evaporated by rotary evaporator. The oily product was precipitated in cold water and centrifuged. The yellow product was dried under vacuum (Figure 3.6). ^{1}H NMR ($CDCl_3$, 500 MHz) δ (ppm): 7.80-7.15 (m, 9H, aromatic), 2.20–1.97 (d, 2H, CH_2).

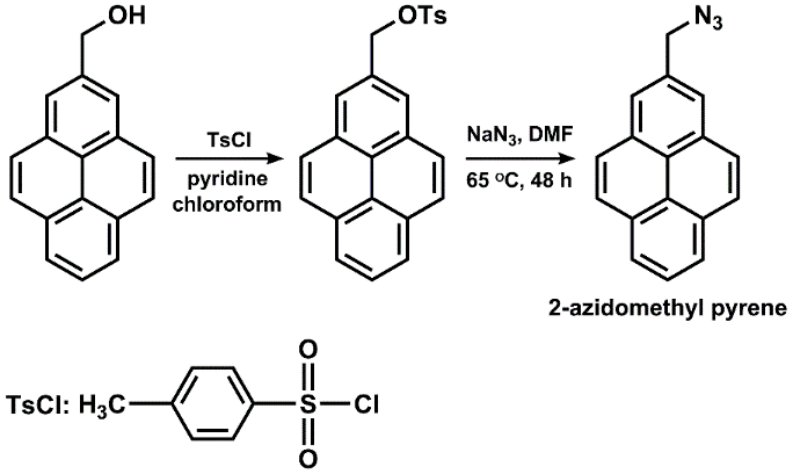

Figure 3.6 : Azidation of 1-pyrenemethanol.

3.3.9 Synthesis of propargyl functionalized MOP (c-MOP)

A flame dried Schlenk flask fitted with a condenser and a magnetic stirring bar was charged with melamine (313 mg, 2.485 mmol), 1,5-dihydroxy-9,10-dione dipropargyl ether (500 mg, 3.728 mmol) and dimethyl sulfoxide (15.5 ml). After degassing by argon bubbling the mixture was heated to 180 °C for 72 h under an inert atomosphere. After cooling to room temperature the precipitated the clickable porous network was isolated by filtration over a Büchner funnel and washed with excess acetone, tetrahydrofurane and dichloromethane. The solvent was removed under vacuum at room temperature to afford the materials as off-black powders in 55 % yield (Figure 3.7).

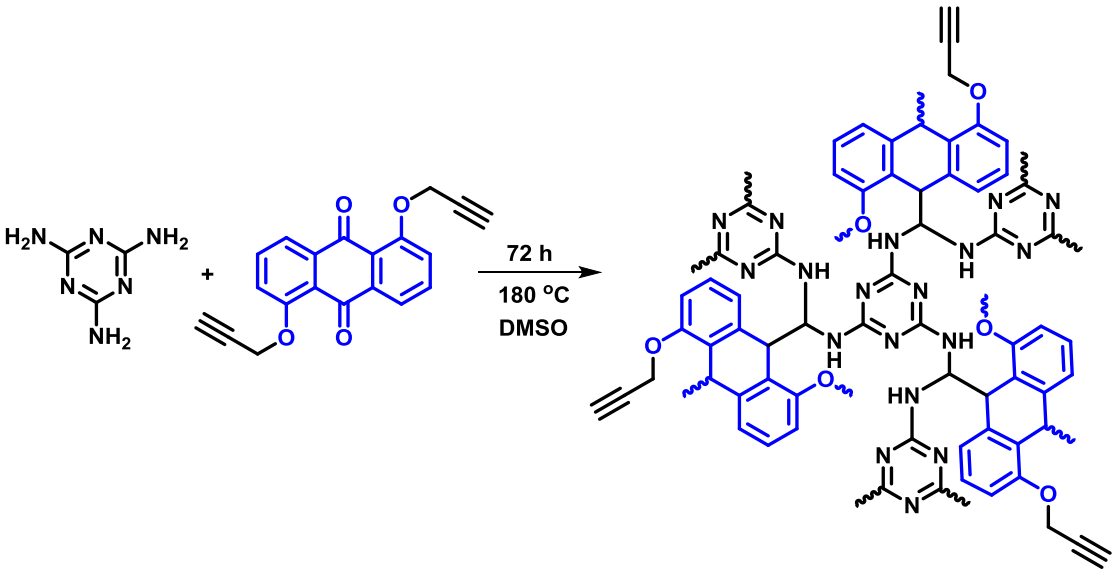

Figure 3.7 : The preparing of clickable microporous organic polymer (c-MOP).

3.3.10 Post-functionalization of propargyl-MOP by click reaction

c-MOP (0.3 mmol), CuBr (0.2 mmol), PMDETA (0.2 mmol), 2-azidomethyl pyrene (0.1 mmol) and 5 mL of DMSO were placed in a Schlenk tube. The reaction mixture was degassed by three freeze-pump-thaw cycles and stirred at 40 ºC during one day. Modification of c-MOP via Huisgen type click reaction was showed in Figure 3.8. This material was washed with deionised water, ammonia solution to remove unreacted reagents. This material was washed with deionised water, ammonia solution to remove unreacted reagents.

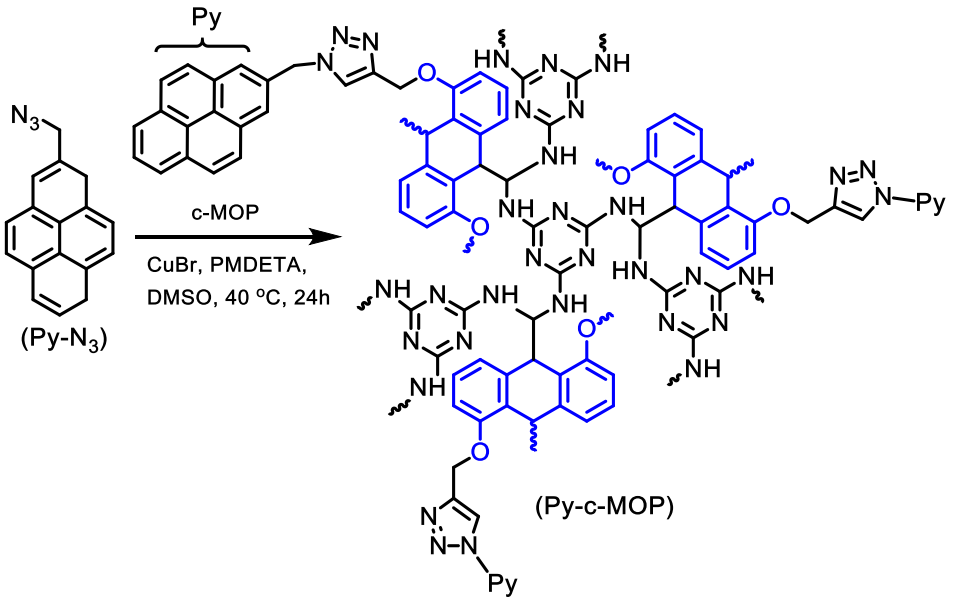

Figure 3.8 : Modification of c-MOP via Huisgen type click reaction.

4. RESULTS AND DISCUSSIONS

4.1 Polybenzoxazine Based Microporous Material

The binding capability of Hg(II) to N and O atoms can give rise to design of many alternative materials for removal of mercury salts. From this point of view, an important high performance material, polybenzoxazines, which contains both nitrogen (amino) and O (phenolic) becomes a cost-effective alternative for mercury removal objective. For this purpose, initially, monomer 6,6'-(propane-2,2-diyl)bis(3-allyl-3,4-dihydro-2H-benzo[e] [1,3]oxazine) (B-ala) was synthesized by typical benzoxazine synthesis method using bisphenol A, allyamine and paraformaldehyde. The structure of the B-ala monomer was confirmed by spectral analysis.

Actually, the specific surface area of such polybenzoxazines is generally lower than 1 $m^2.g^{-1}$. Such stiff polybenzoxazine with low porosity is not suitable for the ultimate use as sorbents since much higher interacting surface area is required for the intended sorption applications. Hence, B-ala was cured in DMSO to generate porosity on polybenzoxazine resin. The curing was performed at 180°C for 3 days. Thereafter, the resin was washed with several organic solvents and swelled in 1,4-dioxane before freeze-drying. Upon freeze-drying, an open, sponge-like network structure, probably originating from the solvent (DMSO) induced phase-separation, is obtained (Figure 4.1 and 4.2). Such a sponge-like morphology is advantageous for applications demanding high mass transport, like adsorbent resins, catalysis etc.

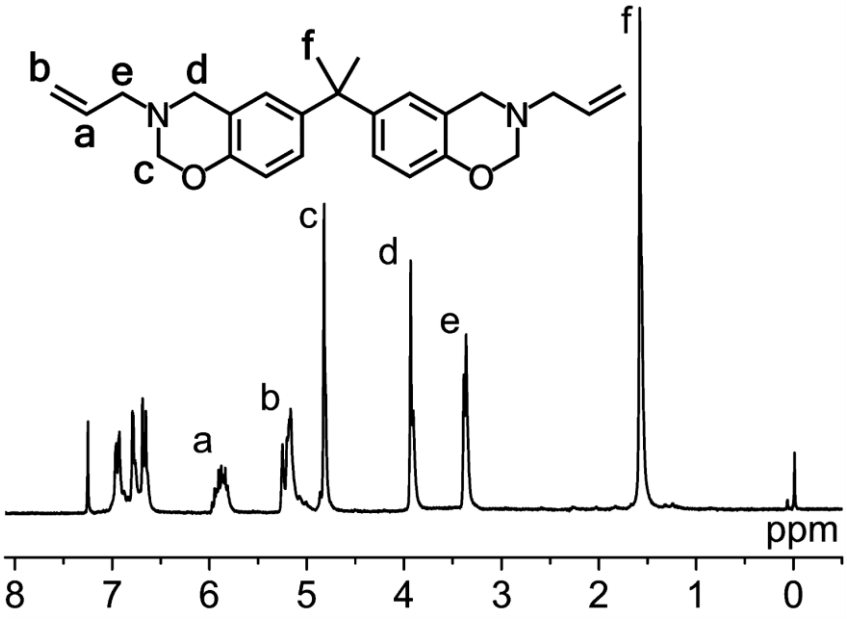

Figure 4.1 ^{1}H NMR spectrum of B-ala monomer.

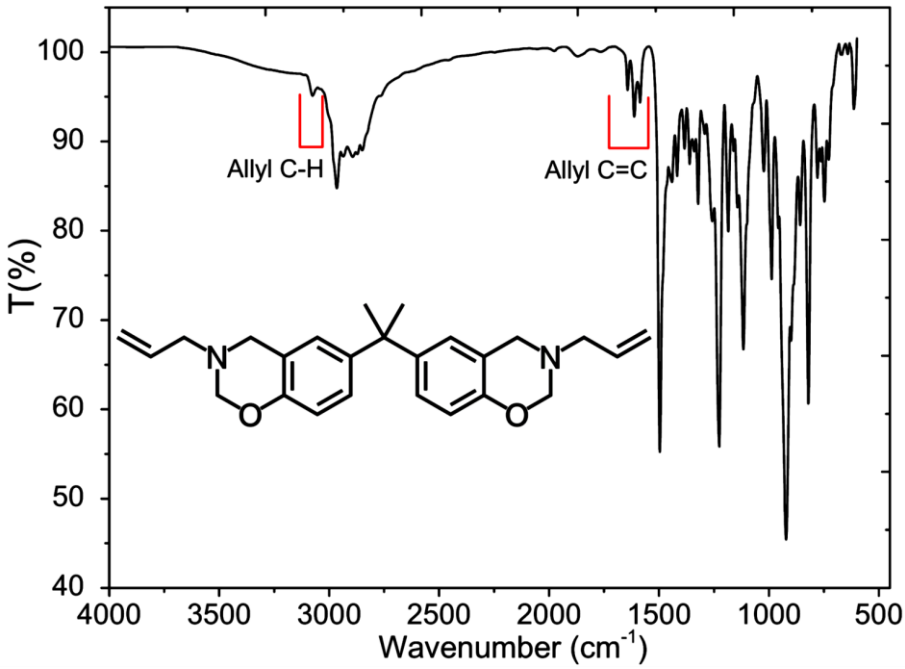

Figure 4.2 FT-IR Spectrum of B-ala monomer.

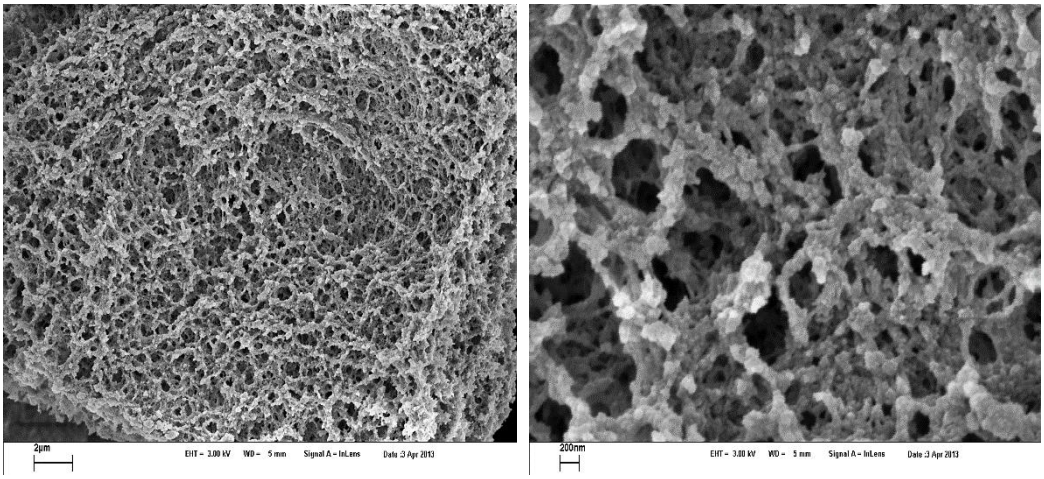

Figure 4.3 : SEM images of B-ala based polybenzoxazine sorbent.

The completion of curing was controlled by DSC analysis. It is well known that 1,3-benzoxazines can be cured by thermally-activated ring-opening polymerization and this can be monitored using DSC since the ring-opening reaction is an exothermic process. The curing maximum of such process varies from 160 to 250 °C, depending on the functionalities present on the benzoxazines. Figure 4.4 reveals that the curing exotherm of B-ala, is between 175-315 °C and the amount of exotherm is calculated to be 355 $j.g^{-1}$. Under the same DSC conditions, the porous polybenzoxazine resin did not exhibit any exotherm indicating complete consumption of benzoxazine rings during thermal treatment.

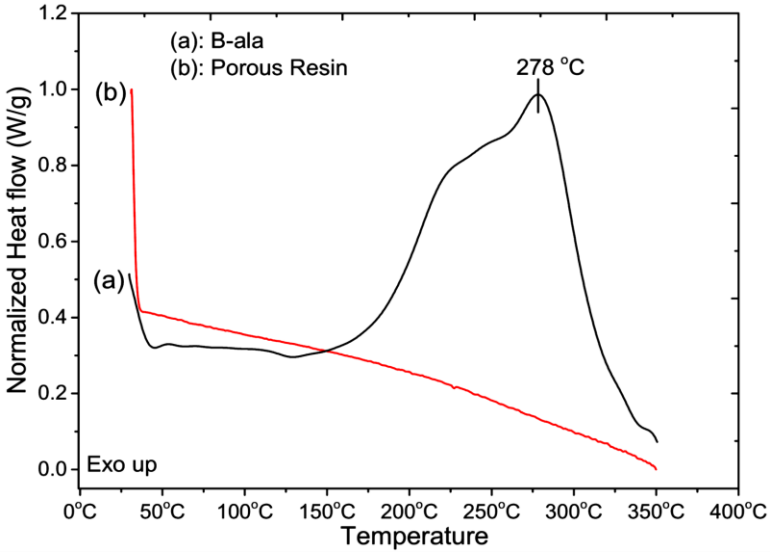

Figure 4.4 : DSC profiles of B-ala (a) and polybenzoxazine resin (b).

The porosity of the materials was analysed by means of N_2 adsorption/desorption at 77.3 K. A representative porosity data derived from the measurements of gas adsorption/desorption isotherm is depicted in Figure 4.5.

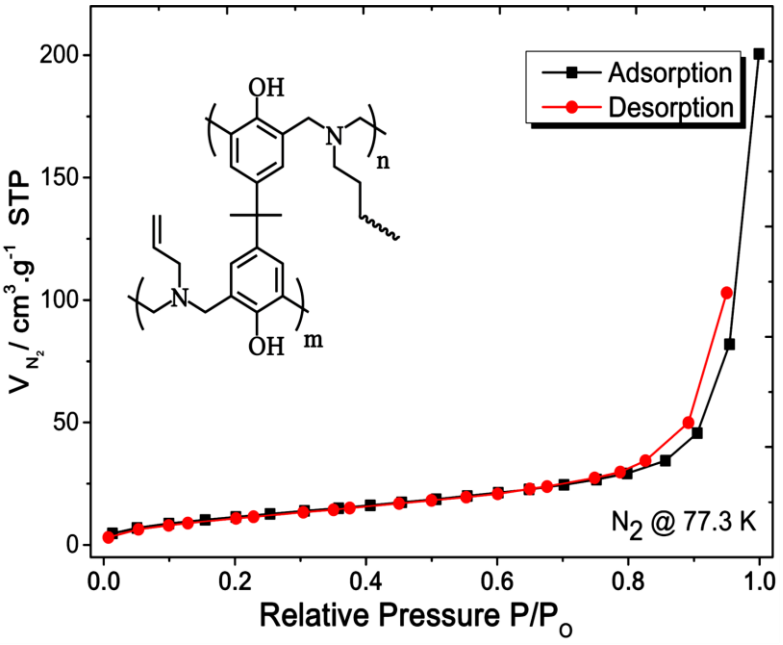

Figure 4.5 : N_2 adsorption/desorption isotherms of polybenzoxazine resin obtained at 77.3K.

The analysis of the polybenzoxazine resin indicated macroporosity with a BET surface ≈45 $m^2.g^{-1}$. The freeze-dried material exhibits a large and much steeper increase in volume at high relative pressures, which is a typical feature for macroporous/nanoparticulate systems. These findings are in complete agreement with the above given nitrogen porosimetry measurements and SEM analysis. In general, the applied drying method mainly influences the macrostructure, i.e. the stability of the interstitial voids between the polymer particles. Since evaporative drying approach leads to some compacting, this may result in the collapse of pores.

Mercury (II) sorption capacity of the polybenzoxazine resin was determined by the atomic absorption spectrometry (AAS-HGV). The samples were prepared in synthetic sea water, and Mercury (II) ion concentration was 1 ppm in all measurements. A hundred milligrams of the polybenzoxazine resin was added to these sample solutions and stirred for three hours. After filtration of the sorbent, the concentration of the remaining mercury (II) was measured. According to residue analysis, sorption of mercury (II) ion was measured as 98% of the dissolved salt. There are several factors must be considered when evaluating sorption capacity. In practice, there are numerous types of impurities present in sea water at different concentration levels. These impurities compete with each other in the sorption process. Hence, apart from mercury (II), various metal salts, namely Pb(II), Fe(II),

Mn(II), Cu(II), Zn(II), Cd(II), were also prepared at the same conditions. Collective determination of the concentrations of these metal ions was performed using an Ion Coupled Plasma Mass Spectroscopy (ICP–MS) and relatively low sorption amounts were detected for these metal ions. The percentage sorption values of the corresponding metal salts, depicted as bar graphs in Figure 4.6, reveals that the polybenzoxazine resin has specific sorption behaviour against mercury (II) salt.

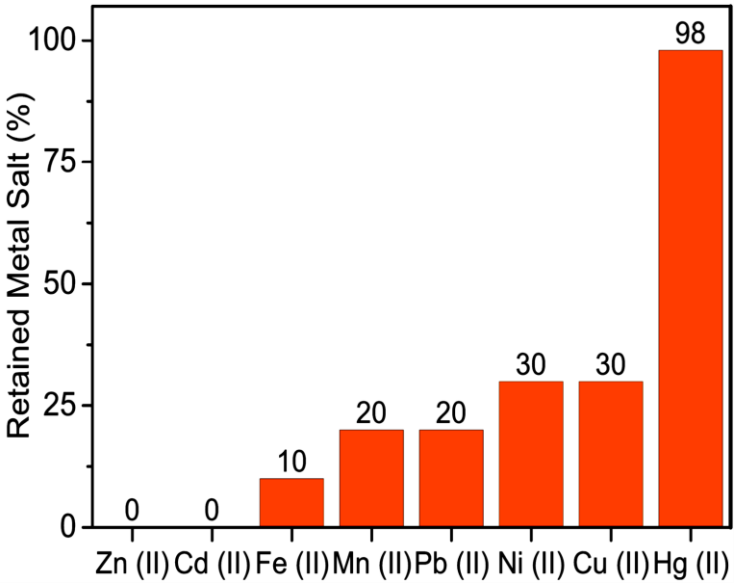

Figure 4.6 : Sorption behaviour of polybenzoxazine resin against several metal ions, based on retained metal salt.

In a sorption process, an economical optimum depends on the sorption behaviours of the sorbent like sorption capacity and specificity. Thus, polybenzoxazine resin's ability to remove Hg(II) salts from salty water is also evaluated using load tests. Figure 4.7 reveals that up to 80 mg of $Hg(NO_3)_2$ can easily be loaded to a fixed amount of polybenzoxazine resin (20 mg) without losing the sorption power and the maximum load capacity of polybenzoxazine is more than 4 mg $Hg(NO_3)_2$ per 1 mg sorbent. Moreover, identical tests were also conducted with different metals salts. Metal salt load tests showed that after 40 mg of loading, the sorption power of polybenzoxazine resin decreases for Cu(II), Ni(II), Pb(II), Mn(II) salts and after loading 60 mg of salt, a steep descent takes place. These data clearly confirm that in addition to specific binding (affinity) of Hg (II) to polybenzoxazine resin, a high load capacity against mercury (II) is present.

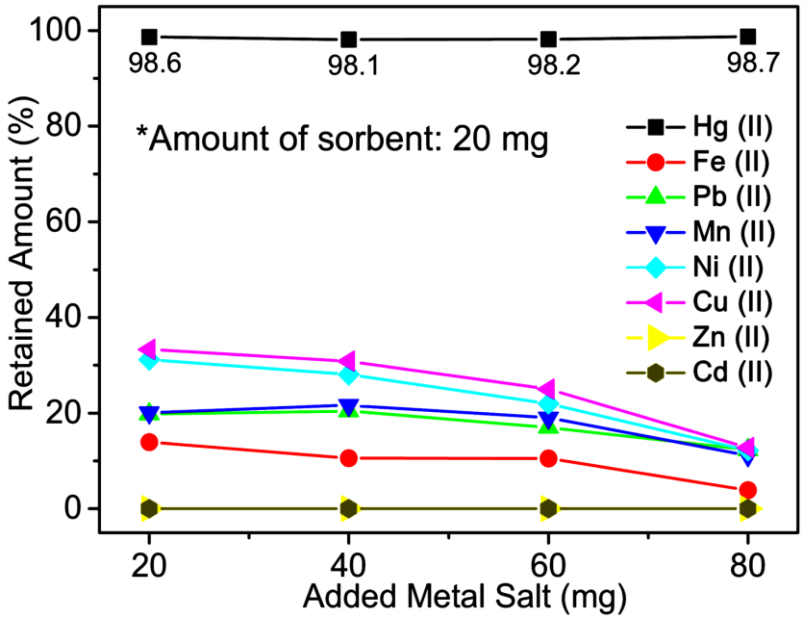

Figure 4.7 : Load capacity trends of polybenzoxazine resin for various metal salts.

A number of studies deal with the coordination abilities of the substituted thio ligands towards various transition metals especially mercury salts. Apart from thio-mercury interactions, the binding capability of Hg(II) to N and O atoms facilitates a cheaper design of many alternative materials for removal of mercury salts. The structure of the polybenzoxazine resin contains free phenolic –OH and an adjacent tertiary amine group, both of which contribute to generate a coordination system with Hg (II) ion (Figure 4.7). It can, thus, be expected from the structure that the sorption mechanism is mainly chemisorption. However, it is also likely that to some extend adsorption contributes to the overall sorption process.

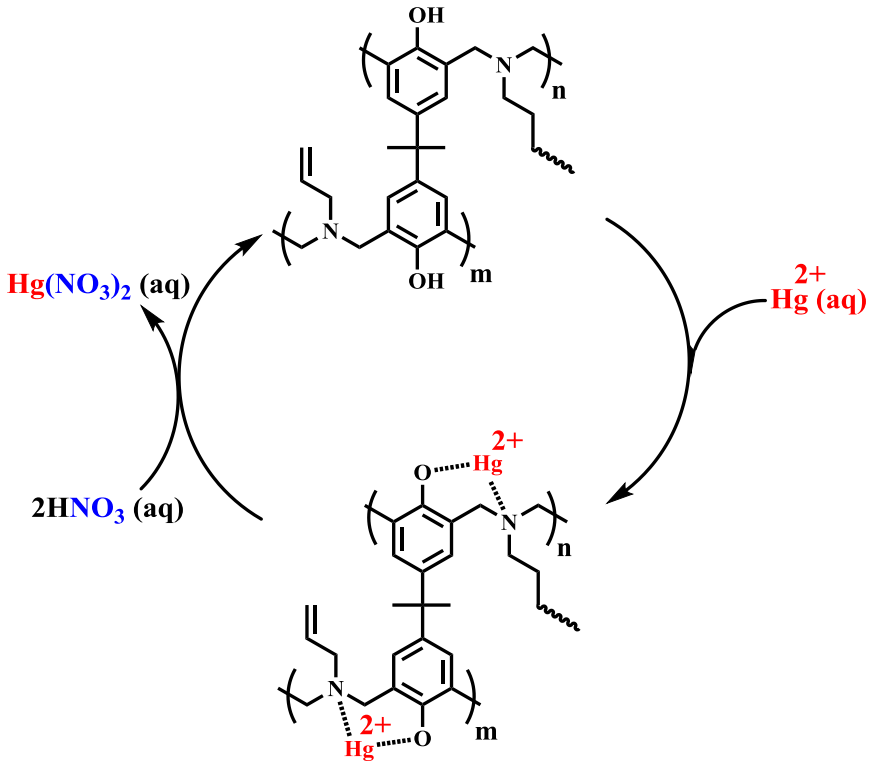

Figure 4.8 : Chemisorption–adsorption and desorption cycle of mercury (II) salt on polybenzoxazine resin.

As presented in Figure 4.8, bonded Hg(II) can be removed from polybenzoxazines using acids and the resin can easily be regenerated for further uses. In order to demonstrate the recycling ability of the polybenzoxazine sorbent, sorption-desorption experiments were conducted. Desorption experiments were intentionally carried out with 2N HNO_3 aqueous solution, so as to apply harsh acidic conditions for most organic compounds.

In polybenzoxazines, two types of hydrogen bonding can be considered; (i) intermolecular hydrogen bonding between two phenolic hydroxyl groups of polybenzoxazine and (ii) intramolecular hydrogen bonding between phenolic hydroxyl groups and nitrogen atoms on the Mannich Bridge. These hydrogen bonding attractions can easily be detected in IR spectrum of polybenzoxazines as broadening of phenolic O-H stretching vibration band. Binding of Hg (II) ion to phenolic –OH and tertiary amine would decrease the number of hydrogen bonding in polybenzoxazine resin and results in a shift of –OH band towards high energy region in IR. Likewise, this shift is clearly detectable in Figure 4.9, evidencing the chemisorption mechanism.

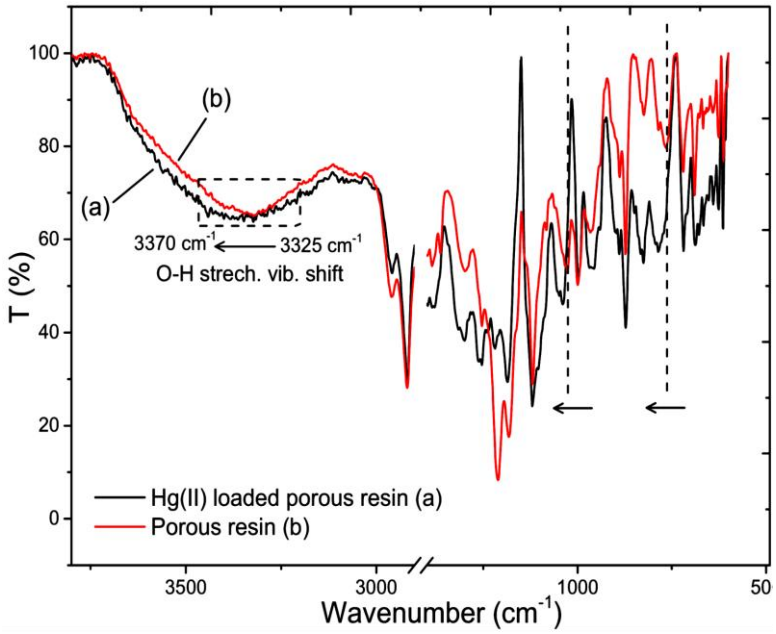

Figure 4.9 : IR spectra of Hg(II) loaded polybenzoxazine resin (a) and pristine polybenzoxazine resin (b).

The presented results demonstrate that polybenzoxazine sorbent can be regenerated and reused for the sorption of mercury salts effectively for at least eight uses. In order to increase the number of reuse, an additional step like washing the resin with NaOH solution to neutralize the protonated amines should be included to the process. However, in our studies we restricted the process to only two steps, namely sorption and desorption. In this connection, it should be pointed out that many other sorbents typically require additional treatment steps and generate large amounts of secondary waste, which is a major challenge in waste management. High recycling ability of polybenzoxazine resin also minimizes the amount of secondary wastes after extraction. Moreover, polybenzoxazine resins are cost effective materials. The starting materials used for the synthesis of this resin are commercially available and relatively cheap. Additionally, the recycling power of this resin increases by its cost effectiveness. Hence, this sorbent can find applications in a variety of environmental fields.

Figure 4.10 shows that the sorption capacity almost remained the same within the first five usages, and up to 7th cycle there is no significant reduction decent in the sorption power. After this point, most probably some decomposition and protonation of amino groups take place in the polybenzoxazine structure arising from the harsh acidic conditions causing pore collapses and structural differences. Additionally,

some nitration reactions favoured by the ring activating effect of phenolic –OH groups are likely to occur.

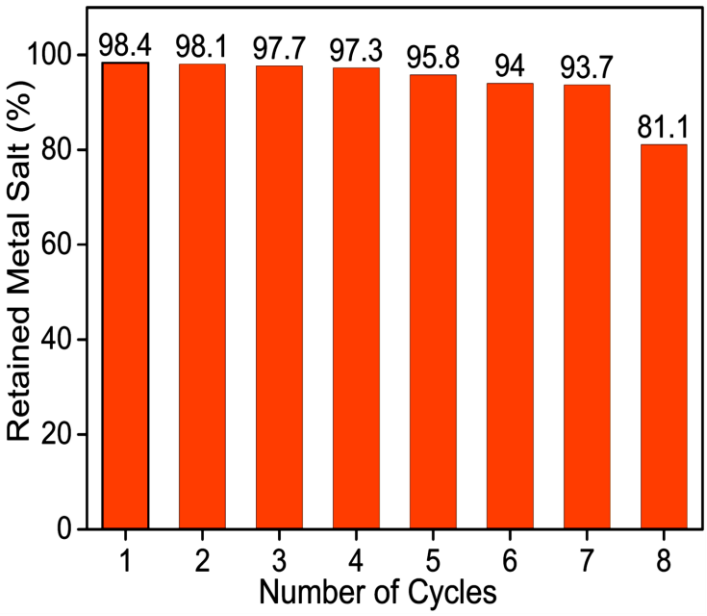

Figure 4.10 : Sorption values of polybenzoxazines after reuse experiments.

4.2 Schiff Base Chemistry Based Microporous Materials

In view of Schiff base chemistry, catalyst-free one-pot synthesis of nitrogen-rich polymer networks with high surface areas can be achievable. For this purpose melamine was selected as nitrogen source and anthraquinone and its propargylated version were prepared as carbonyl monomer.

The porous packing material was obtained using melamine and 1,5-dihydroxy anthraquinone in dimethyl sulfoxide. The mixture was heated to 180 °C for 72 h under an inert atmosphere was washed with selected solvents until it reached the desired purity. At least one of the solvents such as dimethylsulfoxide, tetrahydrofuran and dichloromethane, chloroform, diethylether, acetone, methanol, ethylacetate, toluene was preferred as washing solvent. Finally, the washed material was freeze-dried in order to remove the impurities and to make it ready to be added to the column, and thus pure column filling material in high porosity was obtained. Figure 4.11 illustrates size and 3D shape of smallest possible cavities in network. The resulting rigid and black porous polymer network displays high surface area (215 m^2/g) and similar solvent uptake in both polar and non-polar media, which

explains good compatibility of the material with all mobile phases, from acetonitrile to methanol and water.

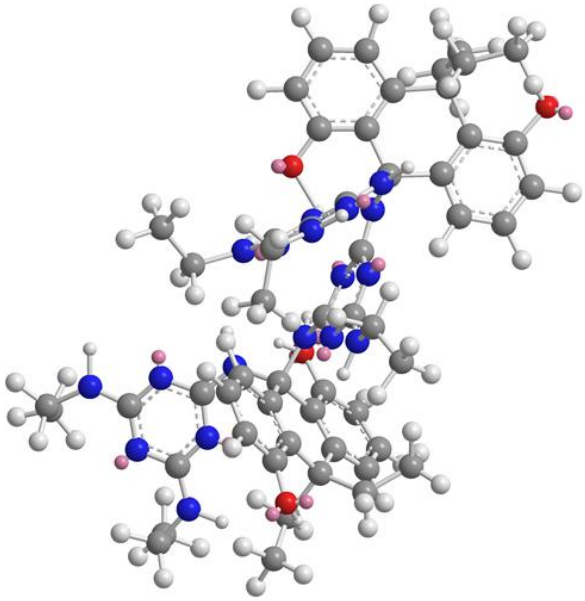

Figure 4.11 : 3D Structure of porous packing material.

Scanning electron microscopy (SEM) photos belong to porous packing material is given below in different scale bar from 1 µm to 3 µm (Figure 4.12).

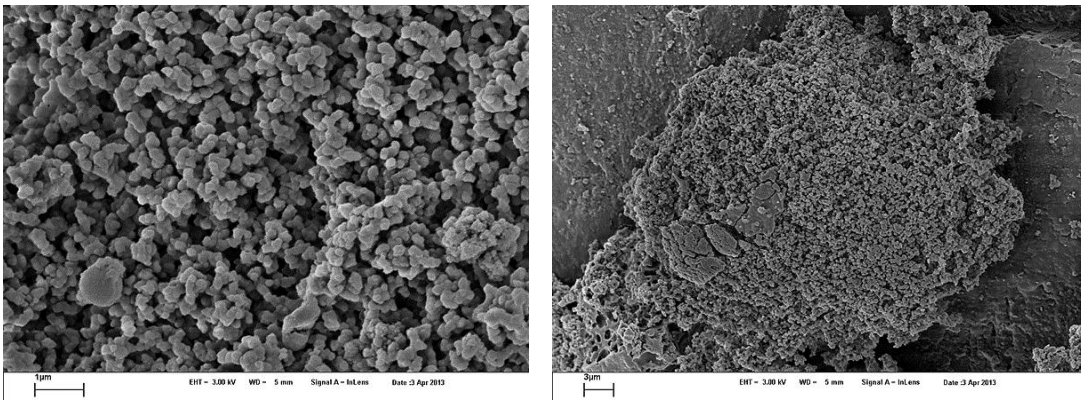

Figure 4.12 : SEM photos of porous packing material.

Fourier transform infrared (FTIR) spectra of material was given in Figure 4.13. Bands which can be attributed to the primary amine group of melamine lie at 3470 and 3420 cm^{-1} (NH_2 stretching) and 1650 cm^{-1} (NH_2 deformation). The hydroxyl and carbonyl function of the anthraquinone are observed in the spectrum at 3300-3500 and 1690 cm^{-1} (C=O stretching).

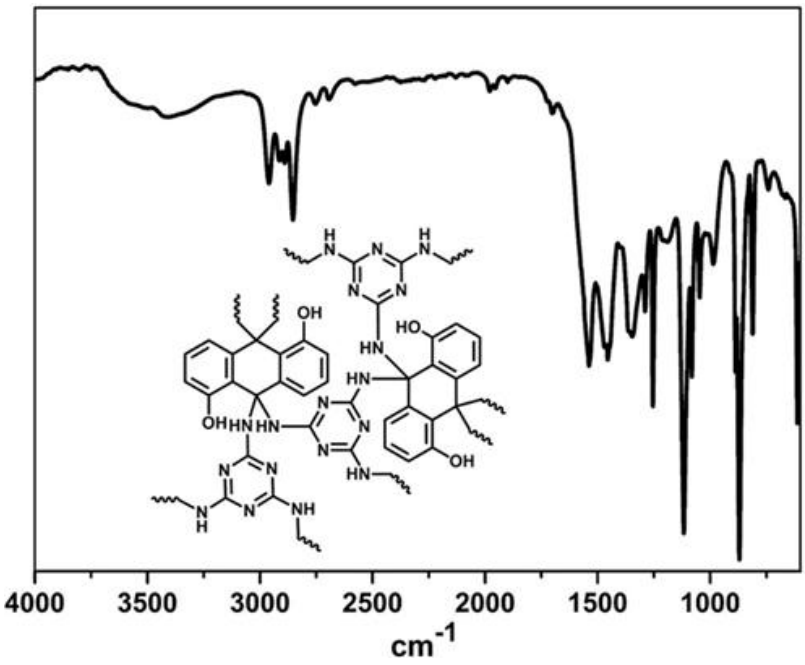

Figure 4.13 : Fourier transform infrared (FTIR) spectra of porous packing material.

The porous properties of the column packing material was analyzed by nitrogen sorption analysis. As seen in Figure 4.14, the adsorption isotherms show a gas uptake at low relative pressures and a regular path in the intermediate section, thus reflecting the microporous nature of the polymer networks. This indicates a high degree of crosslinking of small structural motifs. Remarkably, the Brunauer-Emmet-Teller (BET) surface area 215 m^2/g.

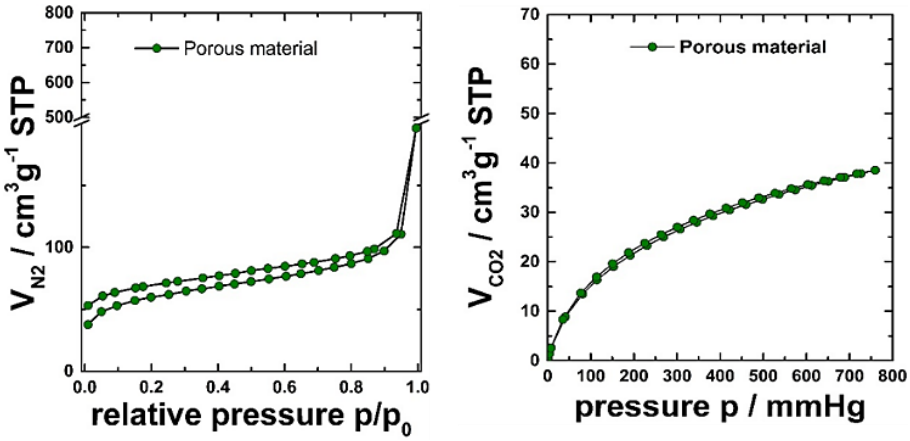

Figure 4.14 : Gas adsorption/desorption isotherms under nitrogen and CO_2.

Chromatograms of PAHs, pesticides, food standards (flavonoids and phenolic acids) are given in Figures 4.15a,b-4.18. For separation of PAH molecule experiments, the standard PAHs mixture which was prepared included each of the following compounds; naphthalene, acenaphthylene, acenaphthene, flourene, phenanthrene,

anthracene, pyrene, fluoranthene and benzo(a)anthracene and was injected into the HPLC. At the end of the measurements, naphthalene, acenaphthylene, acenaphthene, flourene, phenanthrene and anthracene could be determinated. On the contrary, pyrene, fluoranthene and benzo(a)anthracene could not be separated (Figure 4.15a and b). It was clear that the low moleculer weight PAHs (two rings) were separated more successfully. Additionally, acenaphthylene and acenaphthene were also separated from each other more successfully using the second mobile phase (A: methanol %85 and B: water %15). Similarly, phenanthrene was determined well in this phase (Figure 4.15b). The results indicated that the separation can be improved using different mobile phase proportions.

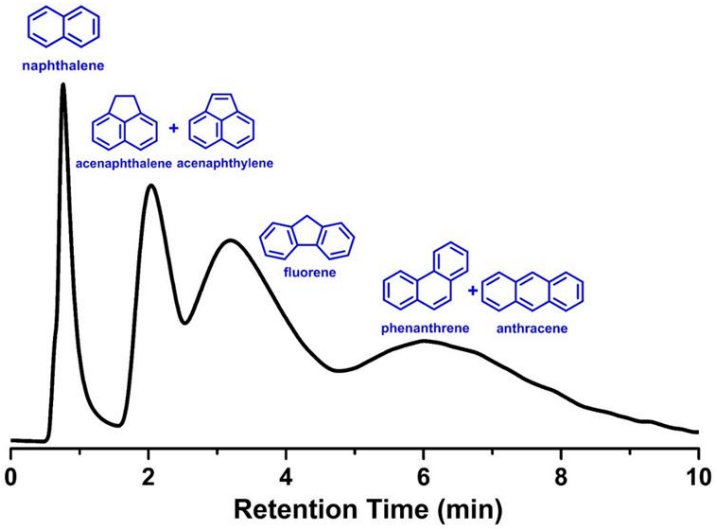

Figure 4.15a : The analysis of [1]PAH standards mixture chromatogram by using acetonitrile as mobile phase.

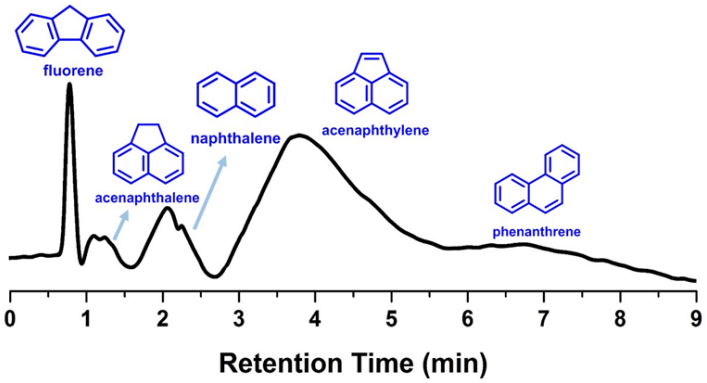

Figure 4.15b : The analysis of [2]PAH standards by using methanol and water as mobile phase.

For separation of pesticide molecules experiments, the standard pesticide mixture which was prepared included each of the following compounds; beta-

hexachlorocyclohexane (HCH), alpha-hexachlorocyclohexane (HCH), 4,4'-dichlorodiphenyldichloroethane (DDD), 4,4'-dichlorodiphenyldichloroethylene (DDE) and dieldirin and was injected into the HPLC. Only the 4,4'-dichlorodiphenyldichloroethane (DDD) and 4,4'-dichlorodiphenyldichloroethylene (DDE) were detected (Figure 4.16).

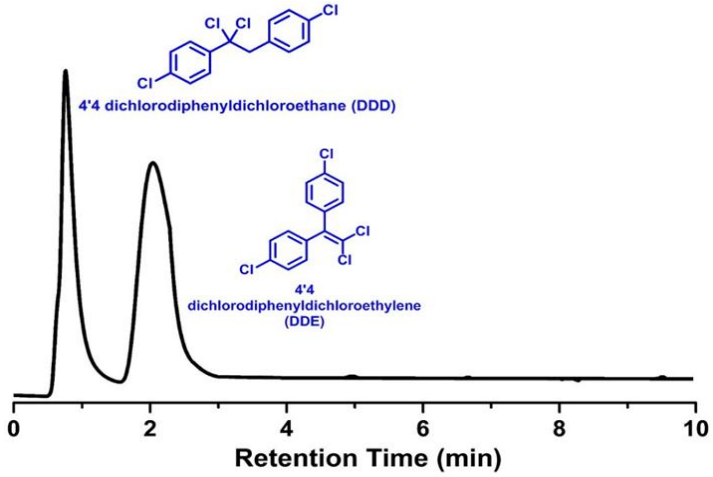

Figure 4.16 : The analysis of pesticide standards.

For the separation of food standards (flovanoid), the (flovanoid) mixture prepared including each of the cadechin hydrate, rutin hydrate, quercetin compounds was injected to HPLC. Figure 4.17 clearly confirms successful separation of the compounds.

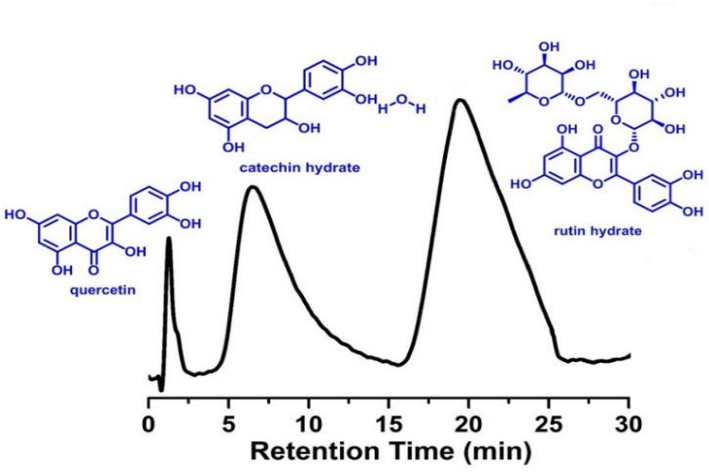

Figure 4.17 : The analysis of flavonoid group standards.

For the separation of an another food standard (phenolic acids) experiment, the prepared phenolic acid mixture included each of the following compounds; phenilic acid, p-coumaric acid, caffeic acid and gallic acid and was injected into the HPLC.

The phenilic acid, caffeic acid and gallic acid were successfully detected, while p-coumaric acid was not perceieved (Figure 4.18).

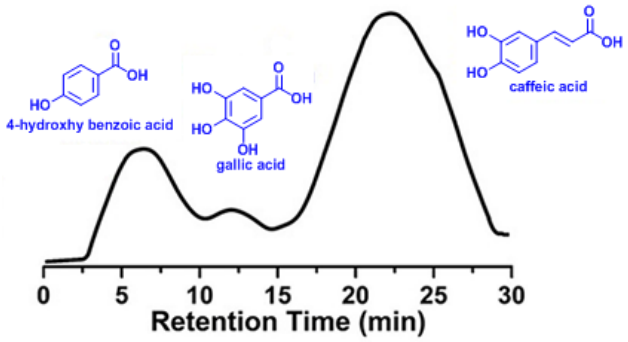

Figure 4.18 : The analysis of phenolic acid group standards.

The synthesized column packing material is not the only adsorption material that exhibits pi-electron donating-accepting properties. The selectivity factor, α for the naphtalene and anthracene, was determined under appropriate random conditions. From data presented in Table 4.1, the corresponding value for the column packing material exhibiting strong pi-interaction activity is very large, since anthracene is retained nearly irreversibly under these conditions. Compared to the other materials, selectivity factor and column efficiency that relates to plates number give promising results.

Table 4.1 : Column properties of various materials for naphthalene and anthracene samples.

Column	Column Size	Capacity factor (k)	Selectivity factor (α)	Plates
Nucleodur C_{18}	250mm*4.6mm*5µm	1.54	1.23	68312
J.T. Baker C_8	250mm*4.6mm*5µm	1.75	1.42	88974
Agilent Hypersil C_8	100mm*4mm*3µm	1.51	1.29	12871
Packing Material	150mm*4.6mm*5µm	1.33	3.25	19044

The function of pi-interactions in liquid chromatography on packing materials can be explained in four parts: a permanent dipole, a hydrogen-donating group, an aliphatic chain and a pi-electron system (Figure 4.19). The retention is mainly controlled by the adsorbent-adsorbate interactions that are due to hydrogen bonding, permanent dipole-dipole and permanent dipole-induced dipole interactions. In our case, the new

column packing material may take place planar stacking of the analyte pi-systems and the adsorbent pi-electron donating-accepting fragments play the important role.

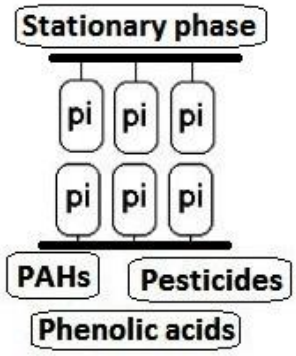

Figure 4.19 : Representative scheme of principal solute/sorbent interaction mechanism.

The other significant factor to mention is the chemical or physical nature of the pi-pi-interactions. In the present system, pi-interactions can be considered as a type of dispersive interaction between conjugated pi-electron systems of packing material and aromatic compounds. The retention of the end group was observed to increase with a rise of pi-electron density gradients in molecules, namely the local dipoles.

Another objective was to obtain the corresponding propargyl containing antraquinone and react with melamine to form clickable MOP. The obtained MOP was successfully modified with azido perylene resulting in fluoresans property with high surface area. The porosity of the materials was analyzed by means of N_2 and CO_2 adsorption/desorption at 77.3 K. A representative porosity data derived from the measurements of gas adsorption/desorption isotherm is depicted in Figure 4.20.

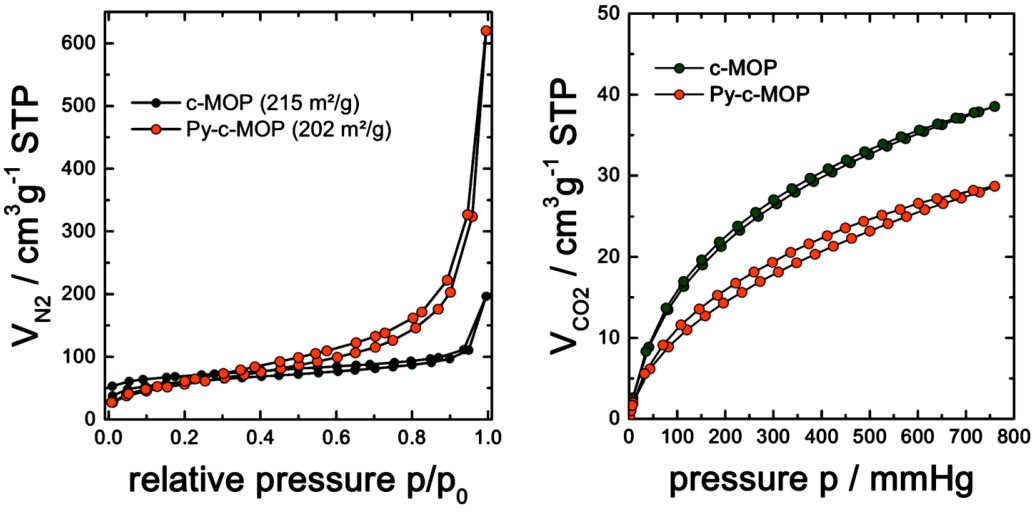

Figure 4.20 : N_2 adsorption/desorption isotherms obtained at 77.3 K; CO_2 adsorption/desorption isotherms obtained at 273 K.

The analysis of the clickable porous material indicated microporosity with a BET surface ≈215 $m^2.g^{-1}$. After click reaction, the BET surface decreased to ≈202 $m^2.g^{-1}$. The freeze-dried material exhibits a large and much steeper increase in volume at high relative pressures, which is a typical feature for microporous/nanoparticulate systems. These findings are in complete agreement the network-featured microporosity, as evidenced with the above given nitrogen porosimetry measurements and SEM analysis pictures (Figure 4.21). In the present work, the freeze-drying technique was chosen as the drying method since it generally influences the microstructure, i.e. the stability of the interstitial voids between the polymer particles. The corresponding evaporative drying approaches lead to some compacting resulting in the collapse of the pores.

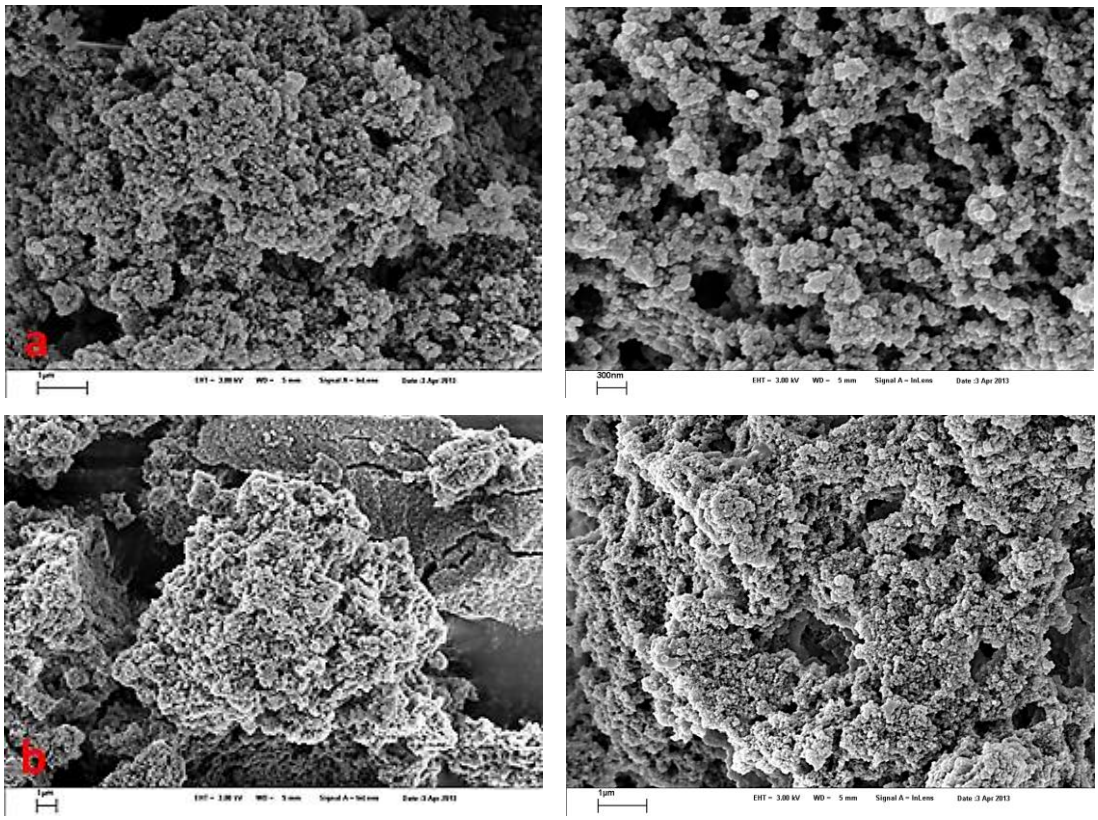

Figure 4.21 : SEM photos of to **a)** porous alkyne, **b)** porous click product.

Upon modification of c-MOP, C=C stretching vibrations of pyrene at 1535-1660 cm^{-1} is detectable and $-N_3$ stretching vibration at 2129 cm^{-1} of Py-N_3 completely disappeared showing that Py-c-MOP does not contain any trapped unreacted Py-N_3 residue in the pores (Figure 4.22c). Expectedly a slight decrease in the BET surface areas was observed. The determined specific surface area was dropped down from 215 to 202 $m^2.g^{-1}$ after the modification. Besides, the isotherms cross each other, with the modified material having a steeper increase at high relative pressures corresponding to a larger fraction of wider pores (Figure 4.22). Figure 4.23 shows solid-state C-NMR spectra of the c-MOP. This effect might be attributed to a change in pore morphology/size, caused by the introduction of pyrene, and change with the geometry of the some pores upon modification from triple bonds towards triazoles. The impact of modification on the networks' geometry on the observable porosity was recently demonstrated. Under the used modification condition pore-filling for the material was not observed and only slight decrease for BET area was observed hence diffusion in the larger micropores is presumably faster the accession restrictions to many micropores may limit the filling of the pores. Additionally, steric

reasons, i.e. taking the size of the molecule (pyrene) to enter the pores into account would also result in a slight modification. (Figure 4.22).

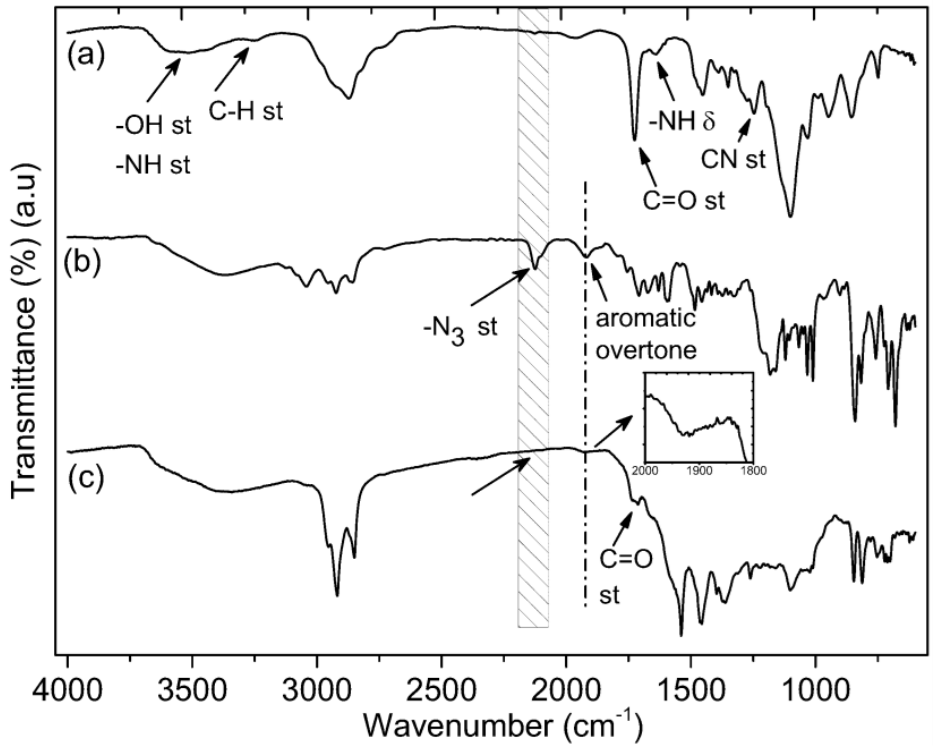

Figure 4.22 : FT-IR spectra of the c-MOP (a), 2-azidomethyl pyrene (b) and pyrene functionalized porous network Py-MOP (c).

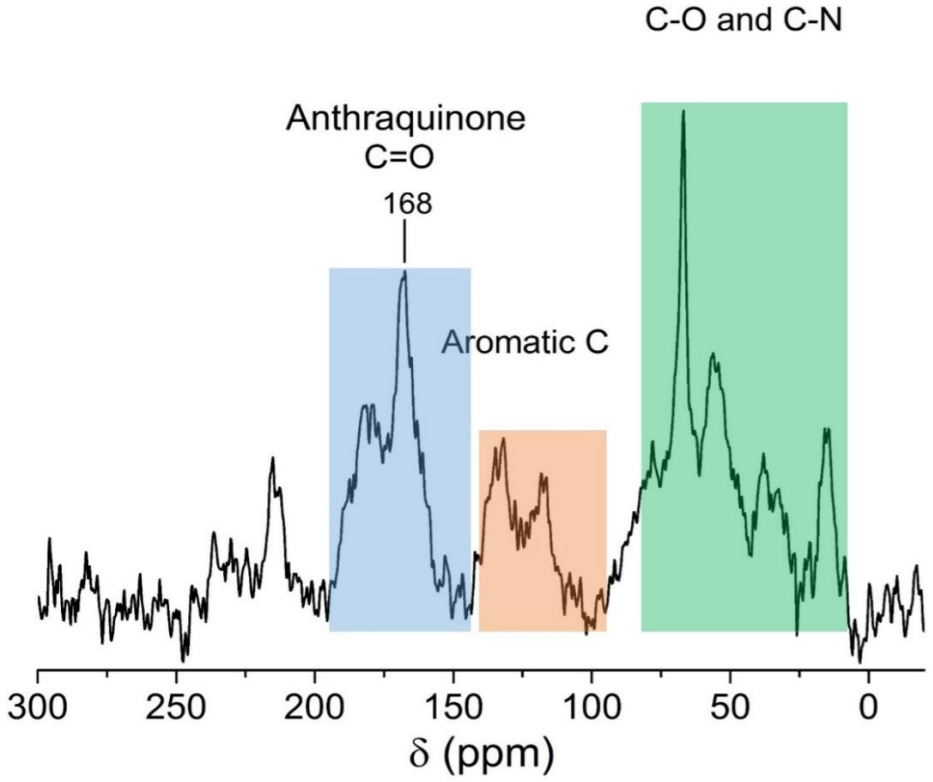

Figure 4.23 : Solid state C-NMR spectra of the c-MOP.

By taking the advantage of fluorescence property, pyrene molecule further evidence for modification of c-MOP can be revealed with a fluorescence spectroscopy. Figure 4.23 shows the solid-state emission spectra of the c-MOP anc py-c-MOP. Non-modified c-MOP shows almost no fluorescence activity, on the other hand incorporation of pyrene bring in fluorescence property to the structure. The excitation at 340 nm should give the characteristic pyrene emission peaks at 375 and 395 nm. However, after attaching of pyrene to c-MOP with a triazole linkage, these characteristic peaks shift to 412 and 459 nm, indicating the successful functionalization other than contamination with pyrene monomer (Figure 4.24).

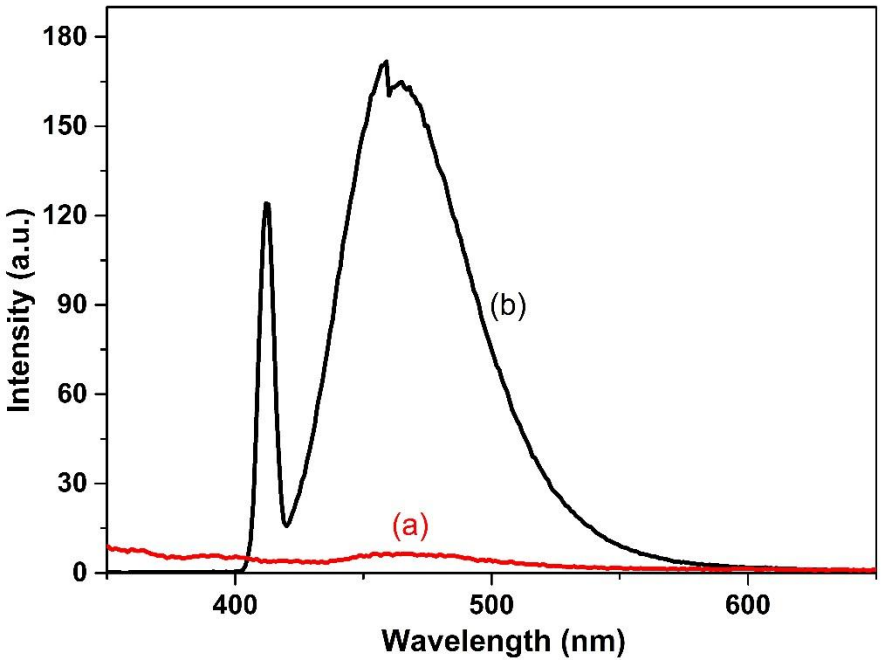

Figure 4.24 : Flourescence spectra of functional porous material a) before and b) after "click" reaction.

5. CONCLUSIONS

Over the last decade, the development of new porous materials, especially micro- and mesoporous materials, opened unprecedented opportunities for a wide range of applications. Microporous materials are characterized by microporous structural features and rich surface properties, which have potential applications in adsorption, separation, ion-exchange, and catalysis. In order to extend the performance of such materials, increasing efforts are undertaken now toward the development of scaffolds containing organic building blocks, which due to their functional diversity would allow for an exquisite control over the chemical nature of the surface areas and the physical properties of the resulting networks. Purely organic, micro and mesoporous materials are however still a contemporary field of research.

Conventional technologies for treatment of aqueous mercury include precipitation, coagulation, reduction, membrane separation, ion exchange, and adsorption. Among these technologies, adsorption has been widely studied because it is easy to operate and cost-effective. Many adsorbents have been studied for Hg(II) removal from aqueous solutions, including activated carbons, silicates, polymers and biomass. In addition, other materials including clays, organic matters, iron oxides, and pyrite, belonging to the general categories of soils, suspended solids/sediments in natural waters and natural minerals have also been extensively studied for their adsorption properties for mercury. Materials effective for mercury removal generally carry sulfur, nitrogen and oxygen containing functional groups as major binding sites for mercury. For example, strong interactions between mercury and organic matters have been attributed to the binding of mercury with reduced sulfur-containing functional groups in these substances.

In the first part of the thesis, a new synthetic approach for the fabrication of porous polybenzoxazine resin with attractive features an efficient mercury (II) ion removal method from seawater was described for the first time. The method presented here is very appealing due to its very simple design and specificity against mercury (II) ion in both load capacity and affinity as evidenced by convincing analytical data. It is

anticipated that with the help of design flexibility of benzoxazine monomers, stemming from vast number of commercially available phenols and amines, the approach can further be expanded to other benzoxazine-based polymers. High recycling ability of polybenzoxazine resin minimizing the amount of secondary wastes makes the system cost effective and therefore, can find applications in environmental industry.

One of the most common techniques used in chemistry to reveal the contents of an unknown sample particularly those concerning envinronmental issues is chromatography. Chromatography is the science of separation from the sample matrix. The technique is based on partitioning between two phases, one stationary and the other mobile.

In the second part of the thesis, the column packing material with porous structure was successfully synthesized through an inventive method. After the synthesis, the analysis of compounds such as polycyclic aromatic hydrocarbons (PAH), pesticides, flavonoids and phenolic acids was performed. The high efficiency arising from the high surface area (surface area, 215 m^2/g) and adsorption properties indicates that the rigid and black porous polymeric material can be used in various chromatographic systems. Compared to the other packing materials, it has good compatibility with all mobile phases, from acetonitrile to methanol and water.

The modification of polymers after the successful achievement of a specific polymerization process represents an important task in macromolecular science. The “click”-type reactions, offers a convenient route for the modification of macromolecular structures. Among them, the metal catalyzed azide/alkyne “click” reaction (a variation of the Huisgen 1,3-dipolar cycloaddition reaction between terminal acetylenes and azides) appears to be the most widely used process. The process is based on the catalytic activity of Copper (Cu) to form a triazole ring through cycloaddition reaction. Sharpless and Fokin independently described it as a reliable catalytic process offering "an unprecedented level of selectivity, reliability, and scope for those organic synthesis endeavors which depend on the creation of covalent links between diverse building blocks.”

In the third part of the thesis, a new approach to form clickable porous materials was described. The concept was further proved by a model reaction incorporating

fluorescent pyrene molecules into the porous material by the click process. The use of such Huisgen-type click reaction in MOPs was first performed by Coopers group. Although they applied similar monomer functionalization strategy, our approach appears to be more simple and utilizes commercially available cheap materials. Thus, the corresponding propargyl containing anthraquinone was synthesized and reacted with melamine to form clickable MOP. The obtained MOP was successfully modified with azido pyrene yielding a porous material with high surface area and fluroscence property.

REFERENCES

[1] Wu, D. C., Xu, F., Sun, B., Fu, R. W., He, H. K. and Matyjaszewski, K. (2012). Design and Preparation of Porous Polymers. *Chemical Reviews, 112(7),* 3959-4015.

[2] Xiao, F. S., Qiu, S. L., Pang, W. Q. and Xu, R. R. (1999). New Developments in Microporous Materials. *Advanced Materials, 11(13),* 1091-1098.

[3] Pan, L., Sander, M. B., Huang, X. Y., Li, J., Smith, M., Bittner, E., Bockrath, B. and Johnson, J. K. (2004). Microporous Metal Organic Materials: Promising Candidates as Sorbents for Hydrogen Storage. *Journal of the American Chemical Society, 126(5),* 1308-1309.

[4] Gokmen, M. T. and Du Prez, F. E. (2012). Porous Polymer Particles-a Comprehensive Guide to Synthesis, Characterization, Functionalization and Applications. *Progress in Polymer Science, 37(3),* 365-405.

[5] McKeown, N. B., Budd, P. M. and Book, D. (2007). Microporous Polymers as Potential Hydrogen Storage Materials. *Macromolecular Rapid Communications, 28(9),* 995-1002.

[6] Nischang, I. (2013). Porous Polymer Monoliths: Morphology, Porous Properties, Polymer Nanoscale Gel Structure and Their Impact on Chromatographic Performance. *Journal of Chromatography A, 1287(*39-58.

[7] Schuth, F. and Schmidt, W. (2002). Microporous and Mesoporous Materials. *Advanced Materials, 14(9),* 629-638.

[8] Schwab, M. G., Fassbender, B., Spiess, H. W., Thomas, A., Feng, X. L. and Mullen, K. (2009). Catalyst-Free Preparation of Melamine-Based Microporous Polymer Networks through Schiff Base Chemistry. *Journal of the American Chemical Society, 131(21),* 7216-+.

[9] Thompson, A. P. and Glandt, E. D. (1996). Polymers in Random Porous Materials: Structure, Thermodynamics, and Concentration Effects. *Macromolecules, 29(12),* 4314-4323.

[10] Hamerton, I., Ennis, K., Howlin, B. J. and McNamara, L. T. (2013). Effects of Thermal History on the Polymerisation Mechanism and Network Development in Aromatic Polybenzoxazines. *Reactive & Functional Polymers, 73(12),* 1612-1624.

[11] Hamerton, I., McNamara, L. T., Howlin, B. J., Smith, P. A., Cross, P. and Ward, S. (2013). Examining the Initiation of the Polymerization Mechanism and Network Development in Aromatic Polybenzoxazines. *Macromolecules, 46(13),* 5117-5132.

[12] Hamerton, I., McNamara, L. T., Howlin, B. J., Smith, P. A., Cross, P. and Ward, S. (2014). Kinetics and Cure Mechanism in Aromatic Polybenzoxazines Modified Using Thermoplastic Oligomers and Telechelics. *Macromolecules, 47(6),* 1935-1945.

[13] Hamerton, I., McNamara, L. T., Howlin, B. J., Smith, P. A., Cross, P. and Ward, S. (2014). Toughening Mechanisms in Aromatic Polybenzoxazines Using Thermoplastic Oligomers and Telechelics. *Macromolecules, 47(6),* 1946-1958.

[14] Hamerton, I., Thompson, S., Howlin, B. J. and Stone, C. A. (2013). New Method to Predict the Thermal Degradation Behavior of Polybenzoxazines from Empirical Data Using Structure Property Relationships. *Macromolecules, 46(19),* 7605-7615.

[15] Mahadik-Khanolkar, S., Donthula, S., Sotiriou-Leventis, C. and Leventis, N. (2014). Polybenzoxazine Aerogels. 1. High-Yield Room-Temperature Acid-Catalyzed Synthesis of Robust Monoliths, Oxidative Aromatization, and Conversion to Microporous Carbons. *Chemistry of Materials, 26(3),* 1303-1317.

[16] Zuniga, C., Lligadas, G., Ronda, J. C., Galia, M. and Cadiz, V. (2012). Renewable Polybenzoxazines Based in Diphenolic Acid. *Polymer, 53(8),* 1617-1623.

[17] Kiskan, B., Ghosh, N. N. and Yagci, Y. (2011). Polybenzoxazine-Based Composites as High-Performance Materials. *Polymer International, 60(2),* 167-177.

[18] Kiskan, B., Koz, B. and Yagci, Y. (2009). Synthesis and Characterization of Fluid 1,3-Benzoxazine Monomers and Their Thermally Activated Curing. *Journal of Polymer Science Part a-Polymer Chemistry, 47(24),* 6955-6961.

[19] Taskin, O. S., Kiskan, B. and Yagci, Y. (2013). Polybenzoxazine Precursors as Self-Healing Agents for Polysulfones. *Macromolecules, 46(22),* 8773-8778.

[20] Tasdelen, M. A. and Yagci, Y. (2013). Light-Induced Click Reactions. *Angewandte Chemie International Edition, 52(23),* 5930-5938.

[21] Gomez-Hortiguela, L., Lopez-Arbeloa, F., Cora, F. and Perez-Pariente, J. (2008). Supramolecular Chemistry in the Structure Direction of Microporous Materials from Aromatic Structure-Directing Agents. *Journal of the American Chemical Society, 130(40),* 13274-13284.

[22] Asakura, Y., Sakamoto, Y. and Kuroda, K. (2014). Silylation of Layered Silicate Rub-51 with Sicl4 and Conversion of the Silylated Derivative to a Crystalline Microporous Material. *Chemistry of Materials, 26(12),* 3796-3803.

[23] Cai, R., Du, Y. P., Peng, S. J., Bi, H. C., Zhang, W. Y., Yang, D., Chen, J., Lim, T. M., Zhang, H., Cao, Y. C. and Yan, Q. Y. (2014). Synthesis of Porous, Hollow Metal Mco3 (M=Mn, Co, Ca) Microstructures and Adsorption Properties Thereof. *Chemistry-a European Journal, 20(2),* 421-425.

[24] Chun, J., Kang, S., Park, N., Park, E. J., Jin, X., Kim, K. D., Seo, H. O., Lee, S. M., Kim, H. J., Kwon, W. H., Park, Y. K., Kim, J. M., Kim, Y. D. and Son, S. U. (2014). Metal-Organic Framework@Microporous Organic Network: Hydrophobic Adsorbents with a Crystalline Inner Porosity. *Journal of the American Chemical Society, 136(19),* 6786-6789.

[25] Comotti, A., Bracco, S., Ben, T., Qiu, S. L. and Sozzani, P. (2014). Molecular Rotors in Porous Organic Frameworks. *Angewandte Chemie-International Edition, 53(4),* 1043-1047.

[26] Esquirol, A. L., Sarazin, P. and Virgilio, N. (2014). Tunable Porous Hydrogels from Cocontinuous Polymer Blends. *Macromolecules, 47(9),* 3068-3075.

[27] He, D. G., He, X. X., Wang, K. M., Zhao, Y. X. and Zou, Z. (2013). Regenerable Multifunctional Mesoporous Silica Nanocomposites for Simultaneous Detection and Removal of Mercury(Ii). *Langmuir, 29(19),* 5896-5904.

[28] Hoai, N. T. and Kim, D. (2009). Synthesis, Structure, and Selective Separation Behavior of Copper-Imprinted Microporous Polymethacrylate Beads. *Aiche Journal, 55(12),* 3248-3254.

[29] Mandal, I., Townsend, M. J., Darton, N. J., Bonyadi, S. and Slater, N. K. H. (2014). A Microporous Walled Micro-Capillary Film Module for Cation-Exchange Protein Chromatography. *Journal of Membrane Science, 466(*123-129.

[30] Pini, R. (2014). Interpretation of Net and Excess Adsorption Isotherms in Microporous Adsorbents. *Microporous and Mesoporous Materials, 187(*40-52.

[31] Saleh, M., Lee, H. M., Kemp, K. C. and Kim, K. S. (2014). Highly Stable Co2/N-2 and Co2/Ch4 Selectivity in Hyper-Cross-Linked Heterocyclic Porous Polymers. *Acs Applied Materials & Interfaces, 6(10),* 7325-7333.

[32] Zhang, G., Presly, O., White, F., Oppel, I. M. and Mastalerz, M. (2014). A Permanent Mesoporous Organic Cage with an Exceptionally High Surface Area. *Angewandte Chemie-International Edition, 53(6),* 1516-1520.

[33] Afeworki, M., Kennedy, G. J., Dorset, D. L. and Strohmaier, K. G. (2006). Synthesis and Characterization of a New Microporous Material. 2. Alpo and Sapo Forms of Emm-3. *Chemistry of Materials, 18(6),* 1705-1710.

[34] Baumgartner, A., Sattler, K., Thun, J. and Breu, J. (2008). A Route to Microporous Materials through Oxidative Pillaring of Micas. *Angewandte Chemie International Edition, 47(9),* 1640-1644.

[35] Del Regno, A. and Siperstein, F. R. (2013). Organic Molecules of Intrinsic Microporosity: Characterization of Novel Microporous Materials. *Microporous and Mesoporous Materials, 176(*55-63.

[36] van Garderen, N., Graule, T., Aneziris, C. G. and Clemens, F. J. (2013). Comparison Methods for Microstructure Analysis on Highly Porous Extrudates Based on Diatomite Filter Aids. *Microporous and Mesoporous Materials, 171(*215-222.

[37] Vila, N., Ghanbaja, J., Aubert, E. and Walcarius, A. (2014). Electrochemically Assisted Generation of Highly Ordered Azide-Functionalized Mesoporous Silica for Oriented Hybrid Films. *Angewandte Chemie-International Edition, 53(11),* 2945-2950.

[38] Wang, D. M., Zhao, T. T., Cao, Y., Yao, S., Li, G. H., Huo, Q. S. and Liu, Y. L. (2014). High Performance Gas Adsorption and Separation of Natural Gas in Two Microporous Metal-Organic Frameworks with Ternary Building Units. *Chemical Communications, 50(63),* 8648-8650.

[39] Wang, J. L., Zhu, H., Chen, G. J., Hu, Z. J., Weng, Y. Y., Wang, X. B. and Zhang, W. D. (2014). Controlled Synthesis and Self-Assembly of Dopamine-Containing Copolymer for Honeycomb-Like Porous Hybrid Particles. *Macromolecular Rapid Communications, 35(11),* 1061-1067.

[40] Wang, Y., Yang, J., Liu, Y. Y. and Ma, J. F. (2013). Controllable Syntheses of Porous Metal-Organic Frameworks: Encapsulation of Ln(Iii) Cations for Tunable Luminescence and Small Drug Molecules for Efficient Delivery. *Chemistry-a European Journal, 19(43),* 14591-14599.

[41] Zhu, Y. L., Yang, H. S., Jin, Y. H. and Zhang, W. (2013). Porous Poly(Aryleneethynylene) Networks through Alkyne Metathesis. *Chemistry of Materials, 25(18),* 3718-3723.

[42] Dybtsev, D. N., Chun, H., Yoon, S. H., Kim, D. and Kim, K. (2004). Microporous Manganese Formate: A Simple Metal-Organic Porous Material with High Framework Stability and Highly Selective Gas Sorption Properties. *Journal of the American Chemical Society, 126(1),* 32-33.

[43] Kondo, M., Shimamura, M., Noro, S., Minakoshi, S., Asami, A., Seki, K. and Kitagawa, S. (2000). Microporous Materials Constructed from the Interpenetrated Coordination Networks. Structures and Methane Adsorption Properties. *Chemistry of Materials, 12(5),* 1288-1299.

[44] Kuhn, P., Forget, A., Su, D. S., Thomas, A. and Antonietti, M. (2008). From Microporous Regular Frameworks to Mesoporous Materials with Ultrahigh Surface Area: Dynamic Reorganization of Porous Polymer Networks. *Journal of the American Chemical Society, 130(40),* 13333-13337.

[45] Zhang, J., Chen, S. M., Wu, T., Feng, P. Y. and Bu, X. H. (2008). Homochiral Crystallization of Microporous Framework Materials from Achiral Precursors by Chiral Catalysis. *Journal of the American Chemical Society, 130(39),* 12882-12890.

[46] McKeown, N. B., Budd, P. M., Msayib, K. J., Ghanem, B. S., Kingston, H. J., Tattershall, C. E., Makhseed, S., Reynolds, K. J. and Fritsch, D. (2005). Polymers of Intrinsic Microporosity (Pims): Bridging the Void between Microporous and Polymeric Materials. *Chemistry- A European Journal, 11(9),* 2610-2620.

[47] Navrotsky, A., Trofymluk, O. and Levchenko, A. A. (2009). Thermochemistry of Microporous and Mesoporous Materials. *Chemical Reviews, 109(9),* 3885-3902.

[48] Treacy, M. M. J. (2003). Describing Ordered Microporous and Mesoporous Materials - Introduction. *Microporous and Mesoporous Materials, 58(1),* 1-2.

[49] Choma, J., Fahrenholz, W., Jamiola, D., Ludwinowicz, J. and Jaroniec, M. (2014). Development of Mesoporosity in Carbon Spheres Obtained by Stober Method. *Microporous and Mesoporous Materials, 185(*197-203.

[50] Fang, Z. L., Durholt, J. P., Kauer, M., Zhang, W. H., Lochenie, C., Jee, B., Albada, B., Metzler-Nolte, N., Poppl, A., Weber, B., Muhler, M., Wang, Y. M., Schmid, R. and Fischer, R. A. (2014). Structural Complexity in Metal-Organic Frameworks: Simultaneous Modification of Open Metal Sites and Hierarchical Porosity by Systematic Doping with Defective Linkers. *Journal of the American Chemical Society, 136(27),* 9627-9636.

[51] Gu, Z. Y., Yang, C. X., Chang, N. and Yan, X. P. (2012). Metal-Organic Frameworks for Analytical Chemistry: From Sample Collection to Chromatographic Separation. *Accounts of Chemical Research, 45(5),* 734-745.

[52] Gucuyener, C., van den Bergh, J., Gascon, J. and Kapteijn, F. (2010). Ethane/Ethene Separation Turned on Its Head: Selective Ethane Adsorption on the Metal-Organic Framework Zif-7 through a Gate-Opening Mechanism. *Journal of the American Chemical Society, 132(50),* 17704-17706.

[53] Li, B. Y., Zhang, Y. M., Krishna, R., Yao, K. X., Han, Y., Wu, Z. L., Ma, D. X., Shi, Z., Pham, T., Space, B., Liu, J., Thallapally, P. K., Liu, J., Chrzanowski, M. and Ma, S. Q. (2014). Introduction of Pi-Complexation into Porous Aromatic Framework for Highly Selective Adsorption of Ethylene over Ethane. *Journal of the American Chemical Society, 136(24),* 8654-8660.

[54] Liu, Q. Q. (2010). Monodisperse Polystyrene Nanospheres with Ultrahigh Surface Area: Application for Hydrogen Storage. *Macromolecular Chemistry and Physics, 211(9),* 1012-1017.

[55] Singh, N. K., Dsouza, R. N., Grasselli, M. and Fernandez-Lahore, M. (2014). High Capacity Cryogel-Type Adsorbents for Protein Purification. *Journal of Chromatography A, 1355(*143-148.

[56] Wang, X. M., Dai, K. L., Chen, L. M., Huang, J. H. and Liu, Y. N. (2014). An Ethylenediamine-Modified Hypercrosslinked Polystyrene Resin: Synthesis, Adsorption and Separation Properties. *Chemical Engineering Journal, 242(*19-26.

[57] Woodward, R. T., Stevens, L. A., Dawson, R., Vijayaraghavan, M., Hasell, T., Silverwood, I. P., Ewing, A. V., Ratvijitvech, T., Exley, J. D., Chong, S. Y., Blanc, F., Adams, D. J., Kazarian, S. G., Snape, C. E., Drage, T. C. and Cooper, A. I. (2014). Swellable, Water- and Acid-Tolerant Polymer Sponges for Chemoselective Carbon Dioxide Capture. *Journal of the American Chemical Society, 136(25),* 9028-9035.

[58] Wu, H. H., Reali, R. S., Smith, D. A., Trachtenberg, M. C. and Li, J. (2010). Highly Selective Co2 Capture by a Flexible Microporous Metal-Organic Framework (Mmof) Material. *Chemistry- A European Journal, 16(47),* 13951-13954.

[59] Siderius, D. W. and Gelb, L. D. (2009). Predicting Gas Adsorption in Complex Microporous and Mesoporous Materials Using a New Density Functional Theory of Finely Discretized Lattice Fluids. *Langmuir, 25(3),* 1296-1299.

[60] Subbiah, A., Pyle, D., Rowland, A., Huang, J., Narayanan, R. A., Thiyagarajan, P., Zon, J. and Clearfield, A. (2005). A Family of Microporous Materials Formed by Sn(Iv) Phosphonate Nanoparticles. *Journal of the American Chemical Society, 127(31),* 10826-10827.

[61] Klemperer, W. G. and Zhong, B. (1996). Preparation of a Microporous Organometallic Material. *Chemistry of Materials, 8(7),* 1353-&.

[62] Unger, K. K. and Liapis, A. I. (2012). Adsorbents and Columns in Analytical High-Performance Liquid Chromatography: A Perspective with Regard to Development and Understanding. *Journal of Separation Science, 35(10-11),* 1201-1212.

[63] Chae, H. K., Siberio-Perez, D. Y., Kim, J., Go, Y., Eddaoudi, M., Matzger, A. J., O'Keeffe, M. and Yaghi, O. M. (2004). A Route to High Surface Area, Porosity and Inclusion of Large Molecules in Crystals. *Nature, 427(6974),* 523-527.

[64] Furukawa, H. and Yaghi, O. M. (2009). Storage of Hydrogen, Methane, and Carbon Dioxide in Highly Porous Covalent Organic Frameworks for Clean Energy Applications. *Journal of the American Chemical Society, 131(25),* 8875-8883.

[65] Rosi, N. L., Eckert, J., Eddaoudi, M., Vodak, D. T., Kim, J., O'Keeffe, M. and Yaghi, O. M. (2003). Hydrogen Storage in Microporous Metal-Organic Frameworks. *Science, 300(5622),* 1127-1129.

[66] Rowsell, J. L. C. and Yaghi, O. M. (2005). Strategies for Hydrogen Storage in Metal-Organic Frameworks. *Angewandte Chemie-International Edition, 44(30),* 4670-4679.

[67] Uribe-Romo, F. J., Hunt, J. R., Furukawa, H., Klock, C., O'Keeffe, M. and Yaghi, O. M. (2009). A Crystalline Imine-Linked 3-D Porous Covalent Organic Framework. *Journal of the American Chemical Society, 131(13),* 4570-4576.

[68] Cote, A. P., Benin, A. I., Ockwig, N. W., O'Keeffe, M., Matzger, A. J. and Yaghi, O. M. (2005). Porous, Crystalline, Covalent Organic Frameworks. *Science, 310(5751),* 1166-1170.

[69] Kiskan, B., Zhang, J. S., Wang, X. C., Antonietti, M. and Yagci, Y. (2012). Mesoporous Graphitic Carbon Nitride as a Heterogeneous Visible Light Photoinitiator for Radical Polymerization. *Acs Macro Letters, 1(5),* 546-549.

[70] Ravikovitch, P. I., Vishnyakov, A., Russo, R. and Neimark, A. V. (2000). Unified Approach to Pore Size Characterization of Microporous Carbonaceous Materials from N-2, Ar, and Co2 Adsorption Isotherms. *Langmuir, 16(5),* 2311-2320.

[71] Shin, Y., Zemanian, T. S., Fryxell, G. E., Wang, L. Q. and Liu, J. (2000). Supercritical Processing of Functionalized Size Selective Microporous Materials. *Microporous and Mesoporous Materials, 37(1-2),* 49-56.

[72] Otsu, T., Yoshida, M. and Tazaki, T. (1982). A Model for Living Radical Polymerization. *Makromolekulare Chemie Rapid Communications, 3(2),* 133-140.

[73] Percec, V. and Barboiu, B. (1995). Living Radical Polymerization of Styrene Initiated by Arenesulfonyl Chlorides and Cu-I(Bpy)(N)Cl. *Macromolecules, 28(23),* 7970-7972.

[74] Taskin, O. S., Yilmaz, G., Tasdelen, M. A. and Yagci, Y. (2014). Photoinduced Reverse Atom Transfer Radical Polymerization of Methyl Methacrylate Using Camphorquinone/Benzhydrol System. *Polymer International, 63(5),* 902-907.

[75] Dinolfo, P. H. and Hupp, J. T. (2001). Supramolecular Coordination Chemistry and Functional Microporous Molecular Materials. *Chemistry of Materials, 13(10),* 3113-3125.

[76] Jiang, T., Ozin, G. A. and Bedard, R. L. (1998). Spectroscopic Properties of Microporous Layered Tin Sulfide Materials. *Journal of Materials Chemistry, 8(7),* 1641-1648.

[77] Milewska-Duda, J., Duda, J. T., Jodlowski, G. and Kwiatkowski, M. (2000). A Model for Multilayer Adsorption of Small Molecules in Microporous Materials. *Langmuir, 16(18),* 7294-7303.

[78] Lorjai, P., Chaisuwan, T. and Wongkasemjit, S. (2009). Porous Structure of Polybenzoxazine-Based Organic Aerogel Prepared by Sol-Gel Process and Their Carbon Aerogels. *Journal of Sol-Gel Science and Technology, 52(1),* 56-64.

[79] Thubsuang, U., Ishida, H., Wongkasemjit, S. and Chaisuwan, T. (2012). Novel Template Confinement Derived from Polybenzoxazine-Based Carbon Xerogels for Synthesis of Zsm-5 Nanoparticles Via Microwave Irradiation. *Microporous and Mesoporous Materials, 156(*7-15.

[80] Ghosh, N. N., Kiskan, B. and Yagci, Y. (2007). Polybenzoxazines - New High Performance Thermosetting Resins: Synthesis and Properties. *Progress in Polymer Science, 32(11),* 1344-1391.

[81] Kiskan, B. and Yagci, Y., 2010. Synthetic Strategies to Combine High Performance Benzoxazine Thermosets with Polymers. In *Polychar-18 World Forum on Advanced Materials,* Mormann, W., Ed.

[82] Kudoh, R., Sudo, A. and Endo, T. (2010). A Highly Reactive Benzoxazine Monomer, 1-(2-Hydroxyethyl)-1,3-Benzoxazine: Activation of

Benzoxazine by Neighboring Group Participation of Hydroxyl Group. *Macromolecules, 43(3),* 1185-1187.

[83] Ning, X. and Ishida, H. (1994). Phenolic Materials Via Ring-Opening Polymerization of Benzoxazines - Effect of Molecular-Structure on Mechanical and Dynamic-Mechanical Properties. *Journal of Polymer Science Part B-Polymer Physics, 32(5),* 921-927.

[84] Ning, X. and Ishida, H. (1994). Phenolic Materials Via Ring-Opening Polymerization - Synthesis and Characterization of Bisphenol-a Based Benzoxazines and Their Polymers. *Journal of Polymer Science Part a-Polymer Chemistry, 32(6),* 1121-1129.

[85] Takeichi, T., Nakamura, K., Agag, T. and Muto, H. (2004). Synthesis of Cresol-Based Benzoxazine Monomers Containing Allyl Groups and the Properties of the Polymers Therefrom. *Designed Monomers and Polymers, 7(6),* 727-740.

[86] Zhang, K., Zhuang, Q., Liu, X., Cai, R., Yang, G. and Han, Z. (2013). Synthesis and Copolymerization of Benzoxazines with Low-Dielectric Constants and High Thermal Stability. *RSC Advances, 3(15),* 5261-5270.

[87] Zhang, K., Zhuang, Q., Zhou, Y., Liu, X., Yang, G. and Han, Z. (2012). Preparation and Properties of Novel Low Dielectric Constant Benzoxazole-Based Polybenzoxazine. *Journal of Polymer Science, Part A: Polymer Chemistry, 50(24),* 5115-5123.

[88] Liu, C., Shen, D., Sebastián, R. M., Marquet, J. and Schönfeld, R. (2013). Catalyst Effects on the Ring-Opening Polymerization of 1,3-Benzoxazine and on the Polymer Structure. *Polymer (United Kingdom), 54(12),* 2873-2878.

[89] Yagci, Y., Kiskan, B. and Ghosh, N. N. (2009). Recent Advancement on Polybenzoxazine-a Newly Developed High Performance Thermoset. *Journal of Polymer Science Part a-Polymer Chemistry, 47(21),* 5565-5576.

[90] Niu, Y. Z., Qu, R. J., Liu, X. G., Mu, L., Bu, B. H., Sun, Y. T., Chen, H., Meng, Y. F., Meng, L. N. and Cheng, L. (2014). Thiol-Functionalized Polysilsesquioxane as Efficient Adsorbent for Adsorption of Hg(Ii) and Mn(Ii) from Aqueous Solution. *Materials Research Bulletin, 52(*134-142.

[91] Rahman, N., Sato, N., Sugiyama, M., Hidaka, Y., Okabe, H. and Hara, K. (2014). Selective Hg(Ii) Adsorption from Aqueous Solutions of Hg(Ii) and Pb(Ii) by Hydrolyzed Acrylamide-Grafted Pet Films. *Journal of Environmental Science and Health Part a-Toxic/Hazardous Substances & Environmental Engineering, 49(7),* 798-806.

[92] Thakur, S., Kumari, S., Dogra, P. and Chauhan, G. S. (2014). A New Guar Gum-Based Adsorbent for the Removal of Hg(Ii) from Its Aqueous Solutions. *Carbohydrate Polymers, 106(*276-282.

[93] Asasian, N. and Kaghazchi, T. (2013). Optimization of Activated Carbon Sulfurization to Reach Adsorbent with the Highest Capacity for Mercury Adsorption. *Separation Science and Technology, 48(13),* 2059-2072.

[94] Bae, K. M., Kim, B. J., Rhee, K. Y. and Park, S. J. (2014). Roles of Metal/Activated Carbon Hybridization on Elemental Mercury Adsorption. *Journal of Nanoscience and Nanotechnology, 14(8),* 5811-5816.

[95] Bidhendi, M. E., Bidhendi, G. R. N., Mehrdadi, N. and Rashedi, H. (2014). Modified Mesoporous Silica (Sba-15) with Trithiane as a New Effective Adsorbent for Mercury Ions Removal from Aqueous Environment. *Journal of Environmental Health Science and Engineering, 12(*6.

[96] Chen, P. H., Hsu, C. F., Tsai, D. D. W., Lu, Y. M. and Huang, W. J. (2014). Adsorption of Mercury from Water by Modified Multi-Walled Carbon Nanotubes: Adsorption Behaviour and Interference Resistance by Coexisting Anions. *Environmental Technology, 35(15),* 1935-1944.

[97] Gao, Y. S., Zhang, Z., Wu, J. W., Duan, L. H., Umar, A., Sun, L. Y., Guo, Z. H. and Wang, Q. (2013). A Critical Review on the Heterogeneous Catalytic Oxidation of Elemental Mercury in Flue Gases. *Environmental Science & Technology, 47(19),* 10813-10823.

[98] Gong, Y. Y., Liu, Y. Y., Xiong, Z. and Zhao, D. Y. (2014). Immobilization of Mercury by Carboxymethyl Cellulose Stabilized Iron Sulfide Nanoparticles: Reaction Mechanisms and Effects of Stabilizer and Water Chemistry. *Environmental Science & Technology, 48(7),* 3986-3994.

[99] He, C., Shen, B. X., Chen, J. H. and Cai, J. (2014). Adsorption and Oxidation of Elemental Mercury over Ce-Mnox/Ti-Pilcs. *Environmental Science & Technology, 48(14),* 7891-7898.

[100] Hu, C. X., Zhou, J. S., Li, J. X., Zheng, J., Wang, Y. C., Luo, Z. Y. and Cen, K. F. (2014). Oxidative Adsorption of Elemental Mercury by Activated Carbon from Coconut Shell in Simulated Flue Gas. *Separation Science and Technology, 49(7),* 1062-1066.

[101] Lopes, C. B., Lopes, I., Rocha, L. S., Duarte, A. C., Soares, A., Rocha, J. and Pereira, E. (2014). A Multidisciplinary Approach to Evaluate the Efficiency of a Clean-up Technology to Remove Mercury from Water. *Bulletin of Environmental Contamination and Toxicology, 93(2),* 138-143.

[102] Mao, Y. X., Li, Y. B., Richards, J. and Cai, Y. (2013). Investigating Uptake and Translocation of Mercury Species by Sawgrass (Cladium Jamaicense) Using a Stable Isotope Tracer Technique. *Environmental Science & Technology, 47(17),* 9678-9684.

[103] Morris, E. A., Kirk, D. W., Jia, C. Q. and Morita, K. (2012). Roles of Sulfuric Acid in Elemental Mercury Removal by Activated Carbon and Sulfur-Impregnated Activated Carbon (Vol 46, Pg 7905, 2012). *Environmental Science & Technology, 46(19),* 10857-10857.

[104] Mullassery, M. D., Fernandez, N. B. and Anirudhan, T. S. (2014). Removal of Mercury(Ii) Ions from Aqueous Solutions Using Chemically Modified Banana Stem: Kinetic and Equilibrium Modeling. *Separation Science and Technology, 49(8),* 1259-1269.

[105] Ravi, S., Selvaraj, M., Park, H., Chun, H. H. and Ha, C. S. (2014). Novel Hierarchically Dispersed Mesoporous Silica Spheres: Effective Adsorbents for Mercury from Wastewater and a Thermodynamic Study. *New Journal of Chemistry, 38(8),* 3899-3906.

[106] Rocha, L. S., Lopes, C. B., Henriques, B., Tavares, D. S., Borges, J., Duarte, A. C. and Pereira, E. (2014). Competitive Effects on Mercury Removal by an Agricultural Waste: Application to Synthetic and Natural Spiked Waters. *Environmental Technology, 35(6),* 661-673.

[107] Saber-Samandari, S. and Gazi, M. (2013). Removal of Mercury (Ii) from Aqueous Solution Using Chitosan-Graft-Polyacrylamide Semi-Ipn Hydrogels. *Separation Science and Technology, 48(9),* 1382-1390.

[108] Saman, N., Johari, K. and Mat, H. (2014). Synthesis and Characterization of Sulfur-Functionalized Silica Materials Towards Developing Adsorbents for Mercury Removal from Aqueous Solutions. *Microporous and Mesoporous Materials, 194(*38-45.

[109] Vernon, J. D. and Bonzongo, J. C. J. (2014). Volatilization and Sorption of Dissolved Mercury by Metallic Iron of Different Particle Sizes: Implications for Treatment of Mercury Contaminated Water Effluents. *Journal of Hazardous Materials, 276(*408-414.

[110] Xu, J. Y., Kleja, D. B., Biester, H., Lagerkvist, A. and Kumpiene, J. (2014). Influence of Particle Size Distribution, Organic Carbon, Ph and Chlorides on Washing of Mercury Contaminated Soil. *Chemosphere, 109(*99-105.

[111] Yuan, Y., Jiang, S. L., Miao, Q. Q., Zhang, J., Wang, M. J., An, L. N., Cao, Q. J. W., Guan, Y. F., Zhang, Q. and Liang, G. L. (2014). Fluorescent Switch for Fast and Selective Detection of Mercury (Ii)

Ions in Vitro and in Living Cells and a Simple Device for Its Removal. *Talanta, 125(*204-209.

[112] Zhou, J. S., Hou, W. H., Qi, P., Gao, X., Luo, Z. Y. and Cen, K. F. (2013). Ceo2-Tio2 Sorbents for the Removal of Elemental Mercury from Syngas. *Environmental Science & Technology, 47(17),* 10056-10062.

[113] Aksu, A., Balkis, N., Taskin, O. S. and Ersan, M. S. (2011). Toxic Metal (Pb, Cd, as and Hg) and Organochlorine Residue Levels in Hake (Merluccius Merluccius) from the Marmara Sea, Turkey. *Environmental Monitoring and Assessment, 182(1-4),* 509-521.

[114] Algan, O., Balkis, N., Cagatay, M. N. and Sari, E. (2004). The Sources of Metal Contents in the Shelf Sediments from the Marmara Sea, Turkey. *Environmental Geology, 46(6-7),* 932-950.

[115] Ates, S., Dizman, C., Aydogan, B., Kiskan, B., Torun, L. and Yagci, Y. (2011). Synthesis, Characterization and Thermally Activated Curing of Polysulfones with Benzoxazine End Groups. *Polymer, 52(7),* 1504-1509.

[116] Atwood, D. A. and Zaman, M. K., 2006. Mercury Removal from Water. In *Recent Developments in Mercury Science,* Atwood, D. A., Ed.

[117] Clarkson, T. W. (1997). The Toxicology of Mercury. *Critical Reviews in Clinical Laboratory Sciences, 34(4),* 369-403.

[118] Economou, A. and Fielden, P. R. (2003). Mercury Film Electrodes: Developments, Trends and Potentialities for Electroanalysis. *Analyst, 128(3),* 205-212.

[119] Jurng, J., Lee, T. G., Lee, G. Y., Lee, S. J., Kim, B. H. and Seier, J. (2002). Mercury Removal from Incineration Flue Gas by Organic and Inorganic Adsorbents. *Chemosphere, 47(9),* 907-913.

[120] Kurun, A., Balkis, H. and Balkis, N. (2007). Accumulations of Total Metal in Dominant Shrimp Species (Palaemon Adspersus, Palaemon Serratus, Parapenaeus Longirostris) and Bottom Surface Sediments Obtained from the Northern Inner Shelf of the Sea of Marmara. *Environmental Monitoring and Assessment, 135(1-3),* 353-367.

[121] Lavoie, R. A., Jardine, T. D., Chumchal, M. M., Kidd, K. A. and Campbell, L. M. (2013). Biomagnification of Mercury in Aquatic Food Webs: A Worldwide Meta-Analysis. *Environmental Science & Technology, 47(23),* 13385-13394.

[122] Miretzky, P. and Fernandez Cirelli, A. (2009). Hg(Ii) Removal from Water by Chitosan and Chitosan Derivatives: A Review. *Journal of Hazardous Materials, 167(1-3),* 10-23.

[123] Morsali, A. and Masoomi, M. Y. (2009). Structures and Properties of Mercury(Ii) Coordination Polymers. *Coordination Chemistry Reviews, 253(13-14),* 1882-1905.

[124] Overman, L. E. (1984). Mercury(Ii)-Catalyzed and Palladium(Ii)-Catalyzed 3,3 -Sigmatropic Rearrangements. *Angewandte Chemie-International Edition in English, 23(8),* 579-586.

[125] Ramadan, H., Ghanem, A. and El-Rassy, H. (2010). Mercury Removal from Aqueous Solutions Using Silica, Polyacrylamide and Hybrid Silica-Polyacrylamide Aerogels. *Chemical Engineering Journal, 159(1-3),* 107-115.

[126] Tchounwou, P. B., Ayensu, W. K., Ninashvili, N. and Sutton, D. (2003). Environmental Exposure to Mercury and Its Toxicopathologic Implications for Public Health. *Environmental Toxicology, 18(3),* 149-175.

[127] Bailey, S. E., Olin, T. J., Bricka, R. M. and Adrian, D. D. (1999). A Review of Potentially Low-Cost Sorbents for Heavy Metals. *Water Research, 33(11),* 2469-2479.

[128] Balkıs, N. and Çağatay, M. N. (2001). Factors Controlling Metal Distributions in the Surface Sediments of the Erdek Bay, Sea of Marmara, Turkey. *Environment International, 27(1),* 1-13.

[129] Dabrowski, A., Hubicki, Z., Podkoscielny, P. and Robens, E. (2004). Selective Removal of the Heavy Metal Ions from Waters and Industrial Wastewaters by Ion-Exchange Method. *Chemosphere, 56(2),* 91-106.

[130] Demir, K. D., Kiskan, B. and Yagci, Y. (2011). Thermally Curable Acetylene-Containing Main-Chain Benzoxazine Polymers Via Sonogashira Coupling Reaction. *Macromolecules, 44(7),* 1801-1807.

[131] Emanuelli, T., Rocha, J. B. T., Pereira, M. E., Porciuncula, L. O., Morsch, V. M., Martins, A. F. and Souza, D. O. G. (1996). Effect of Mercuric Chloride Intoxication and Dimercaprol Treatment on Delta-Aminolevulinate Dehydratase from Brain, Liver and Kidney of Adult Mice. *Pharmacology & Toxicology, 79(3),* 136-143.

[132] Gonzalez, P., Dominique, Y., Massabuau, J. C., Boudou, A. and Bourdineaud, J. P. (2005). Comparative Effects of Dietary Methylmercury on Gene Expression in Liver, Skeletal Muscle, and Brain of the Zebrafish (Danio Rerio). *Environmental Science & Technology, 39(11),* 3972-3980.

[133] Grandjean, P., Weihe, P., White, R. F., Debes, F., Araki, S., Yokoyama, K., Murata, K., Sorensen, N., Dahl, R. and Jorgensen, P. J. (1997).

Cognitive Deficit in 7-Year-Old Children with Prenatal Exposure to Methylmercury. *Neurotoxicology and Teratology, 19(6),* 417-428.

[134] Gupta, R. K., Singh, R. A. and Dubey, S. S. (2004). Removal of Mercury Ions from Aqueous Solutions by Composite of Polyaniline with Polystyrene. *Separation and Purification Technology, 38(3),* 225-232.

[135] Henkel, G. and Krebs, B. (2004). Metallothioneins: Zinc, Cadmium, Mercury, and Copper Thiolates and Selenolates Mimicking Protein Active Site Features - Structural Aspects and Biological Implications. *Chemical Reviews, 104(2),* 801-824.

[136] Hussain, S., Atkinson, A., Thompson, S. J. and Khan, A. T. (1999). Accumulation of Mercury and Its Effect on Antioxidant Enzymes in Brain, Liver, and Kidneys of Mice. *Journal of Environmental Science and Health Part B-Pesticides Food Contaminants and Agricultural Wastes, 34(4),* 645-660.

[137] Hutcheson, M. S., Smith, C. M., Rose, J., Batdorf, C., Pancorbo, O., West, C. R., Strube, J. and Francis, C. (2014). Temporal and Spatial Trends in Freshwater Fish Tissue Mercury Concentrations Associated with Mercury Emissions Reductions. *Environmental Science & Technology, 48(4),* 2193-2202.

[138] Jarup, L. (2003). Hazards of Heavy Metal Contamination. *British Medical Bulletin, 68(*167-182.

[139] Kester, D. R., Iver W. Duedall, Donald N. Connors, Ricardo M. Pytkowicz. (1967). Preparation of Artificial Seawater. *Limnol. Oceanogr., 12(1),* 176-179.

[140] Krishnan, S. V., Gullett, B. K. and Jozewicz, W. (1994). Sorption of Elemental Mercury by Activated Carbons. *Environmental Science & Technology, 28(8),* 1506-1512.

[141] Matlock, M. M., Howerton, B. S., Henke, K. R. and Atwood, D. A. (2001). A Pyridine-Thiol Ligand with Multiple Bonding Sites for Heavy Metal Precipitation. *Journal of Hazardous Materials, 82(1),* 55-63.

[142] Mulligan, C. N., Yong, R. N. and Gibbs, B. F. (2001). Remediation Technologies for Metal-Contaminated Soils and Groundwater: An Evaluation. *Engineering Geology, 60(1-4),* 193-207.

[143] Shah, R. and Devi, S. (1996). Preconcentration of Mercury(Ii) on Dithizone Anchored Poly(Vinyl Pyridine) Support. *Reactive & Functional Polymers, 31(1),* 1-9.

[144] Sinner, F., Buchmeiser, M. R., Tessadri, R., Mupa, M., Wurst, K. and Bonn, G. K. (1998). Dipyridyl Amide-Functionalized Polymers Prepared by Ring-Opening-Metathesis Polymerization (Romp) for the

Selective Extraction of Mercury and Palladium. *Journal of the American Chemical Society, 120(12),* 2790-2797.

[145] Sudo, A., Du, L.-C., Hirayama, S. and Endo, T. (2010). Substituent Effects of N-Alkyl Groups on Thermally Induced Polymerization Behavior of 1,3-Benzoxazines. *Journal of Polymer Science Part A: Polymer Chemistry, 48(13),* 2777-2782.

[146] Sudo, A., Hirayama, S. and Endo, T. (2010). Highly Efficient Catalysts-Acetylacetonato Complexes of Transition Metals in the 4th Period for Ring-Opening Polymerization of 1,3-Benzoxazine. *Journal of Polymer Science Part a-Polymer Chemistry, 48(2),* 479-484.

[147] Tiravanti, G., Petruzzelli, D. and Passino, R. (1996). Low and Non Waste Technologies for Metals Recovery by Reactive Polymers. *Waste Management, 16(7),* 597-605.

[148] Wagemann, R., Trebacz, E., Boila, G. and Lockhart, W. L. (1998). Methylmercury and Total Mercury in Tissues of Arctic Marine Mammals. *Science of the Total Environment, 218(1),* 19-31.

[149] Yavuz, H., Denizli, A., Gungunes, H., Safarikova, M. and Safarik, I. (2006). Biosorption of Mercury on Magnetically Modified Yeast Cells. *Separation and Purification Technology, 52(2),* 253-260.

[150] Yee, K.-K., Reimer, N., Liu, J., Cheng, S.-Y., Yiu, S.-M., Weber, J., Stock, N. and Xu, Z. (2013). Effective Mercury Sorption by Thiol-Laced Metal–Organic Frameworks: In Strong Acid and the Vapor Phase. *Journal of the American Chemical Society, 135(21),* 7795-7798.

[151] Zuo, G. and Muhammed, M. (1995). Selective Binding of Mercury to Thiourea-Based Coordinating Resins. *Reactive and Functional Polymers, 27(3),* 187-198.

[152] Demir, K. D., Kiskan, B., Aydogan, B. and Yagci, Y. (2013). Thermally Curable Main-Chain Benzoxazine Prepolymers Via Polycondensation Route. *Reactive & Functional Polymers, 73(2),* 346-359.

[153] Hanbeyoglu, B., Kiskan, B. and Yagci, Y. (2013). Hydroxyl Functional Polybenzoxazine Precursor as a Versatile Platform for Post-Polymer Modifications. *Macromolecules, 46(21),* 8434-8440.

[154] Cestari, A. R. and Airoldi, C. (1997). Chemisorption on Thiol-Silicas: Divalent Cations as a Function of Ph and Primary Amines on Thiol-Mercury Adsorbed. *Journal of Colloid and Interface Science, 195(2),* 338-342.

[155] Kiskan, B. and Yagci, Y. (2007). Thermally Curable Benzoxazine Monomer with a Photodimerizable Coumarin Group. *Journal of Polymer Science Part a-Polymer Chemistry, 45(9),* 1670-1676.

[156] Nair, C. P. R. (2004). Advances in Addition-Cure Phenolic Resins. *Progress in Polymer Science, 29(5),* 401-498.

[157] Sonmez, H. B., Senkal, B. F. and Bicak, N. (2003). Polymer-Supported Iminodiacetamides for Selective Mercury Extraction. *Journal of Applied Polymer Science, 87(8),* 1316-1321.

[158] Aydogan, C., Kiskan, B., Hacioglu, S. O., Toppare, L. and Yagci, Y. (2014). Electrochemical Manipulation of Adhesion Strength of Polybenzoxazines on Metal Surfaces: From Strong Adhesion to Dismantling. *Rsc Advances, 4(52),* 27545-27551.

[159] Chen, K. C., Li, H. T., Huang, S. C., Chen, W. B., Sun, K. W. and Chang, F. C. (2011). Synthesis and Performance Enhancement of Novel Polybenzoxazines with Low Surface Free Energy. *Polymer International, 60(7),* 1089-1096.

[160] Fu, Z., Xu, K., Liu, X., Wu, J. C., Tan, C. J. and Chen, M. C. (2013). Preparation and Properties of Hybrid Materials Originating from Polybenzoxazines and Silsesquioxanes. *Macromolecular Chemistry and Physics, 214(10),* 1122-1130.

[161] Mahfud, R., Agag, T., Ishida, H., Shaikh, S. and Qutubuddin, S. (2013). Synthesis and Evaluation of Novel Anionic Polymeric Surfactants Based on Polybenzoxazines. *Journal of Colloid and Interface Science, 407(*339-347.

[162] Rimdusit, S., Thamprasom, N., Suppakarn, N., Jubsilp, C., Takeichi, T. and Tiptipakorn, S. (2013). Effect of Triphenyl Phosphate Flame Retardant on Properties of Arylamine-Based Polybenzoxazines. *Journal of Applied Polymer Science, 130(2),* 1074-1083.

[163] Shibayama, Y., Kawauchi, T. and Takeichi, T. (2014). Synthesis and Properties of Polybenzoxazines Containing Pyridyl Group. *High Performance Polymers, 26(1),* 60-68.

[164] Yan, C., Fan, X. Y., Li, J. and Shen, S. Z. (2011). Synthesis and Characterization of Bisphenol a Diphthalimide Bisbenzoxazine Monomers and the Properties of Their Polybenzoxazines. *Journal of Applied Polymer Science, 121(5),* 2778-2787.

[165] Sasaki, A. and Kimura, Y. (1997). Studies on Functionalization of Polymers by Reactive Processing. Part 5. Preparation of Polythiourea-Immobilized Active Charcoal and Its Utilization for Selective Adsorption of Mercury (Ii) Ion. *Nippon Kagaku Kaishi, 12),* 880-886.

[166] Holly, F. W. and Cope, A. C. (1944). Condensation Products of Aldehydes and Ketones with O-Aminobenzyl Alcohol and O-Hydroxybenzylamine. *J. Am. Chem. Soc., 66(11),* 1875-1879.

[167] Li, Y. L., Liu, C., Tan, Y., Xu, K., Lu, C. G. and Wang, P. X. (2014). In Situ Hydrogel Constructed by Starch-Based Nanoparticles Via a Schiff Base Reaction. *Carbohydrate Polymers, 110(*87-94.

[168] Ameloot, R., Liekens, A., Alaerts, L., Maes, M., Galarneau, A., Coq, B., Desmet, G., Sels, B. F., Denayer, J. F. M. and De Vos, D. E. (2010). Silica-Mof Composites as a Stationary Phase in Liquid Chromatography. *European Journal of Inorganic Chemistry, 24),* 3735-3738.

[169] Ongkudon, C. M., Kansil, T. and Wong, C. (2014). Challenges and Strategies in the Preparation of Large-Volume Polymer-Based Monolithic Chromatography Adsorbents. *Journal of Separation Science, 37(5),* 455-464.

[170] Zobel, S., Helling, C., Ditz, R. and Strube, J. (2014). Design and Operation of Continuous Countercurrent Chromatography in Biotechnological Production. *Industrial & Engineering Chemistry Research, 53(22),* 9169-9185.

[171] Berek, D. (1998). Liquid Chromatography of Macromolecules under Limiting Conditions of Desorption. 1. Principles of the Method. *Macromolecules, 31(24),* 8517-8521.

[172] Davankov, V., Sychov, C. S., Ilyin, M. M. and Sochilina, K. O. (2003). Hypercrosslinked Polystyrene as a Novel Type of High-Performance Liquid Chromatography Column Packing Material - Mechanisms of Retention. *Journal of Chromatography A, 987(1-2),* 67-75.

[173] Hao, G.-P., Li, W.-C., Qian, D., Wang, G.-H., Zhang, W.-P., Zhang, T., Wang, A.-Q., Schueth, F., Bongard, H.-J. and Lu, A.-H. (2011). Structurally Designed Synthesis of Mechanically Stable Poly(Benzoxazine-Co-Resol)-Based Porous Carbon Monoliths and Their Application as High-Performance CO_2 Capture Sorbents. *Journal of the American Chemical Society, 133(29),* 11378-11388.

[174] Kerckhoffs, J., ten Cate, M. G. J., Mateos-Timoneda, M. A., van Leeuwen, F. W. B., Snellink-Ruel, B., Spek, A. L., Kooijman, H., Crego-Calama, M. and Reinhoudt, D. N. (2005). Selective Self-Organization of Guest Molecules in Self-Assembled Molecular Boxes. *Journal of the American Chemical Society, 127(36),* 12697-12708.

[175] Cappiello, A., Palma, P. and Mangani, F. (1991). New Materials and Packing Techniques for Micro-Hplc Packed Capillary Columns. *Chromatographia, 32(7-8),* 389-391.

[176] Hosoya, K., Teramachi, M., Tanaka, N., Kobayashi, A., Kanda, T. and Ohtsu, Y. (2001). Preparation Strategy for Uniformly Sized, Polymer-Based Hplc Packing Materials Having Practically Acceptable Column

Efficiency. 1. Copolymerization Technique. *Analytical Chemistry, 73(24),* 5852-5857.

[177] Komarova, N. I., Rogachev, A. D., Chernyak, E. I., Morozov, S. V., Fomenko, V. V. and Salakhutdinov, N. F. (2009). Quantitative Hplc Determination of Main Flavonoid Content of Rhododendron Adamsii Leaves and Stems. *Chemistry of Natural Compounds, 45(1),* 27-31.

[178] Oguni, K., Ito, M., Isokawa, A. and Matsumoto, A. (1996). C-13 Nuclear Spin-Spin Relaxation Times (T(2c)S) of Enantiomers in the Presence of Column Packing Material and Solvents for Chiral Discrimination Hplc. *Chirality, 8(5),* 372-376.

[179] Wilson, T. D. and Simmons, D. M. (1993). A Particle-Size Distribution Analysis of Used Hplc Column Packing Material. *Chromatographia, 35(5-6),* 295-301.

[180] Luo, Y. L., Li, B. Y., Wang, W., Wu, K. B. and Tan, B. (2012). Hypercrosslinked Aromatic Heterocyclic Microporous Polymers: A New Class of Highly Selective Co2 Capturing Materials. *Advanced Materials, 24(42),* 5703-5707.

[181] Mistry, K., Cortes, H., Meunier, D., Schmidt, C., Feibush, B., Grinberg, N. and Krull, I. (2002). Nonaqueous Capillary Electrochromatographic Separation of Synthetic Neutral Polymers by Size Exclusion Chromatography Using Polymeric Stationary Phases. *Analytical Chemistry, 74(3),* 617-625.

[182] Potschka, M. (1991). Size Exclusion Chromatography of DNA and Viruses - Properties of Spherical and Asymmetric Molecules in Porous Networks. *Macromolecules, 24(18),* 5023-5039.

[183] Ciogli, A., Simone, P., Villani, C., Gasparrini, F., Lagana, A., Capitani, D., Marchetti, N., Pasti, L., Massi, A. and Cavazzini, A. (2014). Revealing the Fine Details of Functionalized Silica Surfaces by Solid-State Nmr and Adsorption Isotherm Measurements: The Case of Fluorinated Stationary Phases for Liquid Chromatography. *Chemistry-a European Journal, 20(26),* 8138-8148.

[184] Li, W. B., Ibanez, E., Malik, A. and Lee, M. L. (1996). Evaluation of a Fluorocarbon Bonded Silica Using Packed Capillary Column Supercritical Fluid Chromatography. *Journal of Microcolumn Separations, 8(3),* 175-181.

[185] Luo, C. Y., Zou, X. L., Li, Y. Q., Sun, C. J., Jiang, Y. and Wu, Z. Y. (2011). Determination of Flavonoids in Propolis-Rich Functional Foods by Reversed Phase High Performance Liquid Chromatography with Diode Array Detection. *Food Chemistry, 127(1),* 314-320.

[186] Paek, C., McCormick, A. V. and Carr, P. W. (2010). Preparation and Evaluation of Carbon Coated Alumina as a High Surface Area Packing Material for High Performance Liquid Chromatography. *Journal of Chromatography A, 1217(42),* 6475-6483.

[187] Wang, Z. X. and Marcus, R. K. (2014). Determination of Pore Size Distributions in Capillary-Channeled Polymer Fiber Stationary Phases by Inverse Size-Exclusion Chromatography and Implications for Fast Protein Separations. *Journal of Chromatography A, 1351(*82-89.

[188] Skvortsov, A. M. and Fleer, G. J. (2002). End-Functionalized Polymer as a Tool to Determine the Pore Size and the Interaction Parameters in Liquid Chromatography. *Macromolecules, 35(22),* 8609-8620.

[189] Stegeman, G., Kraak, J. C., Poppe, H. and Tijssen, R. (1993). Hydrodynamic Chromatography of Polymers in Packed-Columns. *Journal of Chromatography A, 657(2),* 283-303.

[190] Sychov, C. S., Ilyin, M. M., Davankov, V. A. and Sochilina, K. O. (2004). Elucidation of Retention Mechanisms on Hypercrosslinked Polystyrene Used as Column Packing Material for High-Performance Liquid Chromatography. *Journal of Chromatography A, 1030(1-2),* 17-24.

[191] Patrushev, Y. V. and Sidelnikov, V. N. (2014). The Properties of Capillary Columns with Silica Organic-Inorganic Mcm-41 Type Porous Layer Stationary Phase. *Journal of Chromatography A, 1351(*103-109.

[192] Uliyanchenko, E., Cools, P., van der Wal, S. and Schoenmakers, P. J. (2012). Comprehensive Two-Dimensional Ultrahigh-Pressure Liquid Chromatography for Separations of Polymers. *Analytical Chemistry, 84(18),* 7802-7809.

[193] Voisin, A., Thienpont, A. and Heroguez, V. (2012). Separation Study of Organic Bases on New Polymeric Stationary Phases under Basic Conditions. *European Polymer Journal, 48(1),* 228-234.

[194] Capanoglu, E., Beekwilder, J., Boyacioglu, D., Hall, R. and De Vos, R. (2008). Changes in Antioxidant and Metabolite Profiles During Production of Tomato Paste. *Journal of Agricultural and Food Chemistry, 56(3),* 964-973.

[195] Cheng, X. L., Yan, H. Y., Wang, X. L., Sun, N. and Qiao, X. Q. (2014). Vortex-Assisted Magnetic Dispersive Solid-Phase Microextraction for Rapid Screening and Recognition of Dicofol Residues in Tea Products. *Food Chemistry, 162(*104-109.

[196] Dai, J. and Mumper, R. J. (2010). Plant Phenolics: Extraction, Analysis and Their Antioxidant and Anticancer Properties. *Molecules, 15(10),* 7313-7352.

[197] George, S., Brat, P., Alter, P. and Amiot, M. J. (2005). Rapid Determination of Polyphenols and Vitamin C in Plant-Derived Products. *Journal of Agricultural and Food Chemistry, 53(5),* 1370-1373.

[198] Chikushi, N., Ohara, E., Hisama, A. and Nishide, H. (2014). Porphyrin Network Polymers Prepared Via a Click Reaction and Facilitated Oxygen Permeation through Their Membranes. *Macromolecular Rapid Communications, 35(10),* 976-980.

[199] Jin, T. N., Yan, M. and Yamamoto, Y. (2012). Click Chemistry of Alkyne-Azide Cycloaddition Using Nanostructured Copper Catalysts. *Chemcatchem, 4(9),* 1217-1229.

[200] Li, L. Y., Zhao, H. X., Wang, J. Y. and Wang, R. H. (2014). Facile Fabrication of Ultrafine Palladium Nanoparticles with Size- and Location-Control in Click-Based Porous Organic Polymers. *Acs Nano, 8(5),* 5352-5364.

[201] Liu, Z. S., Ou, J. J., Lin, H., Wang, H. W., Dong, J. and Zou, H. F. (2014). Preparation of Polyhedral Oligomeric Silsesquioxane-Based Hybrid Monolith by Ring-Opening Polymerization and Post-Functionalization Via Thiol-Ene Click Reaction. *Journal of Chromatography A, 1342(*70-77.

[202] Turgis, R., Arrachart, G., Delchet, C., Rey, C., Barre, Y., Pellet-Rostaing, S., Guari, Y., Larionova, J. and Grandjean, A. (2013). An Original "Click and Bind" Approach for Immobilizing Copper Hexacyanoferrate Nanoparticles on Mesoporous Silica. *Chemistry of Materials, 25(21),* 4447-4453.

[203] Xiao, L. Q., Cai, S. J., Liu, Q. Y., Liao, L. Q., Guo, X., Li, Y., Jia, X. X., Li, F. F. and Liu, L. J. (2014). One-Step Synthesis of Polypyrazoles and Self-Assembled Polypyrazole-Copper Catalysts for Click Chemistry. *Polymer Chemistry, 5(2),* 607-613.

[204] Xiong, X. Y., Peng, Z. Q., Shu, Y., He, H. Q., Chen, Y. Z. and Chen, B. (2014). Application of Thiol-Ene "Click" Reactions in the Preparation of Monolithic Columns. *Progress in Chemistry, 26(1),* 152-157.

[205] Zhang, C., Huang, B., Chen, Y. and Cui, D. M. (2013). Porous Copper Catalyzed Click Reaction in Water. *New Journal of Chemistry, 37(9),* 2606-2609.

[206] Zhong, H., Gong, Y. Q., Zhang, F. S., Li, L. Y. and Wang, R. H. (2014). Click-Based Porous Organic Framework Containing Chelating Terdentate Units and Its Application in Hydrogenation of Olefins. *Journal of Materials Chemistry A, 2(20),* 7502-7508.

[207] Hong, V., Udit, A. K., Evans, R. A. and Finn, M. G. (2008). Electrochemically Protected Copper(I)-Catalyzed Azide-Alkyne Cycloaddition. *Chembiochem, 9(9),* 1481-1486.

[208] Stowell, M. H. B., McPhillips, T. M., Rees, D. C., Soltis, S. M., Abresch, E. and Feher, G. (1997). Light-Induced Structural Changes in Photosynthetic Reaction Center: Implications for Mechanism of Electron-Proton Transfer. *Science, 276(5313),* 812-816.

[209] Jacob, K. and Stolle, A. (2014). Microwave-Assisted Azide-Alkyne Cycloaddition in Water Using a Heterogeneous Cu-Catalyst. *Synthetic Communications, 44(9),* 1251-1257.

[210] Sun, Q., Lv, Z. F., Du, Y. Y., Wu, Q. M., Wang, L., Zhu, L. F., Meng, X. J., Chen, W. Z. and Xiao, F. S. (2013). Recyclable Porous Polymer-Supported Copper Catalysts for Glaser and Huisgen 1,3-Diolar Cycloaddition Reactions. *Chemistry-an Asian Journal, 8(11),* 2822-2827.

[211] Tasdelen, M. A., Yilmaz, G., Iskin, B. and Yagci, Y. (2012). Photoinduced Free Radical Promoted Copper(I)-Catalyzed Click Chemistry for Macromolecular Syntheses. *Macromolecules, 45(1),* 56-61.

CURRICULUM VITAE

Name Surname: Ömer Suat TAŞKIN

Place and Date of Birth: Istanbul – 27.08.1987

University and College Degrees obtained:

2010 - 2014 Philosophy of Doctorate

Organic Chemistry, Istanbul Technical University, Graduate School of Science Engineering and Technology

2008 - 2010 Master of Science

Chemical Oceanography, Institute of Marine Sciences and Management, Istanbul University

2004 - 2008 Bachelor of Science

Chemistry, Faculty of Art and Sciences, Sakarya University, Sakarya

2001 - 2004 High School

Cumhuriyet High School, Istanbul

Professional Experience and Awards:

2009 PhD Chemistry Scholarship Award from Republic of Turkey

2010 Research Assistant, Org. Chem., Istanbul Technical University

2013 A Novel Porous Column Material for Chromatographic Analysis of Aromatic Hydrocarbons, 3. Re.& De. Project Market Activity Awards, Third Degree, Turkish Exporters Assembly

Publications from thesis:

- **Taskin O.S**., Kiskan B., Aksu A., Balkis N., Weber J., Yagci Y. Polybenzoxazine: A Powerful Tool for Removal of Mercury Salts from Water. *Chemistry - A European Jorunal,* 2014, 20(35), 10953-10958.

- **Taskin O.S.**, Kiskan B., Weber J., Yagci Y. One-pot, One-step Strategy for the Preparation of Clickable Melamine Based Porous Material. *Submitted.*

- **Taskin O.S.**, Kiskan B., Aksu A., Balkis N., Weber J., Yagci Y. Catalyst-free Preparation of Microporous Column Packing Material. *Submitted*.

Publications:

- Balkıs, N., Aksu, A., Erşan, M.S., Muftuoglu, A.E., Zeki, S., Demir, V., **Taskin, O.S.** Tracing of the Leachate in the Marine Medium. *Asian Journal of Chemistry*. 2010, 22(8), 5859-5864.

- Aksu, A., Balkıs, N., **Taskin, O.S.**, Erşan, M.S. Toxic Metal (Pb, Cd, As and Hg) and Organochlorine Residue Levels in Fishes Hake (*Merluccius Merluccius)* from The Marmara Sea, Turkey. *Environmental Monitoring and Assessment.* 2010, 182(1-4), 509-521.

- **Taskin, O.S.**, Aksu, A., Balkıs, N., Metal (Al, Fe, Mn and Cu) distributions and origins of polycyclic aromatic hydrocarbons (PAHs) in the surface sediments of the Marmara Sea and the coast of Istanbul, Turkey. *Marine Pollution Bulletin*, 2011, 62, 2568-2570.

- **Taskin, O.S.**, Aksu, A. Organochlorine residue and toxic metal (Pb, Cd and Cr) levels in the surface sediments of the Marmara Sea and the coast of Istanbul, Turkey. *Marine Pollution Bulletin.* 2012, 64(5), 1060-1062.

- **Taskin, O.S.**, Yilmaz G., Tasdelen M.A., Yagci Y. Photoinduced reverse atom transfer radical polymerization of methyl methacrylate using camphorquinone/benzhydrol system. *Polymer International.* 2014, 63(5), 902–907.

- **Taskin, O.S.**, Kiskan B., Yagci Y. Polybenzoxazine Precursors as Self-Healing Agents for Polysulfones. *Macromolecules* 2013. 46(22), 8773-8778.

- **Taskin O.S.**, Erel-Goktepe I, Ahmed Khan MA, Pispas S and Yagci Y. Polystyrene-*b*-poly(2-vinyl phenacyl pyridinium) salts as photoinitiators for free radical and cationic polymerizations and their photoinduced molecular associations. *Journal of Photochemistry and Photobiology A: Chemistry*. 2014, 285, 30-36.

- **Taskin O.S**., Temel BA., Tasdelen MA., Yagci Y. Synthesis of Block Copolymers by Selective H-Abstraction and Radical Coupling Reactions Using Benzophenone/Benzhydrol Photoinitiating System. *European Polymer Journal*. 2014, DOI: 10.1016/j.eurpolymj.2014.07.007.

Patents:

- **Taskin, O.S.**, Kiskan B., Yagci Y. Adsorban Bir Malzeme ve Üretim Yöntemi. *Turkish Patent*. PT 2013/11012. 2013.

- **Taskin, O.S.**, Kiskan B., Aksu A., Balkis N., Yagci Y. Bir Kolon Dolgu Malzemesi ve Üretim Yöntemi. *Turkish Patent*. PT 2013/13450. A Novel Porous Column Material for Chromatographic Analysis of Aromatic Hydrocarbons. Pending application for *PCT (International Patent)*, 2013.

- **Taskin, O.S.**, Kiskan B., Yagci Y. Bir Katalizör ve Üretim Yöntemi. *Turkish Patent.* PT 2013/14776. A Novel Approach for Atom Transfer Radical Polymerization using Heterogeneous Catalyst without copper residue. Pending application for PCT (*International Patent*), 2013.

Chapters:

- Doran, S., **Taskin, O.S.**, Tasdelen MA. and Yagci, Y. Controlled photopolymerization and novel architectures. *Dyes and Chromophores in Polymer Science*. 2014. *In preparation.*

- Yagci Y, Tasdelen MA, Kiskan B, Ciftci M, Dadashi-Silab S, **Taskin O.S.**, Yilmaz G. Visible light-induced atom transfer radical polymerization for macromolecular syntheses. *ACS Symposium Series Publication*. 2014. *In preparation*.